Hydrodynamic & Dispersal Modeling in FISH Project Focal Areas

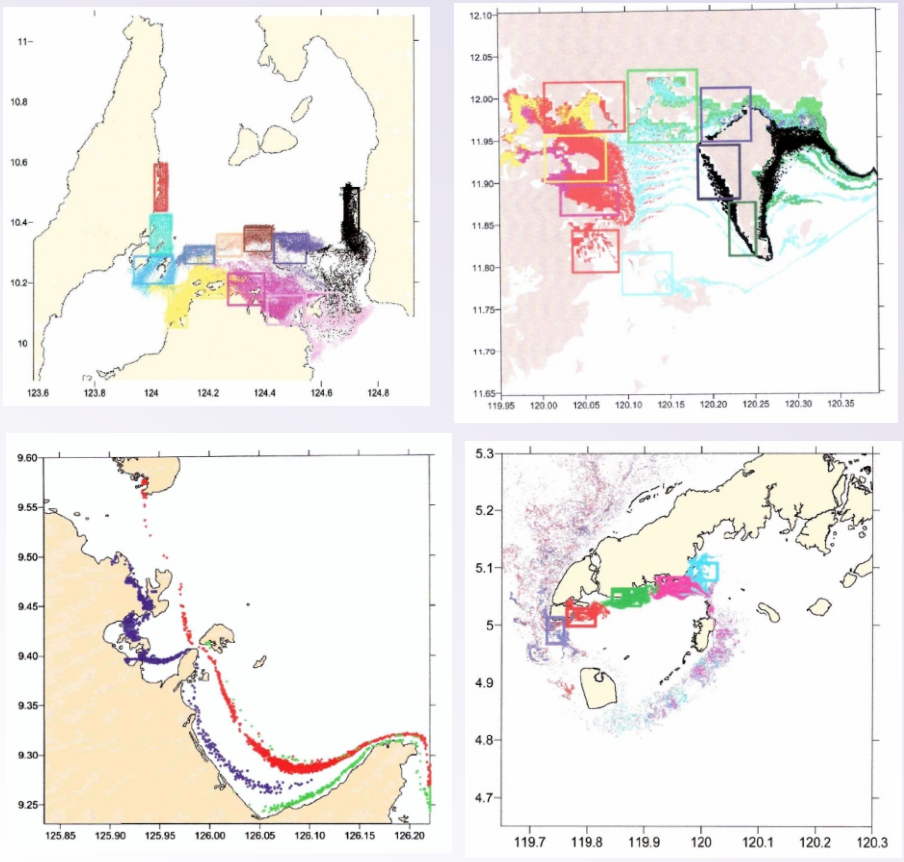

Prepared by:
Cesar L. Villanoy, Ph.D., Olivia C. Cabrera, Marites M. Magno-Canto, Marilou C. Martin, Erlinda E. Salamante and Kathleen M. Silvano

In compliance with the requirements of:

USAID FROM THE AMERICAN PEOPLE

The Fisheries Improved for Sustainable Harvest (FISH) Project

Hydrodynamic & Dispersal Modeling in FISH Project Focal Areas

Prepared by:

Cesar L. Villanoy, Ph.D., Olivia C. Cabrera,
Marites M. Magno-Canto, Marilou C. Martin,
Erlinda E. Salamante and Kathleen M. Silvano

University of the Philippines-Marine Science Institute

2006

In compliance with the requirements of:

The Fisheries Improved for Sustainable Harvest (FISH) Project of the United States Agency for International Development (USAID) and the Department of Agriculture-Bureau of Fisheries and Aquatic Resources (DA-BFAR)

This report was made possible through support provided by the United States Agency for International Development (USAID) under the terms of Contract No. AID 492-C-00-03-00022-00. The opinions expressed therein are those of the author(s) and do not necessarily reflect the views of USAID.

Citation: Villanoy C.L., O.C. Cabrera, M.M. Magno-Canto, M.C. Martin, E.E. Salamante and K.M. Silvano. 2006. Hydrodynamic and Dispersal Modeling in FISH Project Focal Areas. University of the Philippines-Marine Science Institute and the Department of Agriculture-Bureau of Fisheries and Aquatic Resources (DA-BFAR) Fisheries Improved for Sustainable Harvest (FISH) Project. 93 p..

TABLE OF CONTENTS

Study 1

LIST OF FIGURES

LIST OF TABLES

Study 2

LIST OF FIGURES

LIST OF TABLES

LIST OF FIGURES

LIST OF TABLES

Study 4

LIST OF FIGURES

LIST OF TABLES

NUMERICAL SIMULATIONS OF LARVAL DISPERSAL PATTERNS IN BOHOL

1 INTRODUCTION

Bohol is one of the four focal sites of the USAID funded Fisheries Improvements for Sustainable Harvests (FISH) Project. The goal of the project is to improve fish stocks by as much as 10% over a 5-year project. One of the interventions to address this goal is the establishment of fish sanctuaries. Studies (Ward et al., 2001) have suggested that synergistic effects of sanctuary or MPA networks will be more beneficial to the fisheries through larval spillover than just by adult spillover. It is assumed that these networks are established on the basis of larval connectivities and dispersal. The aim of this study is to determine, using numerical models, the potential dispersal patterns of larvae of fish, which may help in selecting locations of future MPAs, and MPA networks.

1.1 Description of Study Site

Bohol is located south of the Camotes Sea bounded by the Bohol Strait in the west and by the Canigao Channel in the east. North of Bohol facing the Camotes Sea is the Danahon Bank distinguished by a double barrier reef system. The presence of complex topographic features in this reef system, both due to shallow extensive reefs and numerous small islands, heavily influences the circulation pattern in the area. That is, the barriers obstruct and divert the flow parallel to these barriers. An interesting consequence of this topographic feature is the occurrence of wakes, eddies and turbulence which can occur in tidal streams behind such obstructions that affects transport of particles (i.e., fish and coral larvae) within the area.

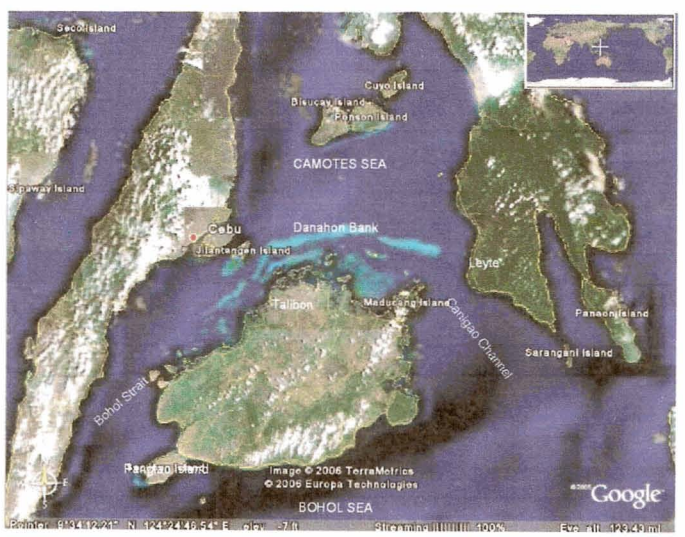

Figure 1 Image showing the study area and surrounding waters.

In terms of bathymetry, Danahon Bank is very shallow with depths not exceeding 100m. The shelf is narrower at the western side along Tubigon but wider that extends across the Canigao Channel towards southern Leyte. Although the Canigao Channel provides a wider shelf compared through the Cebu/Bohol Strait, it marks the shallower connection to the waters of Bohol Sea in the south at the point closest to the coast of eastern Bohol. On the other side is a deeper link with depths twice as much (>200m) the deepest point in the Bank. The deeper connections to the Bohol Sea suggests that during the southwest monsoon, water comes in from the south in the eastern side of Bohol, enters the barrier system and exits to the west and through the few passes along the barrier system. The area is exposed during the northeast monsoon but the presence of the barriers prevents the development of large waves. The net transport direction over the area is most likely from east to west.

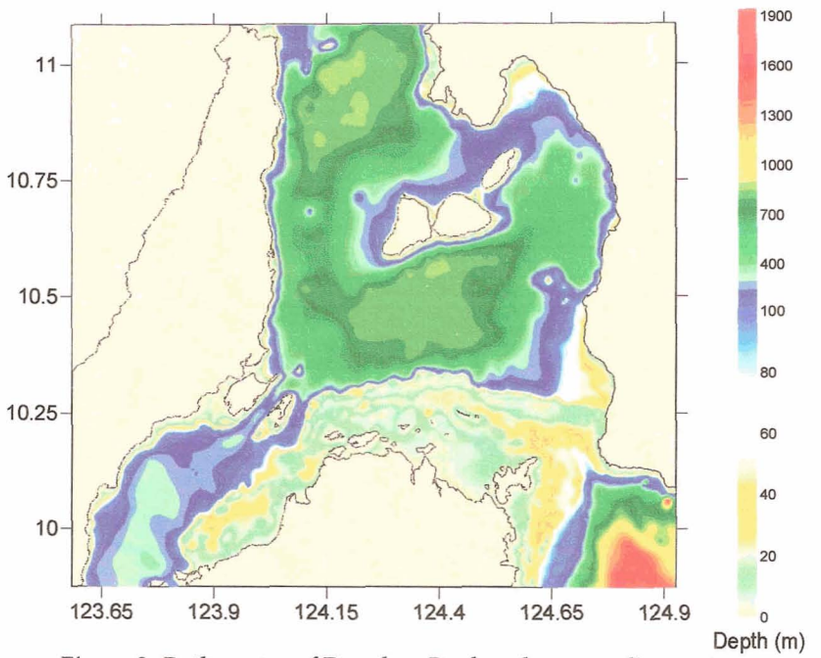

Figure 2 Bathymetry of Danahon Bank and surrounding waters.

1.2 Specific Objectives

The objectives of this study are:

- Characterize circulation patterns in the Danahon Bank in scales relevant to the dispersal of larvae
- Simulate larval dispersal patterns from different areas in Danahon Bank and surrounding waters and to characterize potential larval exchange between these areas

2 METHODOLOGY

2.1 Field Survey

A field survey was conducted last December 7-11, 2005 to collect baseline information on the distribution of temperature, salinity, chlorophyll and surface currents. The stations occupied during the survey are shown in Figure 3. At each

station, the temperature, salinity and chlorophyll profiles were obtained using a Seabird SBE19 CTD with a Turner SCUFA Fluorometer. The surface currents were measured using a 0.5m diameter holey-sock drogue. A handheld GPS in tracking mode was attached to the drogue and measures the position of the drogue as it drifts with the currents. A handheld anemometer and an electronic compass were used to measure wind speed and direction, respectively.

2.2 Hydrodynamic Modeling

The three-dimensional circulation of the waters in Bohol was modeled using the Princeton Ocean Model (Mellor, 2003). This model is a three-dimensional primitive-equation sigma coordinate model and is used in numerous applications ranging from estuarine to global ocean models. The model domain for Bohol model covers the area shown in Figure 2. The model grid resolution is 900m x 900m. At the boundaries, the model is forced by the tides and offshore currents and at the surface by the wind. The tidal forcing prescribed at the open boundaries was derived from the Oregon State University Tidal Inversion Software (OTIS) model applied to Philippine waters by Magno (2005). Open ocean currents at the model open boundaries were obtained from the monthly mean barotropic velocities computed by the Pacific HYCOM Simulations (http://hycom.rsmas.miami.edu/data/information. html#pacific). Separate runs were made to represent seasonal circulation patterns. Each run was allowed to run for 30 days of model time for each seasonal boundary forcing. The model is also forced at the surface by winds derived from satellite altimetry (http://manati.orbit.nesdis.noaa.gov/hires/).

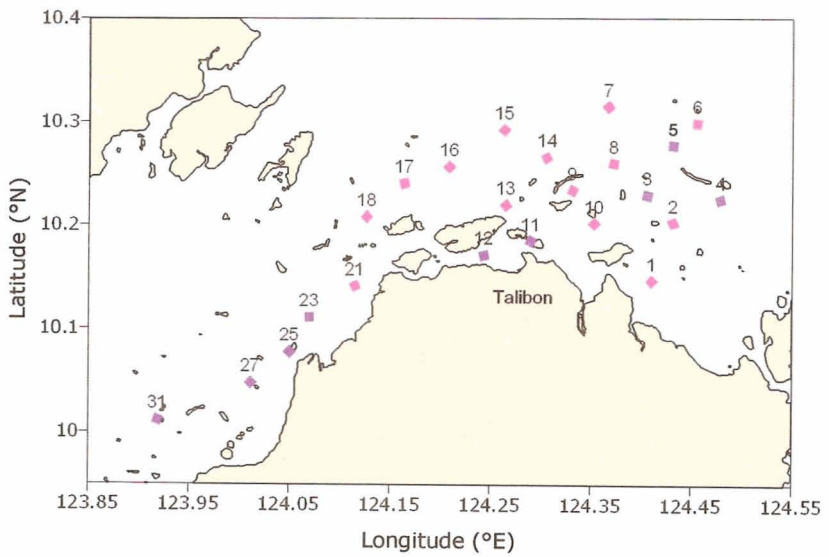

Figure 3. Map showing the location of stations occupied during the field survey. Diamonds in magenta color denote stations occupied during flood tide while violet diamonds show stations surveyed during ebb tide.

The parameters for the simulation experiments conducted for this study are listed in Table 1. Three seasons were considered, northeast monsoon season (January 2003 forcing), southwest monsoon season (August 2003 forcing) and the spring monsoon transition (April 2003 forcing).

Table 1. Summary of hydrodynamic simulations

Run No	Tides	HYCOM Boundary forcing	Winds
1	√		
2		√ August 2003 data	
3		√ August 2003 data	√
4		√ April 2003 data	
5		√ April 2003 data	√
6		√ January 2003 data	
7		√ January 2003 data	√

2.3 Lagrangian dispersal model

The dispersal model is adapted from the model of Polovina et al. (1999). In this model, the larvae are represented as neutrally buoyant passive particles and their position over time is tracked using the following equations:

$$x_{t+\Delta t} = x_t + \left(u_{x,y,t}\Delta t + \varepsilon\sqrt{D\Delta t}\right)$$
$$y_{t+\Delta t} = y_t + \left(v_{x,y,t}\Delta t + \varepsilon\sqrt{D\Delta t}\right) \quad (1)$$

where x and y are the coordinates of a particle; u and v are the advection velocities from the hydrodynamic model, Δt is the integration time step, ε is a randomly generated number ranging from -1 to 1, and D is the eddy diffusion rate (m^2s^{-1}). Each particle when released has attributes, which identifies it individually from the other particles. These attributes include age from release, location of release, date and time of release. These attributes will enable us to estimate the degree of exchange of simulated particles between areas based on the method used by Sauers et al. (2003) in analyzing drifter card data.

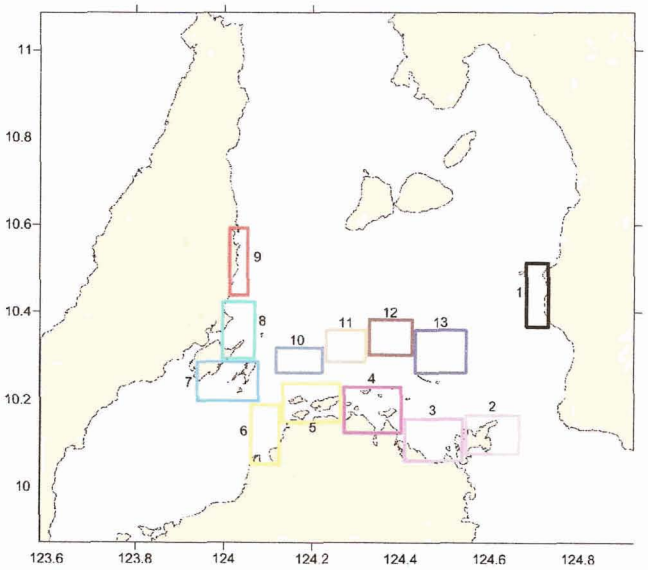

Figure 4. Areas used for dispersal simulation as larval source or sink areas.

To determine the exchange between areas, several areas were designated as source and sink areas around the study area. The sizes and locations of these areas, shown in Figure 4, vary and were chosen to represent different areas all around northern

Bohol and important surrounding waters as closely as possible. The dispersal model was used to simulate the dispersal of particles released from these boxes. Separate runs were used for dispersal periods of 10, 20 and 30 days duration to represent short, medium, and long-range dispersal. Dispersal simulations based on the tidal component of the circulation was also conducted. After each of these simulations, the location of the particles and where they were released were noted and used in the analysis.

3 RESULTS AND DISCUSSION

3.1 Field Survey

The tides during the survey period were mixed mainly semidiurnal (Table 2). The differences in the phases of the tide during the field survey may indicate some degree of variation in the pattern of circulation within the area. To address this, measurements obtained were grouped according to tidal regime (e.g., ebb and flood tide) which is expected to show some short period reversals.

The surface current measurements conducted during the field survey are shown in Figure 5. Strong flows were consistently observed for the duration of the survey but with magnitudes not exceeding 3m/s. Surface currents measured during flood tide generally flows parallel the barriers and southwestward towards the Cebu/Bohol Strait. However, some of the stations have flow directions modified by the presence of the small islands as well. Contrary to what was expected, current patterns for stations covered during ebb tide are also consistent both in direction and magnitude with the flood tide surface currents. Overall, results for the surface current measurements reflect how the presence of the small numerous islands and reefs along the Bank interferes with the flow pattern in the area among other factors.

Table 2. Predicted tides for the survey period from December 8-10, 2005 (source: NAMRIA, 2005)

Date	Time	Height
8	0242	1.40
	1104	-0.12
9	0339	1.21
	1205	-0.01
	1932	0.49
	2132	0.48
10	0448	0.98
	1249	0.1
	1925	0.67

Temperature, Salinity and Chlorophyll

Although wind measurements were not conducted for this survey due to technical constraints, it was well noted that strong winds were prevailing for the entire duration of the sampling. This in fact is also evident in the profiles obtained for the different hydrographic parameters. In general, vertical profiles of temperature, salinity and chlorophyll, both for ebb and flood tide stations show homogenous

profile with depth and indicate a very well mixed water column (Figure 6). The mixed layer extends to about 35m for ebb stations and 25m for flood stations, which could be possible in events of strong winds in conjunction with strong flow resulting to efficient mixing. Furthermore, these conditions may also account for the lack of conceivable differences (i.e., reversal of surface currents from flood to ebb) in the circulation pattern expected for different tidal phases. This may also suggest that the effects of tide in controlling the circulation pattern may not be as significant as the other factor such as surface winds.

3.2 Hydrodynamic Model Results

The hycom-forced current patterns are distinct and complex for the different seasons considered (Figure 7). Along Bohol/Cebu Strait, the flow is directed northward and continues into the Camotes Sea during January and April but reverses during August. For the two former months, these currents become deflected eastward as it approaches the shallow shelf south of the Olango Island located in the middle portion of the strait. It then continues eastward and moves parallel the barrier reefs but become further modified as it encounters the complex topography within the area. Along this area, currents moving eastward also come across the strong currents from the southwest. During August, this current pattern is reversed and the flow advances westward then southward through the Bohol/Cebu Strait.

It seems counterintuitive why barotropic currents along Cebu Strait move northwards during the northeast monsoon and southwards during the southward monsoon until the circulation in the whole Visayan Sea is examined. The Pacific HYCOM results show that most of the seas in the Visayas area flow along the direction of the wind except in the Camotes Sea, which appears to respond to the flow in the neighboring basins. It may have something to do with the fact that the Camotes Sea area is practically closed in the south except for the very narrow straits between Cebu and Bohol. This makes the Camotes Sea receptive to what is happening to the north. For instance, during the southwest monsoon, water from the Visayan Sea may pile up water in the northern part of the Camotes Sea. The presence of this meridional pressure gradient in the Camotes Sea may result in pushing the water southward, opposite the direction of the wind. It must be noted that the preceding statements were based on the results of the Pacific HYCOM Model and that no field observations have been made or is available to confirm such speculation.

For all seasons, the strongest currents were consistently present in the shallow shelf along the Canigao Channel connecting the mainland Bohol and southern Leyte. Currents within this area are obviously influenced by the bottom topography as the currents generally follow its contour and increases in magnitude as water depths become shallower. Currents are also stronger in the shallow areas between Poro and Ponson Islands and along the west coast of Bohol.

The flow in the Danahon Banks in constrained by the presence of the double barrier system resulting in the dominance of the alongshore flow (Figure 8). The net flow appears to move towards the west and is consistent with the field measurements

conducted. Landsat images of the Danahon Bank show island wakes formed in northwest sides of the islands suggesting flow is going into the Danahon Banks area. To the east, in the channel between Bohol and Leyte, flow reverses seasonally and since the flow in Danahon is always westward, the source waters for the Danahon area is from the Bohol Sea during the northeast monsoon and the monsoonal transition (April), and from the Camotes Sea during the southwest monsoon.

Tidal circulation in the Danahon Banks is weak. Model results show that the magnitude of the tidal circulation is roughly only about a third of the wind-driven circulation. This is again consistent with the field observations where the general trend of the flow is westward despite the fact that the measurements were made during both flood and ebb tide conditions. The tidal circulation patterns, which show the current reversals, are shown in Figure 9. The strongest tidal currents are found in the shallow channel between Bohol and Leyte. During ebb, water flows from the Bohol Sea to the Camotes Sea and reverses during flood tide.

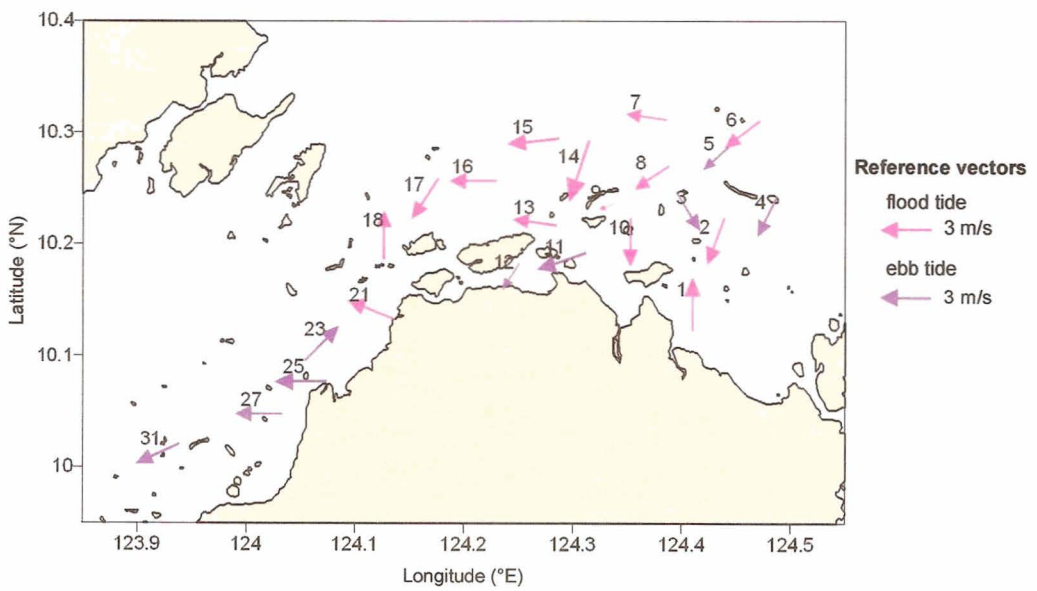

Figure 5. Measured surface currents from surface drogue. Colors of arrow denote different sampling days.

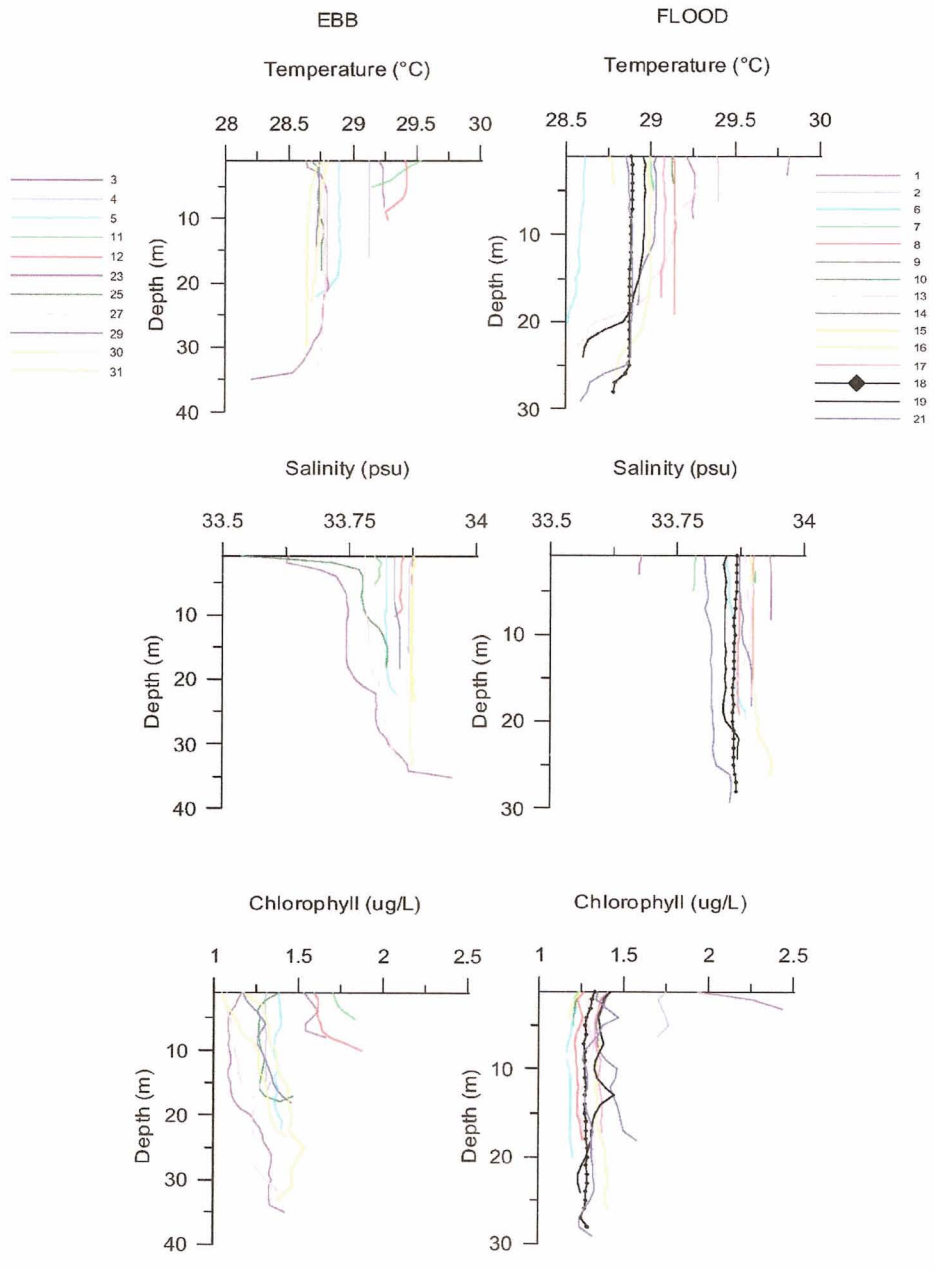

Figure 6. Vertical profiles of temperature, salinity and chlorophyll of stations occupied during flood and ebb tides.

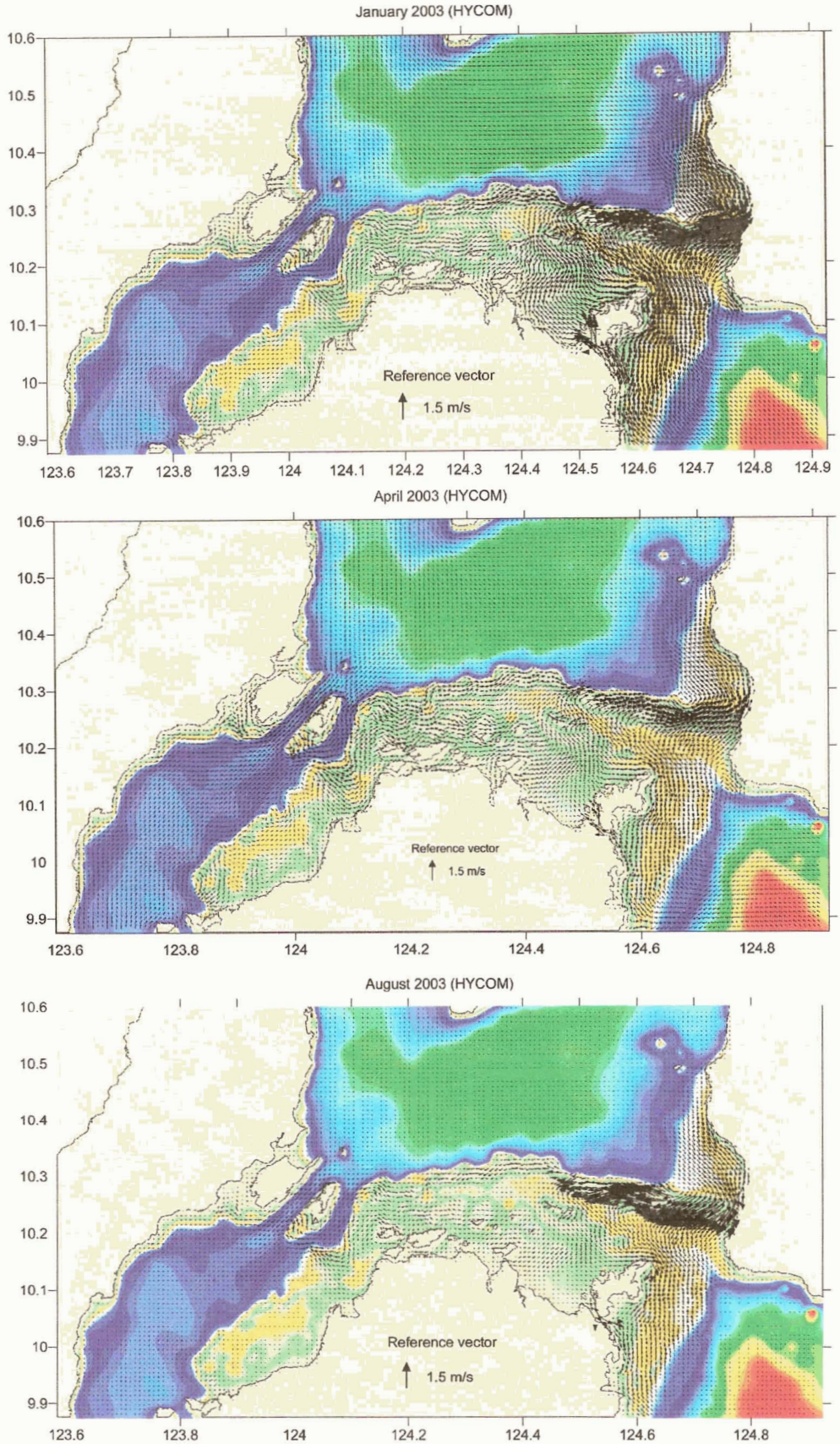

Figure 7. Modeled surface circulation forced by HYCOM barotropic velocities at the open boundaries.

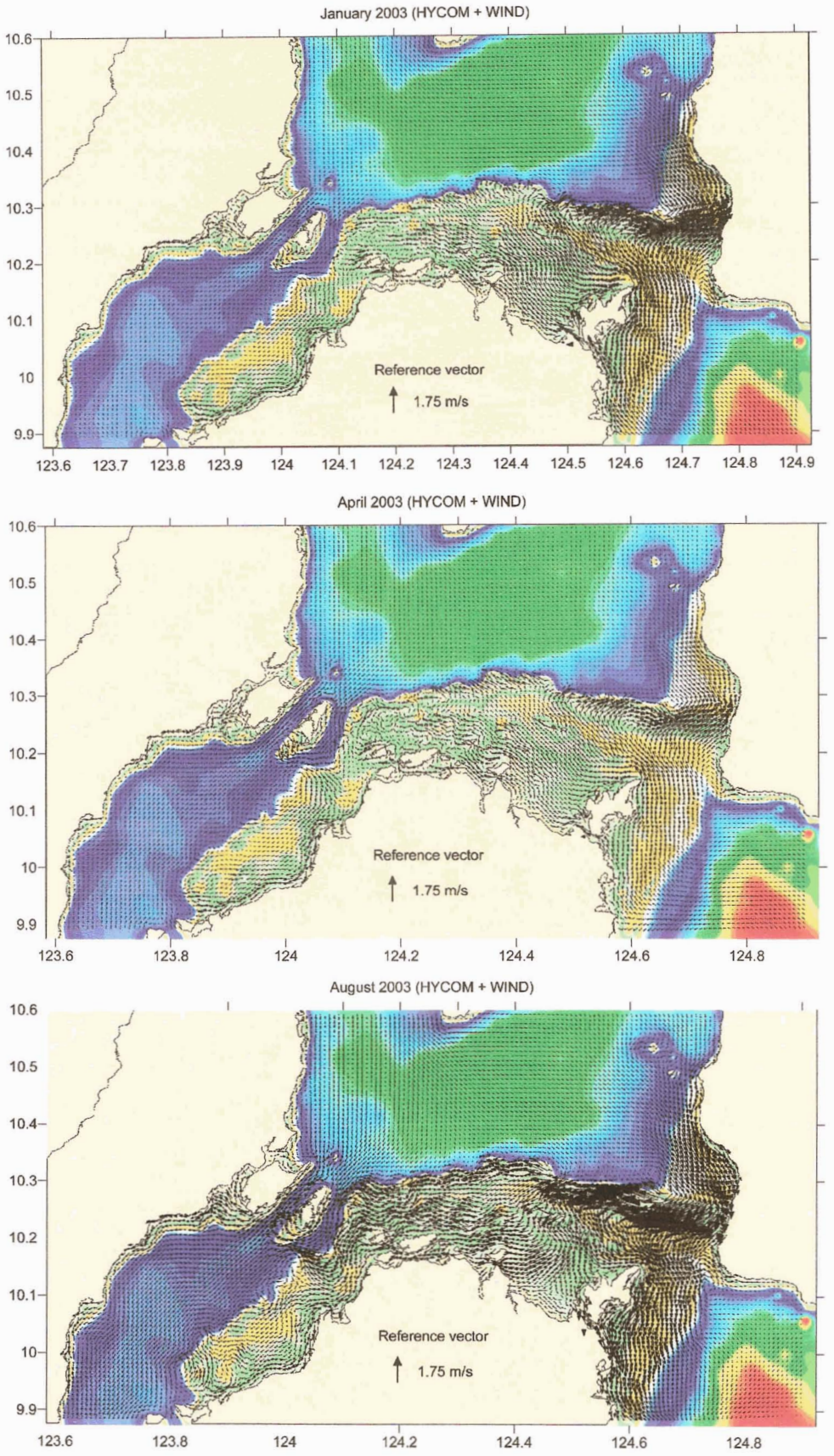

Figure 8. Modeled surface circulation forced by HYCOM at the open boundaries and monthly climatological winds

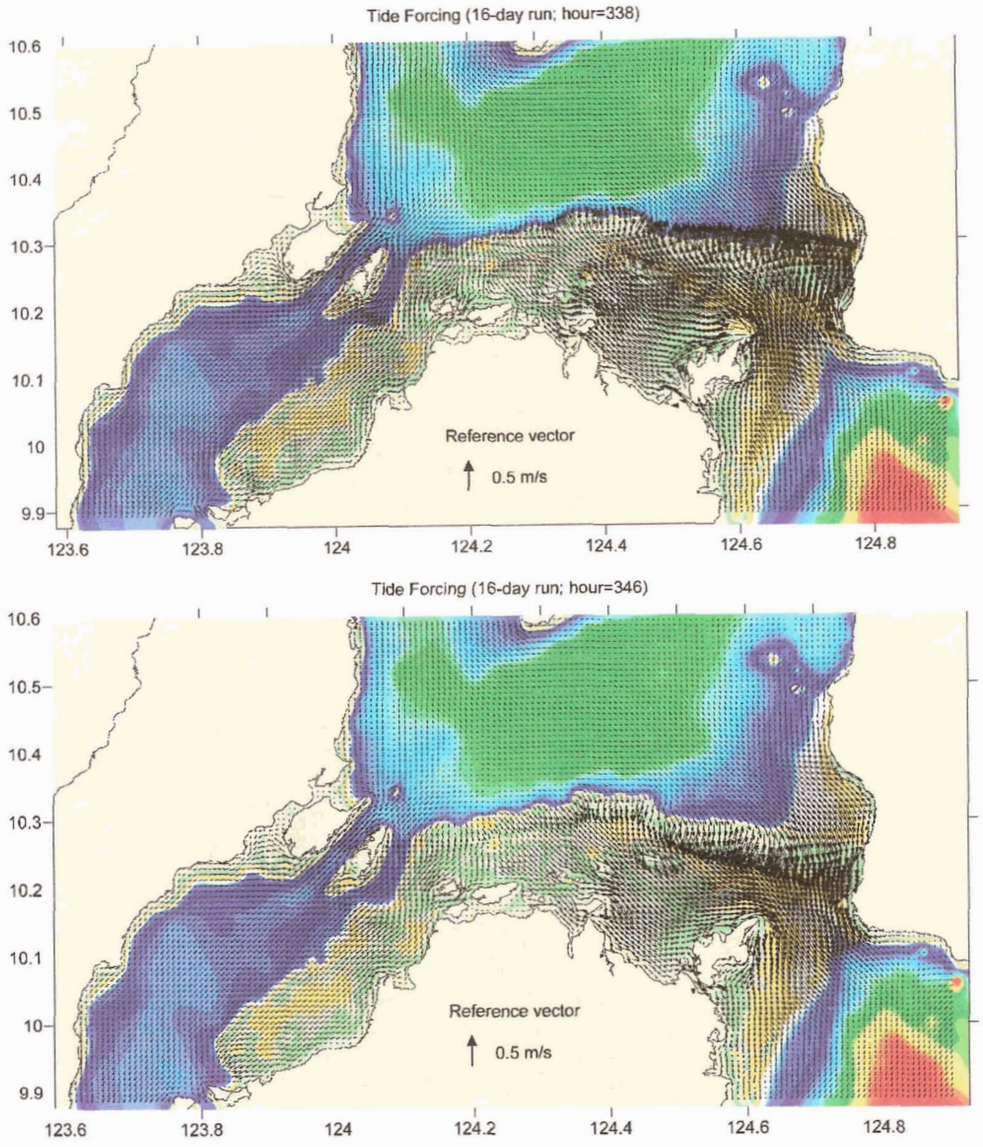

Figure 9. Modeled tidal velocities during ebb (top) and flood (bottom) conditions.

3.3 Larval Dispersal Patterns

The net westward flow of the waters of Danahon Bank will definitely have some implications on the larval dispersal patterns in the area. The results of the dispersal simulations are shown in Figures 10-12 representing dispersal patterns during January, April and August, respectively. The colored dots represent the location of dispersed particles and the source of these dots is indicated by the box of the same color. The net westward dispersal is evident in the figures but seasonal differences in dispersal can be observed in the eastern part of the Danahon Banks. For instance, particles released from Ubay and Pres Carlos P. Garcia were advected northward during January and April and westward during August. Particles released off Talibon were always advected westwards exiting towards Tubigon. The August simulations show almost all particles moving westwards within the Danahon Banks.

The particles released along the double barrier flowed along the barrier but off Buenavista and Hinabanga, the particles moved closer to shore and traveled southwestwards close to the shore. These well defined, almost unidirectional patterns are an important consideration in designing MPA networks and are an important justification for a network.

The dispersal patterns due to the tidal circulation are shown in Figure 13. The dispersal of particles off the areas to the east of Getafe shows a slight net displacement to the east and southeast. However, because of the weaker magnitudes of the tides, dispersal is expected to be dominated by the wind-driven component.

Since we are interested in the potential for larval exchange between specific areas, we can quantify the exchange by determining how many of the particles released ended up within the boundaries of pre-defined areas. For this study, initial areas were selected, defined as the boxes shown in the succeeding figures. The figures are divided into two groups, the first group (Figure 14-16) showing the sink areas where particles released from a particular box ended up and the other group (Figure 17-19) showing the origin of the particles settling in a particular box.

Short term larval durations, as described by the 10-day simulation show that some areas of the Danahon Bank show a potential for self seeding. These areas include the Tubigon (green square), and the boxes in the outer barrier. This potential can be seen in Figure 14 as those boxes where the longest colored bar in a box has the same color as the box. The northward dispersal in the eastern part and the western advection in the northern and western part of Danahon are evident in the figure. In the 20-day simulation, the number of potential self seeding boxes decreases to only 1 box out of 9 simulated. This means that particles are being advected farther away from their source. The remaining self-seeding box is the western edge of the outer barrier and is the box closest to Cebu (medium blue box). This box, together with the box off Tubigon remains the major sink box of their larvae for the long term larval durations (30 days).

Figures 17-19 also summarizes the origin of particles settling in particular boxes for all the simulations conducted. The information provided by these figures can be helpful in selecting sites for MPAs which can be designed as larvae settlement areas. For the January and April simulations, the boxes in the western part of the Danahon banks show the most number of bars, indicating that it is receiving particles from the most number of sources. On the other hand, the August simulations indicate that the eastern edge of the outer barrier is receiving relatively more from different sources compared to the other boxes. The seasonal differences highlight the fact that settlement and dispersal patterns are not static processes and it is important that MPA design should also consider the fact that MPAs can be both larvae exporters and settlement areas but the role of each function may change with season.

The dispersal patterns driven by tides also show the potential of each area for self seeding. In most of the boxes in Figure 20, the largest bar is almost always the bar of the same color as the box which suggests that majority of particles settling in the box were released from the same box. Of course, this may be a function of the size of the box and the strength of advection. The weaker tidal circulation and resulting short distance dispersal coupled with the large sizes of the area of release resulted in a larger number of particles retained.

4 SUMMARY AND CONCLUSIONS

These results highlight the importance of MPA networks in an area where larval dispersal distances is potentially large and predominantly along one direction. The waters in the Danahon Banks are highly influenced by the main topographic feature, which is the double barrier sand bank/reef. Flow inferred from circulation models and also from the short field observation conducted, is dominated by flow to the west parallel to the barrier reef system. The water flowing through this area is sourced from either the Bohol Sea (during January and April) or from the Camotes (during August). Tidal reversal of the currents was not observed during the field survey indicating the weak contribution of the tides.

The dispersal patterns and the use of source and sink boxes were used to identify areas which are potential source areas (larvae exporter) and sink areas (larval settlement areas). In a system where larval advection is dominantly along one direction, this distinction becomes clearer. For instance, the dispersal model shows that the boxes in the western part of the Danahon Banks are potential settlement areas because it receives larvae from a greater number of source boxes compared to the other areas. On the other hand, boxes on the eastern side probably function best as larvae exporters (shown in the figure as contributing to the settled particles in a greater number of boxes). Although seasonal differences may occur, the above show the general patterns in the dispersal of larvae in the Danahon Banks.

5 REFERENCES

Magno MM, 2005. Estimation of entrainment potential in Philippine Coastal Waters: The physical consequence of island wakes and eddies. MSc Thesis. College of Science, University of the Philippines, Diliman, Quezon City.

Mellor, G. L., 2003. Users guide for a three-dimensional, primitive equation, numerical ocean model (June 2003 version), 53 pp., Prog. in Atmos. and Ocean. Sci, Princeton University.

NAMRIA, 2005. Tide and Current Tables Philippines 2005. The Coast and Geodetic Survey Department, National Mapping and Resource Information Authority. Department of Environment and Natural Resources.

Polovina JJ, Kleiber P, Kobayashi DR. 1999. Application of TOPEX-POSEIDON satellite altimetry to simulate transport dynamics of larvae of spiny lobster, *Panulirus marginatus*, in the northeastern Hawaiian Islands, 1993-1996. Fish. Buyll. 97:132-143.

Sauers KA, Klinger T, Coomes C, Ebbesmeyer CC. 2003. Synthesis of 41,300 Drift Cards Released in Juan de Fuca Strait (1975-2002). Proceedings of the 2003 Georgia Basin/Puget Sound Research Conference. http://www.psat.wa.gov/Publications/01_proceedings/sessions/oral/7c_sauer.pdf

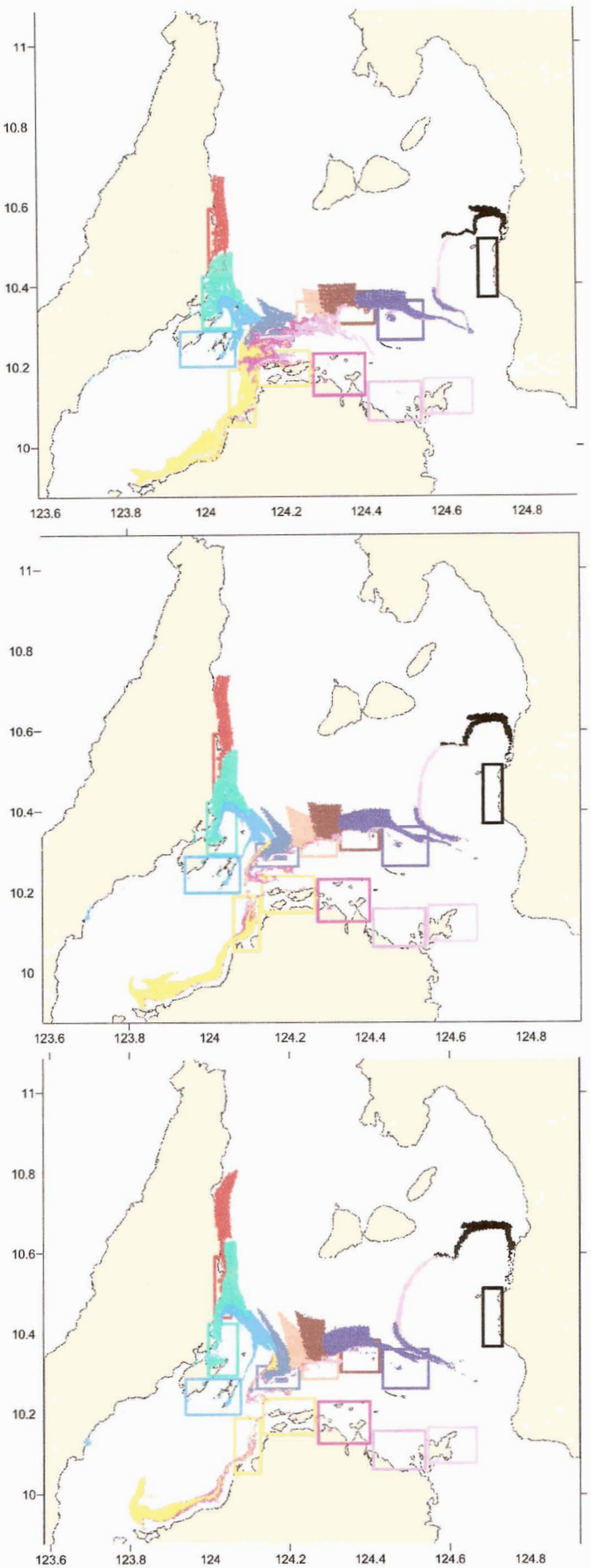

Figure 10. Dispersal of particles released from different locations for January 2003.

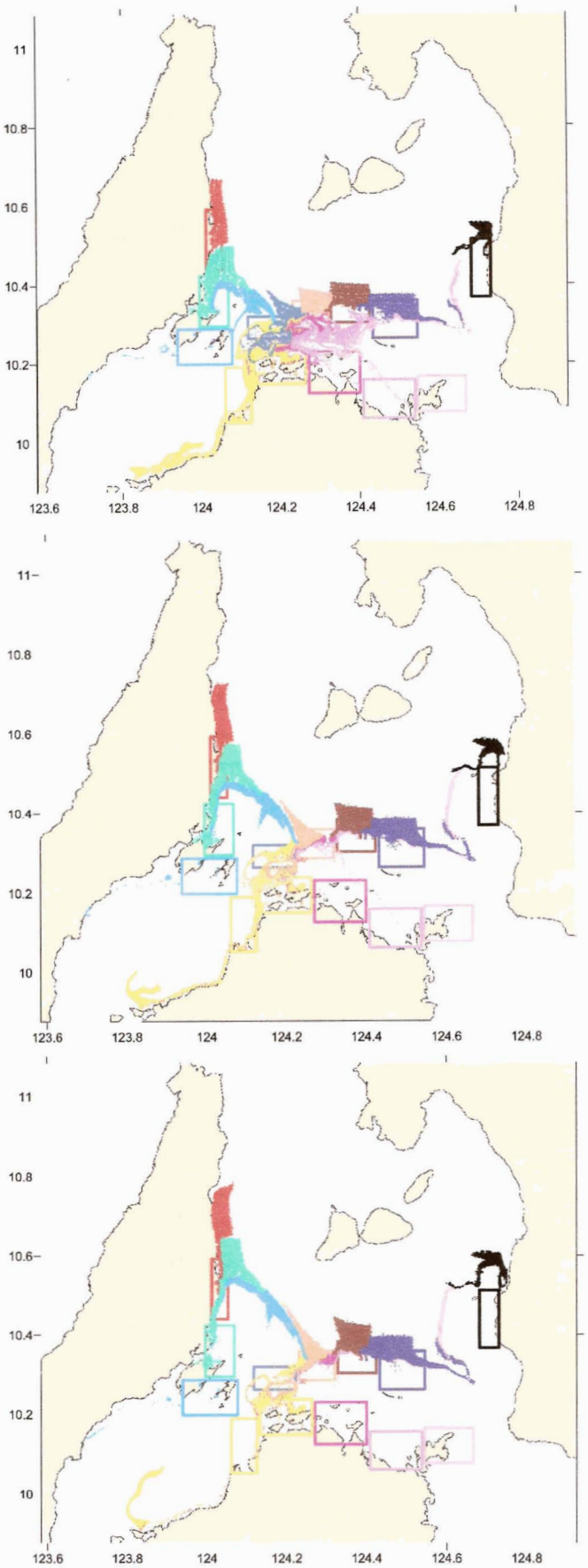

Figure 11. Dispersal of particles released from different locations for April 2003.

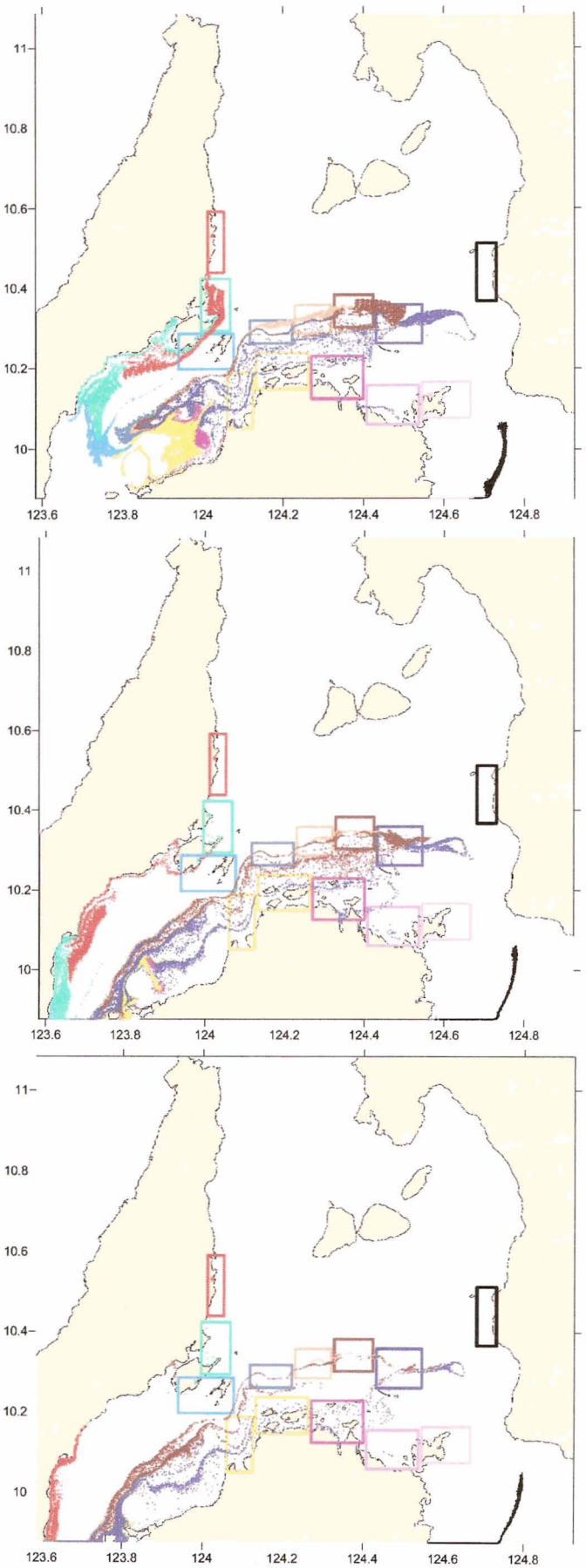

Figure 12. Dispersal of particles released from different locations for August 2003.

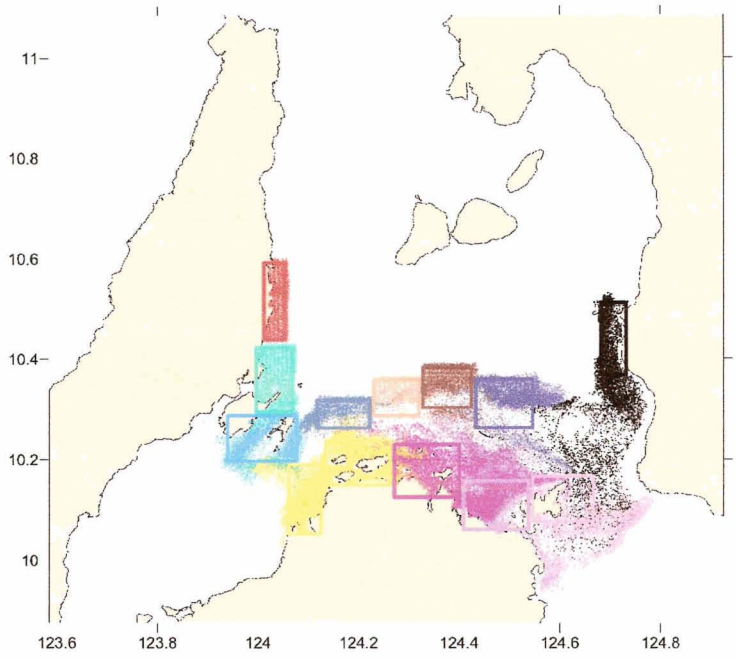

Figure 13. Dispersal of particles released from different locations forced by tidal velocities

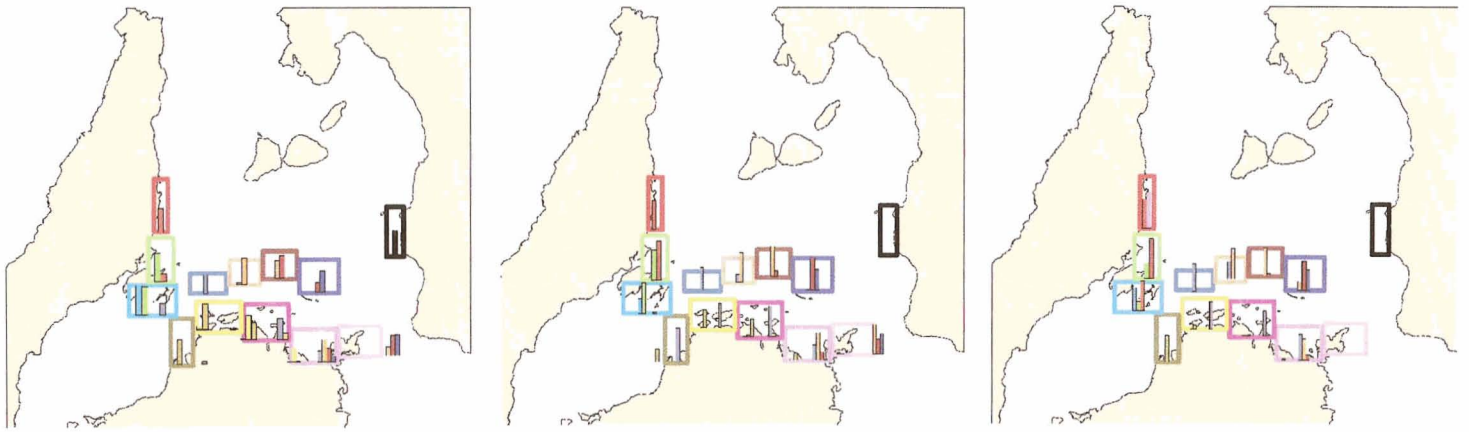

A B C

Figure 14. Relative distribution of sink areas during January for 10-day (A), 20-day (B) and 30-day (C) dispersal simulations. The colored boxes represent release areas for dispersed particles. Colored bars represent where particles from a specific box ended up

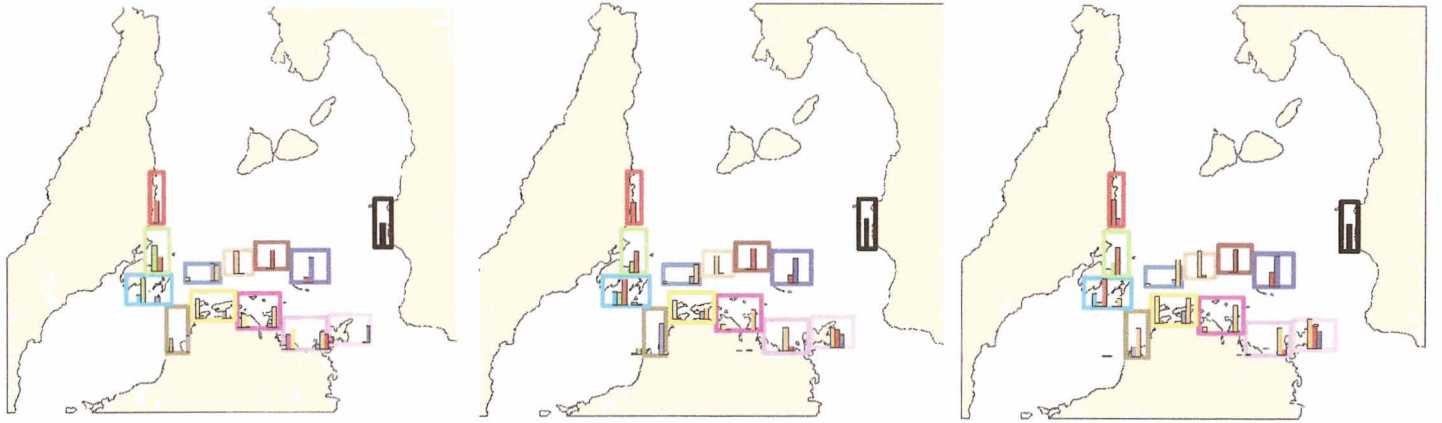

A B C

Figure 15. Relative distribution of sink areas during April for 10-day (A), 20-day (B) and 30-day (C) dispersal simulations. The colored boxes represent release areas for dispersed particles. Colored bars represent where particles from a specific box ended up

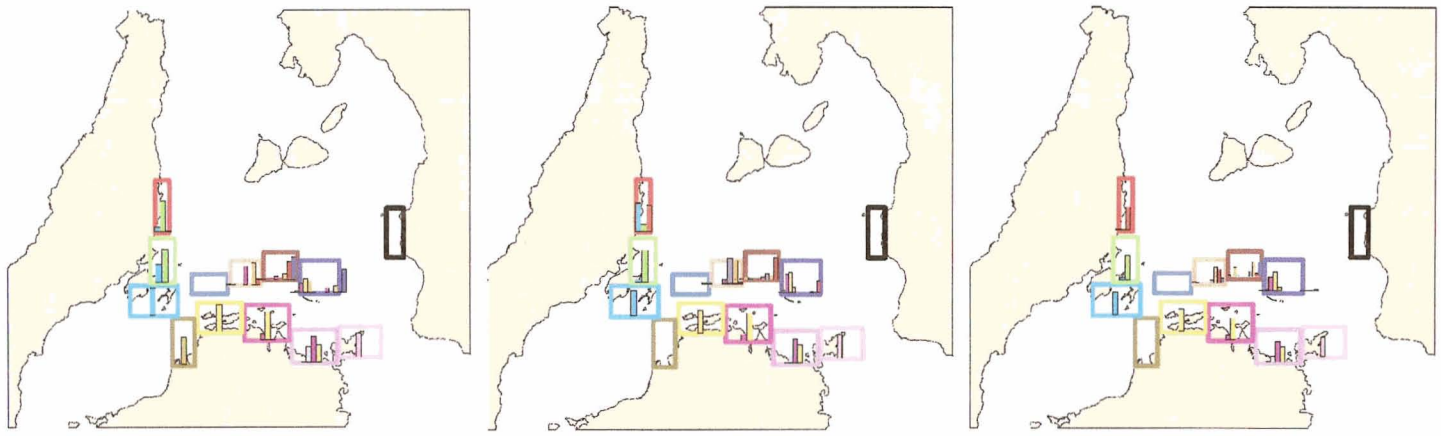

Figure 16. Relative distribution of sink areas during August for 10-day (A), 20-day (B) and 30-day (C) dispersal simulations. The colored boxes represent release areas for dispersed particles. Colored bars represent where particles from a specific box ended up

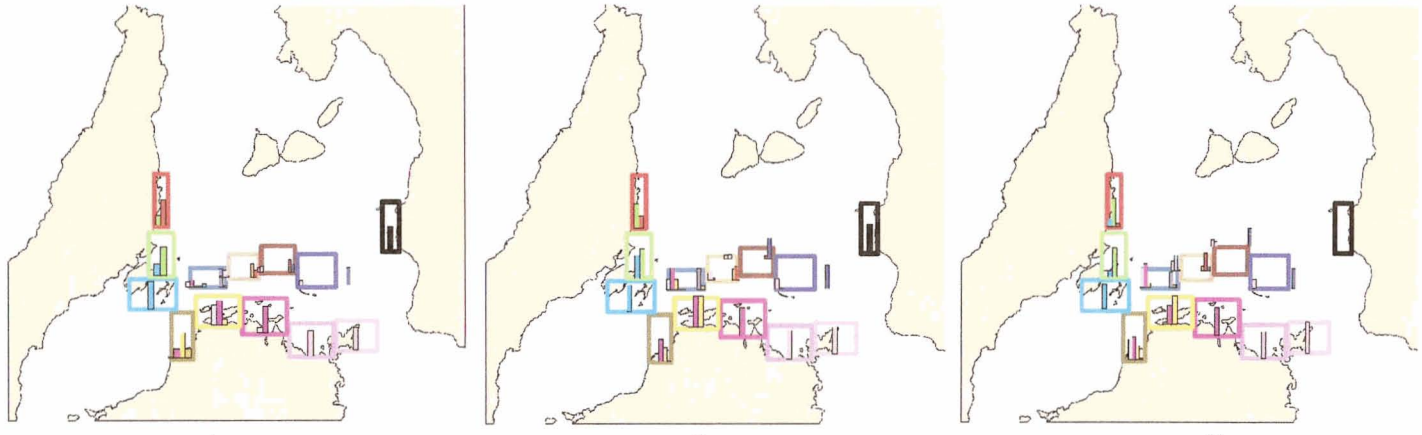

Figure 17. Relative distribution of source areas during January for 10-day (A), 20-day (B) and 30-day (C) dispersal simulations. The colored boxes represent release areas for dispersed particles. Colored bars represent sources of particles that settled at a specific box

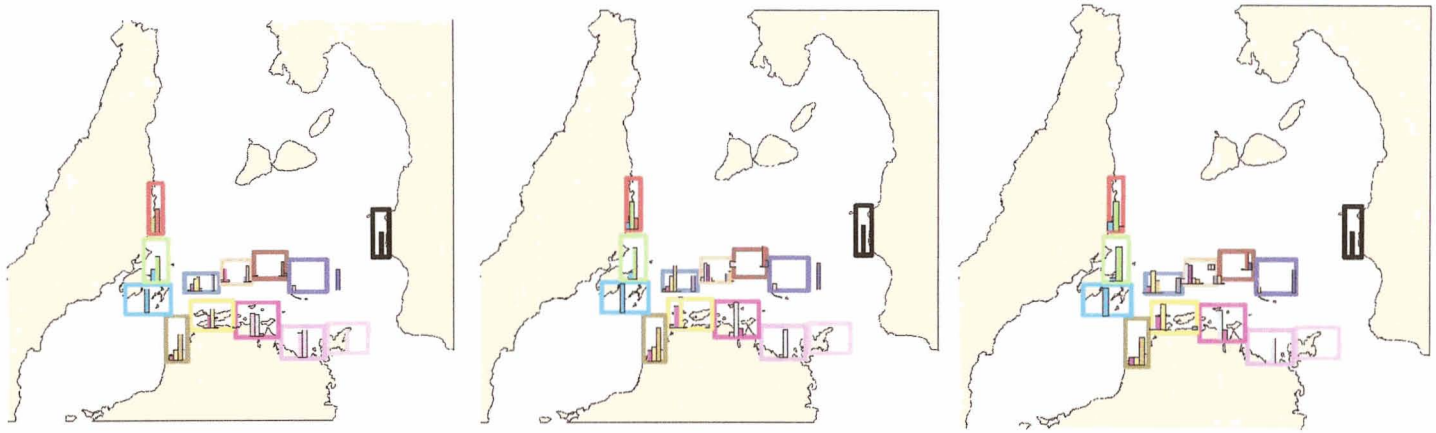

A B C

Figure 18. Relative distribution of source areas during April for 10-day (A), 20-day (B) and 30-day (C) dispersal simulations. The colored boxes represent release areas for dispersed particles. Colored bars represent sources of particles that settled at a specific box

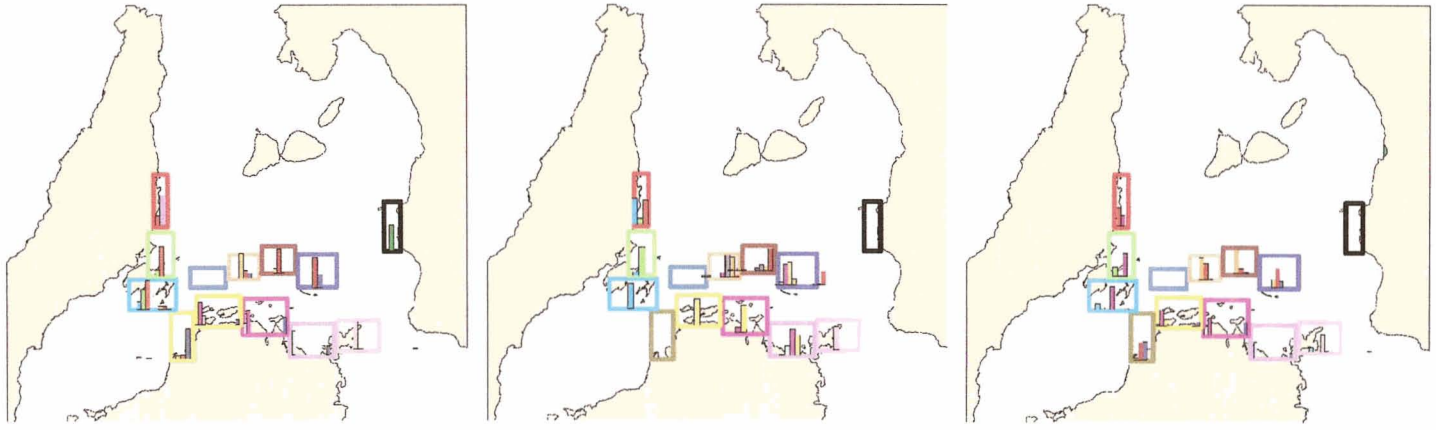

A B C

Figure 19. Relative distribution of source areas during August for 10-day (A), 20-day (B) and 30-day (C) dispersal simulations. The colored boxes represent release areas for dispersed particles. Colored bars represent sources of particles that settled at a specific box

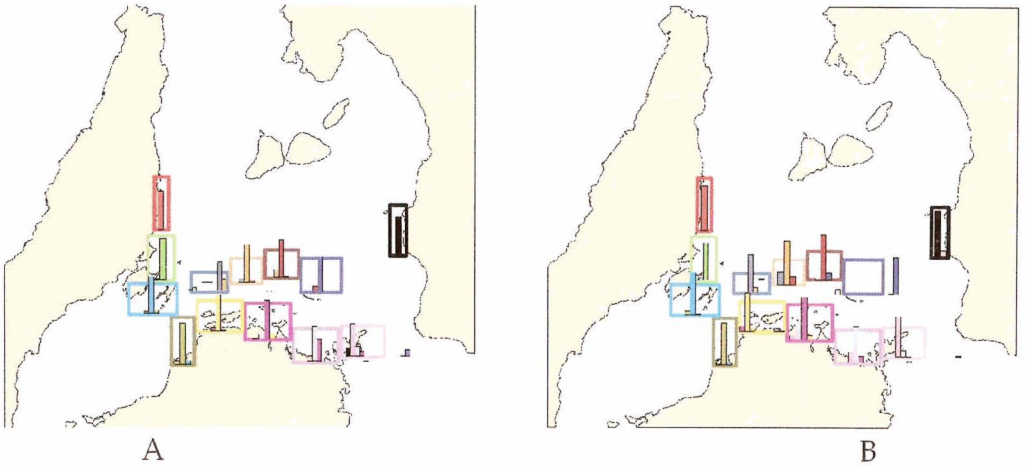

Figure 20. Relative distribution of (A) source and (B) sink areas for 30-day dispersal simulations forced by the tides. The colored boxes represent release areas for dispersed particles.

NUMERICAL SIMULATIONS OF LARVAL DISPERSAL PATTERNS IN CORON BAY

1 INTRODUCTION

Coron Bay is one of the four focal areas of the USAID funded Fisheries Improvements for Sustainable Harvests (FISH) Project. The goal of the project is to improve fish stocks by as much as 10% over a 5-year project. One of the interventions to address this goal is the establishment of fish sanctuaries. Studies (Ward et al., 2001) have suggested that synergistic effects of sanctuary or MPA networks will be more beneficial to the fisheries through larval spillover than just by adult spillover. It is assumed that these networks are established on the basis of larval connectivities and dispersal. The aim of this study is to determine, using numerical models, the potential dispersal patterns of larvae of fish, which may help in selecting locations of future MPAs, and MPA networks.

1.1 Description of Study Site

Unlike other bays in the Philippines, Coron Bay is an embayment sandwiched between two islands, Busuanga and Culion (Figure 1). Hence, it has two connections to the open sea and in the case of Coron Bay, it opens into the Sulu Sea to the southeast and to the South China Sea to the northeast. The narrowest portion of the Bay is towards the northwest and is where Busuanga and Culion Islands are closest to each other. The depth at this northwest passage is only 20m but can probably contribute significantly to the exchange of water in Coron Bay between the South China Sea and Sulu Sea.

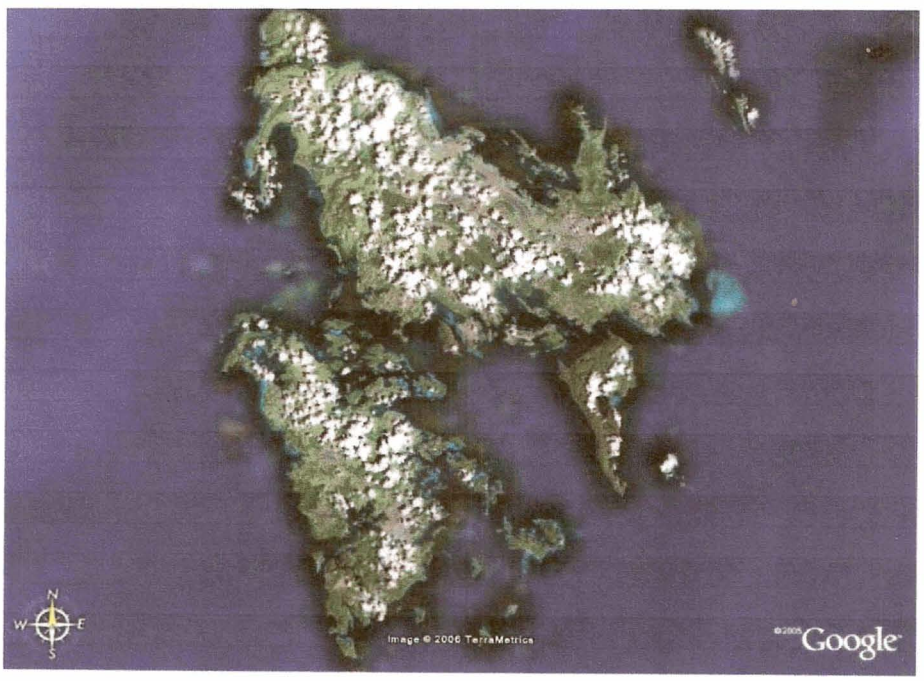

Figure 1 Satellite Map of Culion and Busuanga Island.

Coron Bay is very shallow with depths not exceeding 100m (Figure 2). Beyond the bay mouth, the shelf extends further by about almost 40km before the start of the shelf break. Along the sides of the bay are numerous islands and island passages. The biggest marginal island is Coron Island, which also forms the northeast boundary of the bay.

1.2 Specific Objectives

The objectives of this study are:

- Characterize circulation patterns in Coron Bay in scales relevant to the dispersal of larvae
- Simulate larval dispersal patterns from different areas in Coron Bay and to characterize potential larval exchange between these areas

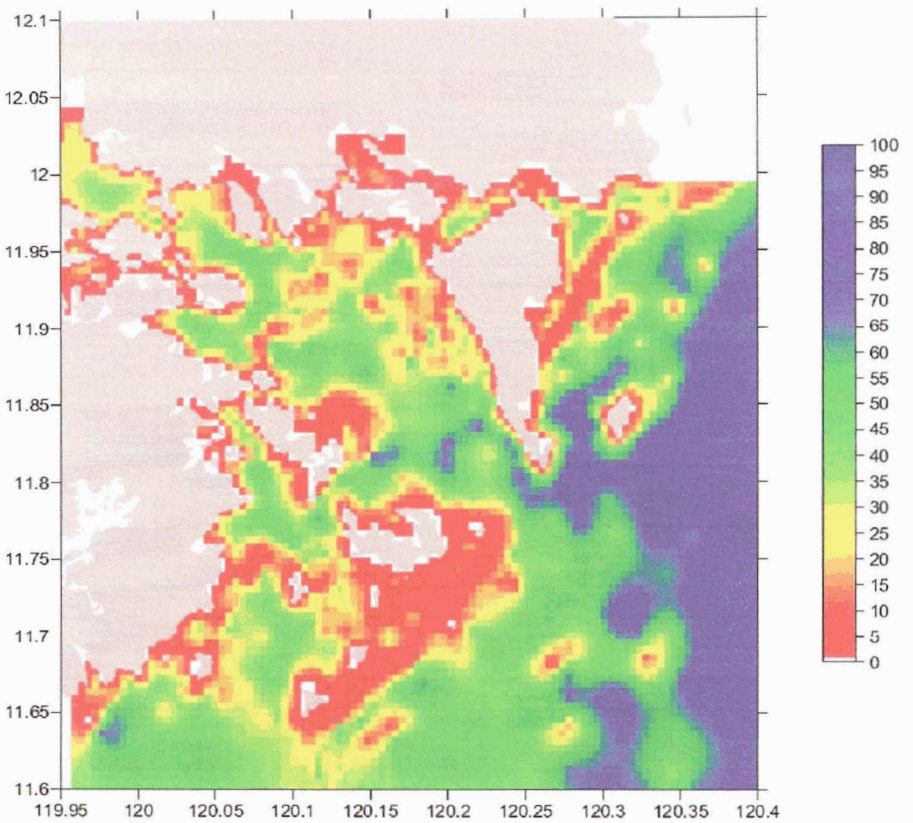

Figure 2 Bathymetry of Coron Bay and vicinity

2 METHODOLOGY

2.1 Field Survey

A field survey was conducted last October 24-26, 2005 to collect baseline information on the distribution of temperature, salinity, chlorophyll and surface currents. The stations occupied during the survey are shown in Figure 3. At each station, the temperature, salinity and chlorophyll profiles were obtained using a Seabird SBE19 CTD with a Turner SCUFA Fluorometer. The surface currents were measured using a 0.5m diameter holey-sock drogue. A handheld GPS in tracking mode was attached

to the drogue and measures the position of the drogue as it drifts with the currents. A handheld anemometer and an electronic compass were used to measure wind speed and direction, respectively.

2.2 Hydrodynamic Modeling

The three-dimensional circulation of the waters in Coron Bay was modeled using the Princeton Ocean Model (Mellor, 2003). This model is a three-dimensional primitive-equation sigma coordinate model and is used in numerous applications ranging from estuarine to global ocean models. The model domain for the Coron Bay model covers the area shown in Figure 2. The model grid resolution is 500m x 500m. The model is forced at the boundaries by the tides and offshore currents and at the surface by the wind. The tidal forcing prescribed at the open boundaries was derived from the Oregon State University Tidal Inversion Software (OTIS) model applied to Philippine waters by Magno (2005). Open ocean currents at the model open boundaries were obtained from the monthly mean barotropic velocities computed by thePacific HYCOM Simulations (http://hycom.rsmas.miami.edu/data/information.html#pacific) . Separate runs were made to represent seasonal circulation patterns. Each run was allowed to run for 30 days of model time for each seasonal boundary forcing. The model is also forced at the surface by winds derived from satellite altimetry (http://manati.orbit.nesdis.noaa.gov/hires/).

The parameters for the simulation experiments conducted for this study are listed in Table 1. Three seasons were considered, northeast monsoon season (January 2003 forcing), southwest monsoon season (August 2003 forcing) and the spring monsoon transition (April 2003 forcing).

Table 1 Summary of hydrodynamic simulations

Run No	Tides	HYCOM Boundary forcing	Winds
1	√	x	x
2	x	√ August 2003 data	x
3	x	√ August 2003 data	√
4	x	√ April 2003 data	x
5	x	√ April 2003 data	√
6	x	√ January 2003 data	x
7	x	√ January 2003 data	√

2.3 Lagrangian dispersal model

The dispersal model is adapted from the model of Polovina et al. (1999). In this model, the larvae are represented as neutrally buoyant passive particles and their position over time are tracked using the following equations:

$$x_{t+\Delta t} = x_t + \left(u_{x,y,t}\Delta t + \varepsilon\sqrt{D\Delta t}\right)$$
$$y_{t+\Delta t} = y_t + \left(v_{x,y,t}\Delta t + \varepsilon\sqrt{D\Delta t}\right) \quad (1)$$

where x and y are the coordinates of a particle; u and v are the advection velocities from the hydrodynamic model, Δt is the integration time step, ε is a randomly generated number ranging from -1 to 1, and D is the eddy diffusion rate (m^2s^{-1}). Each particle when released has attributes, which identifies it individually from the other particles. These attributes include age from release, location of release, date and time of release. These attributes will enable us to estimate the degree of exchange of simulated particles between areas based on the method used by Sauers et al. (2003) in analyzing drifter card data.

To determine the exchange between areas, several areas were designated as source and sink areas around the Bay. The sizes and locations of these areas, shown in Figure 3, vary in size and were chosen to represent different areas all aound the Bay as closely as possible. The dispersal model was used to simulate the dispersal of particles released from these boxes. Separate runs were used for dispersal periods of 10, 20 and 30 days duration to represent short, medium, and long-range dispersal. After each of these simulations, the location of the particles and where they were released were noted and used in the analysis.

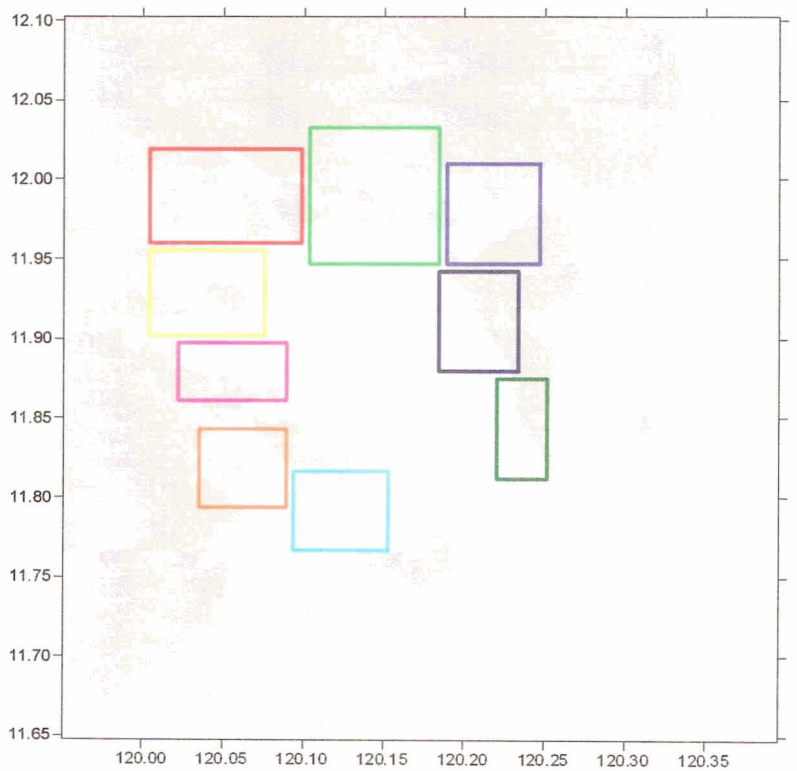

Figure 3 Areas used for dispersal simulation as larval source or sink areas.

3 Results and Discussion

3.1 Field Survey

Prevailing winds during the field survey were from the west (Figure 4). It was apparent that the opening to the west between Busuanga and Culion Island was funneling winds from the South China Sea. The strongest winds were measured on October 25 at the northern part of Coron Bay. The maximum wind speed was around

13 knots. When the other parts of the bay were surveyed, wind speeds were significantly lower. While the wind speed was generally weaker, the general direction of the wind remained the same.

Additionally, tides during the survey period were flooding in the morning and ebbing in the afternoon (Table 2 ***Predicted tides for the survey period from October 24-26, 2005 (source: NAMRIA, 2005)***). The tides were mainly diurnal and is characteristic of the tides in the South China Sea (Magno, 2005)

Table 2 Predicted tides for the survey period from October 24-26, 2005 (source: NAMRIA, 2005)

Date	Time	Height
24	0108	1.16
	1109	0.00
25	0202	1.10
	1227	0.02
26	0313	1.03
	1322	0.05

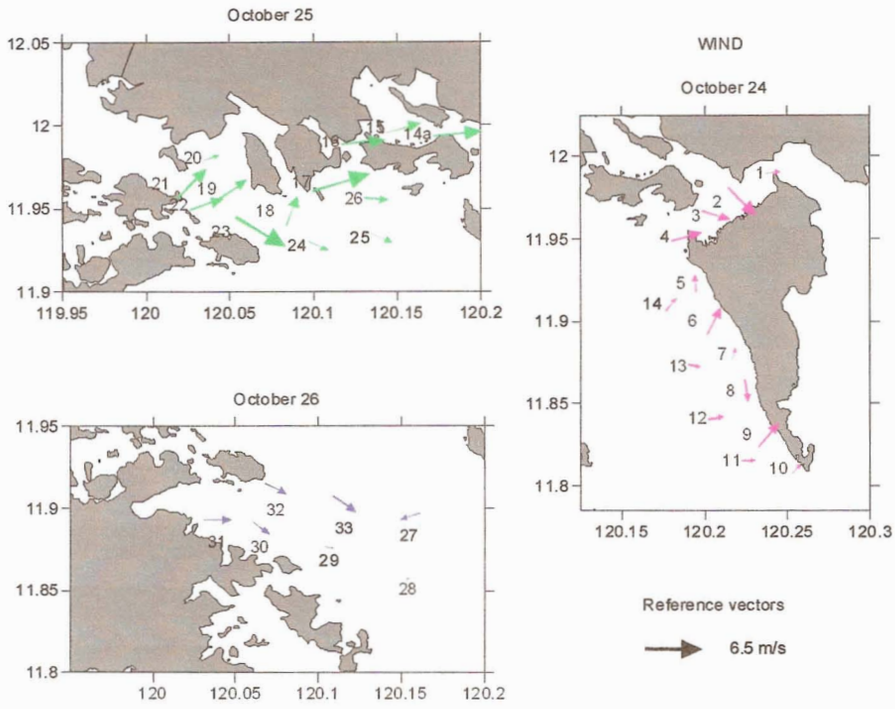

Figure 4 Measured surface winds during the field survey period

The surface current measurements conducted during the field survey are shown in Figure 5. Despite the strong eastward winds in the northern part of Coron Bay, the surface currents were flowing mostly towards the west. This suggests that wind forcing along the narrow channels on the northwestern part may not be significant because of the limited fetch afforded by the numerous islands along the channel. The same direction was observed on the eastern part of the bay (off Coron and along the western coast of Coron Island) but current magnitudes are much weaker. The weak correlation of the surface currents with the wind during the survey suggests that surface circulation is dominated more by the flow between the Busuanga and Culion

Islands be it the tides or exchange between the South China Sea and the Sulu Sea. This is probably one of the unique characteristics of Coron Bay because it is open to the open ocean on opposite ends of the Bay and results in relatively faster flushing compared to typical bays where the only connection to the open sea is through the bay mouth.

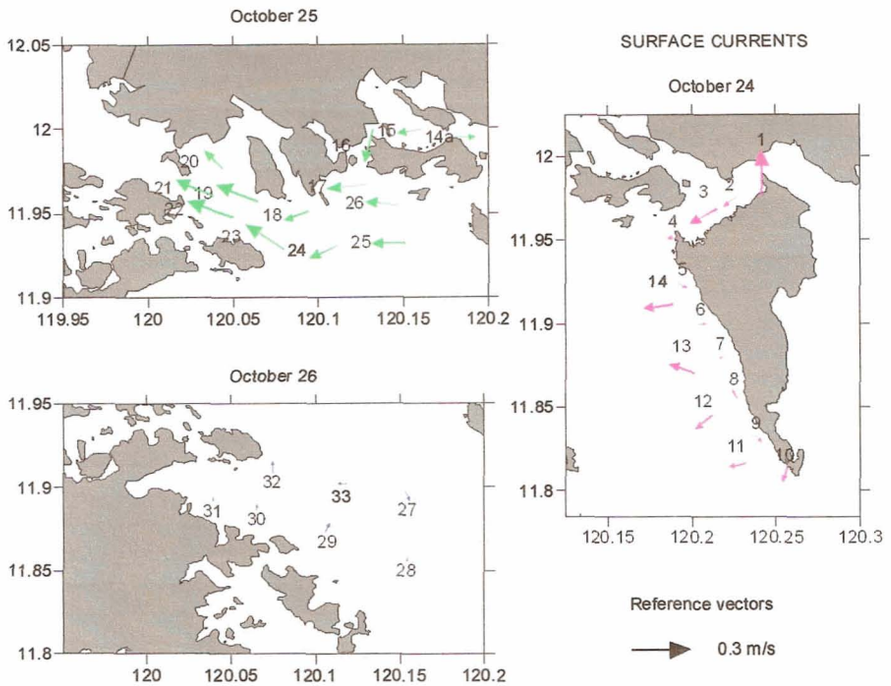

Figure 5. Measured surface current measurements from surface drogues.

3.2 Hydrodynamic Model Results

The general tidal circulation in Coron Bay generated by the model is dominated by the diurnal tides (*Figure 6*). During flood, the tide enters from the Sulu Sea and exits at Tampel Pass (Pass between Bulalacao and Tampel Islands on the southwestern part of Coron Bay. During ebb, the flow is reversed (Figure 7). The maximum currents are found at Tampel Pass and this pass plays a significant role in the circulation of the Bay as it acts like the third passage (aside from the Coron Bay mouth and the northwest opening into the South China Sea) where exchange with Coron Bay waters and the open ocean occur.

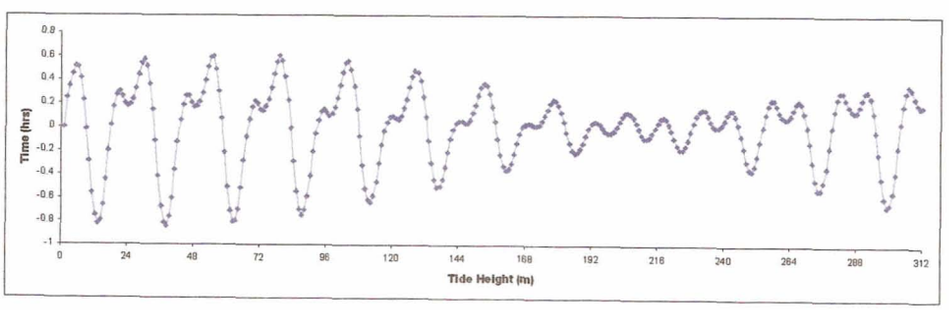

Figure 6. Tidal curves in Coron Bay

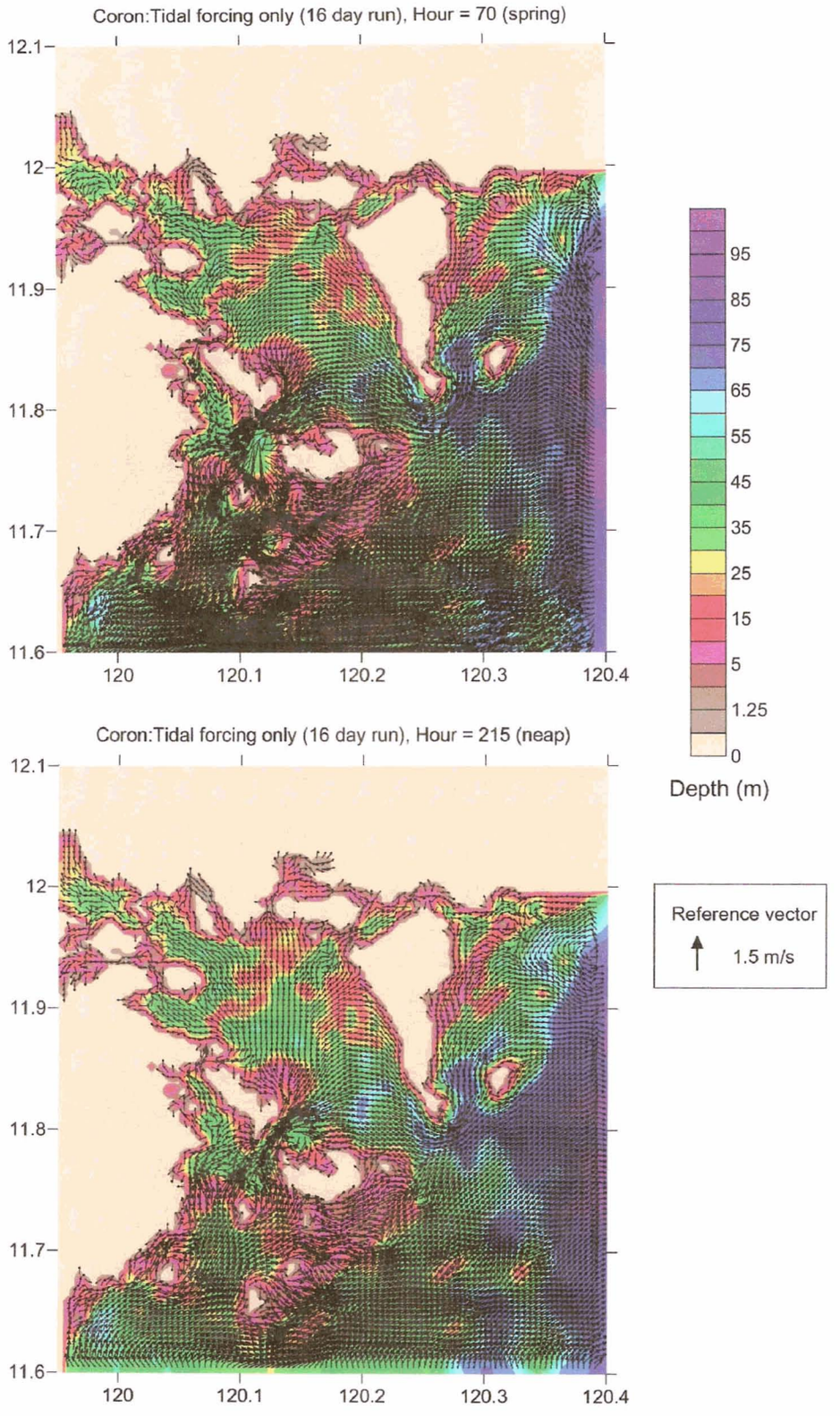

Figure 7. Tidal circulation patterns in Coron Bay

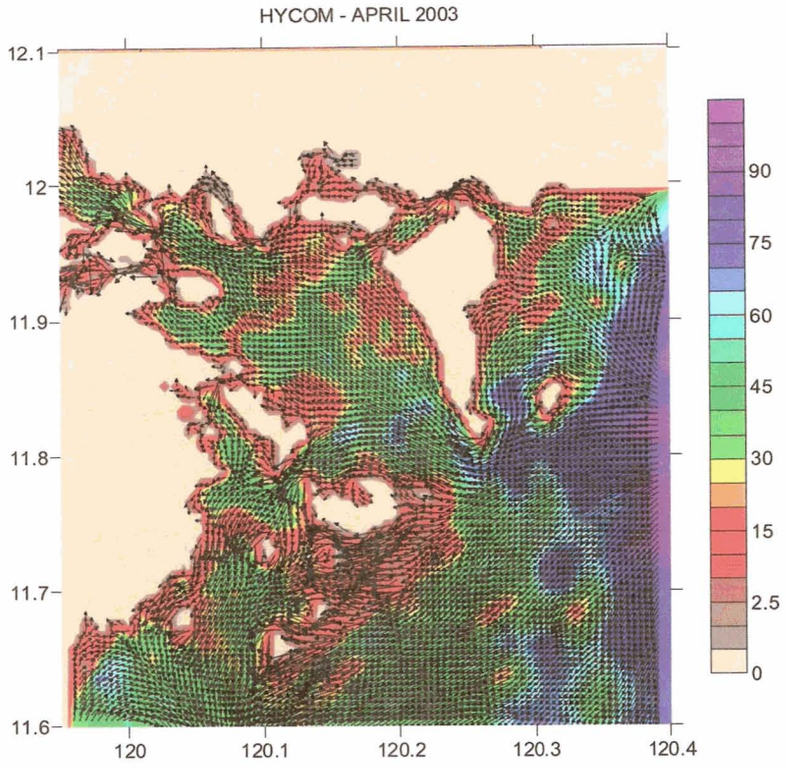

Figure 8 . Coron Bay circulation driven by April 2003 Pacific HYCOM Currents at the open boundaries.

The modeled circulation for Coron Bay for April conditions is shown in Figure 8. Offshore of Coron Bay, flow is predominantly southward but easterly winds during this season may also push water into Coron Bay. Water leaves Coron Bay through Tampel Pass to the west and the narrow passage between Culion and Busuanga Island to the northeast. The velocities between these two passes may be considerable. Strong westward flow can also be observed in the passages between Busuanga and Coron Island, Uson Island and the other small islands to the west. During August, flow off the mouth of Coron Bay is towards the north (Figure 9). Inside Coron Bay, the net flow is towards the mouth (i.e. southeastwards). In Tampel Pass, water flows northward merging with the outgoing flow from inside Coron Bay and exiting at the mouth. This outgoing flow turns around to the north at the tip of Coron Island. The January circulation pattern (Figure 10) also shows the major features of the flow in Coron Bay. A strong current flows into Coron Bay entering around the tip of Coron Island and exits to the southwest along Tampel Pass. This flow between the Bay mouth, Tampel Pass and the northwest passage appears to form the major current system within Coron Bay.

3.3 Larval Dispersal Patterns

The larval dispersal patterns from each of the boxes in Figure 3 were simulated by the Lagrangian dispersal model using surface current patterns derived from the April, August and January hydrodynamic model runs, as well as for surface current patterns due to tidal forcing. For the seasonal runs, the dispersal simulations were

conducted for 10, 20 and 30 day periods. The tidal dispersal was conducted for 15 days to represent a spring-neap cycle. Examples of the results of the dispersal simulations are shown in Figure 11 and Figure 12. At release, particles were uniformly distributed within the source box and were advected by surface currents and diffused randomly using a prescribed diffusion coefficient. Particles of the same color represent particles released instantaneously at the same time. Different colors represent the different positions of the particles after release.

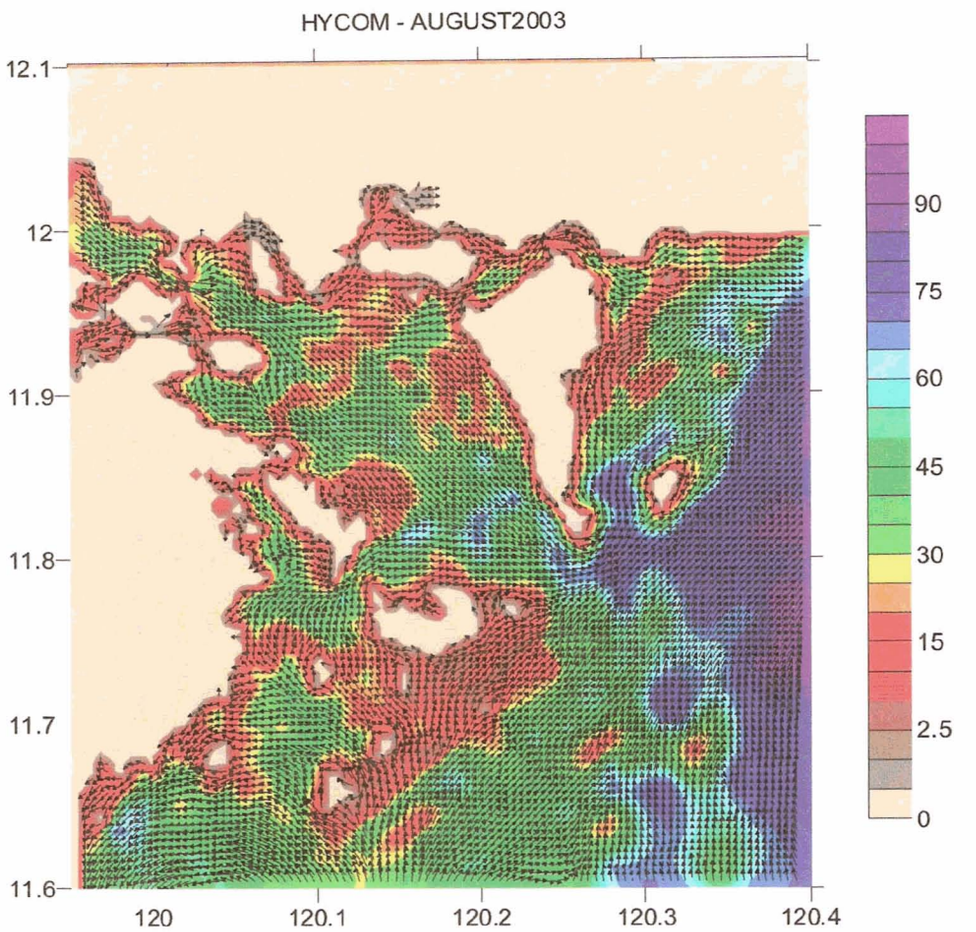

Figure 9. Coron Bay circulation driven by August 2003 Pacific HYCOM Currents at the open boundaries.

To determine the magnitude of potential larval exchange between predefined areas clearly, the sources of particles settling in a particular box were plotted for different conditions/seasons (Figure 14). The bars within each colored box represent the sources of particles found within each box at the end of the dispersal period. For instance, if the blue box contains both blue and green bars, this indicates that particles settling within the boundaries of the blue box originated from both the blue and green boxes. The relative sizes of the colored bars represent the relative number of particles from the different sources. Thus a box containing a lot of colored bars indicates that it is potentially a good larval sink area.

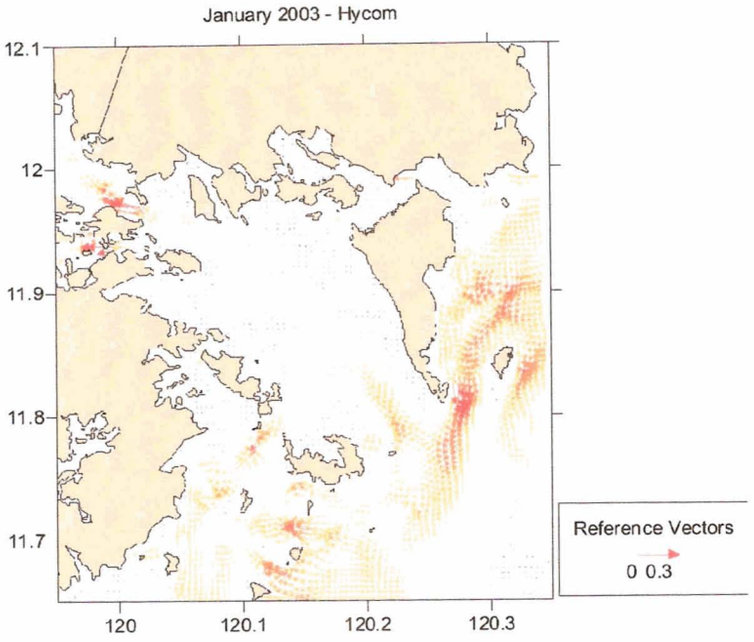

Figure 10. Coron Bay circulation driven by January 2003 Pacific HYCOM Currents at the open boundaries.

Conversely, a similar plot is shown in Figure 15 but considers the sink areas. The colored bars within a box represent which boxes the particles released from a particular box ended up after the simulation period. Thus a box with numerous colored bars mean that particles released from this box ended up in several neighboring boxes and this may mean that this box may be a good larval source area, dispersal wise.

Examination of Figure 14 and Figure *15* suggests three major clusters in terms of potential connectivity. The first cluster includes the northern stretch of Coron Bay extending from Coron Town westwards towards the eastern opening of Coron Bay. This area contains several islands and island passages and dispersal simulations suggest considerable exchange between these areas (e.g. areas defined by the blue, green and red square in Figure 14. The next cluster is the western and southern coasts of Coron Island where particles from both boxes ended up within these two boxes. Particles which ended up in areas outside any of these boxes were not considered in the analysis and it should be noted that at times, the number of particles ending up within any of the boxes represent only a portion of the total number of particles released. The third cluster is the area covered by the yellow and pink boxes. The area off Culion Town (orange box) is fairly isolated and particles settling within the orange box are mostly particles released locally.

The dispersal patterns from the tidal circulation are consistent with the above clusters (Figure 13). The main differences are that particles released in the vicinity of Tampel Pass were dispersed northward covering the entire bay and the particles released west and south of Coron Island were dispersed around the island. Basically, dispersal distances for tide forced circulation are more widespread within the bay.

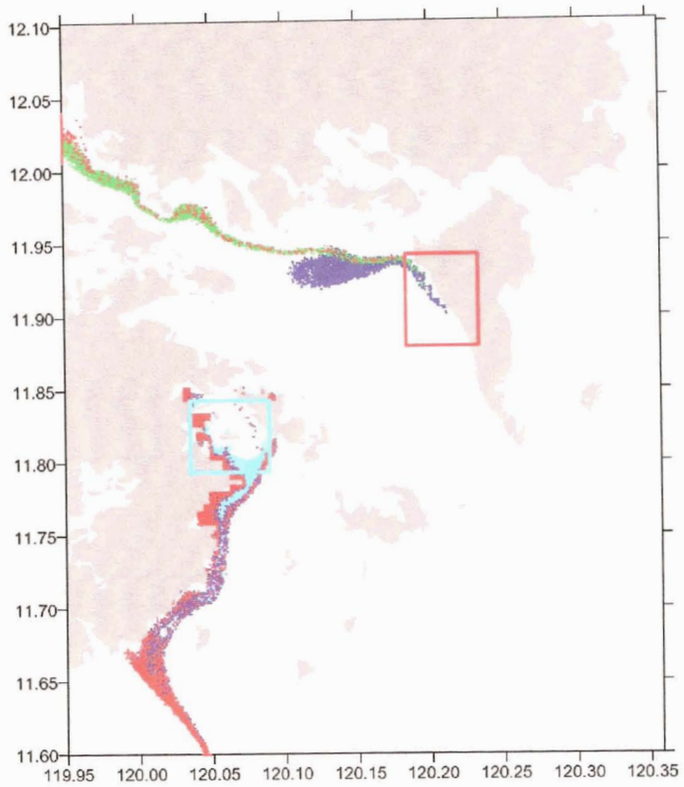

Figure 11 Dispersal of particles from areas marked by the red and blue boxes during April.

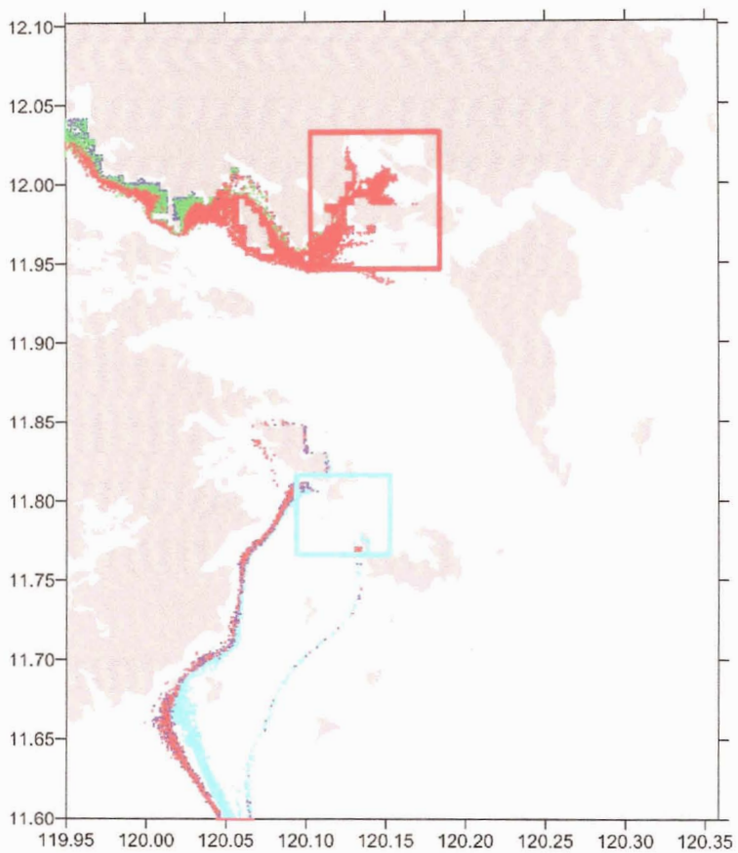

Figure 12. Dispersal of particles from areas marked by the red and blue boxes during April.

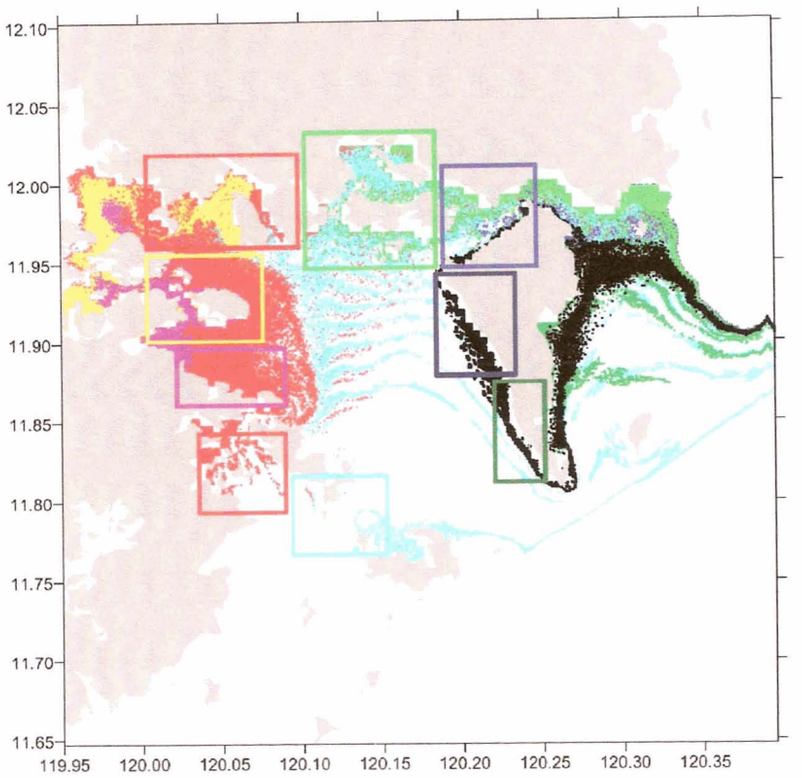

Figure 13. Particle dispersal from areas enclosed in boxes. Particles from particular boxes identified by same color.

4 SUMMARY AND CONCLUSIONS

The circulation of Coron Bay is highly influenced by the opening to the South China Sea to the west of the Bay. Unlike other Bays, Coron Bay is unique because it is open at both ends although the western opening is shallower and narrower. This result in a significant exchange between these two openings resulting in a Bay, which is more highly flushed, compared to bays with only one open ocean connection. The results show seasonal reversal of the flows and the main flow paths are between the Bay mouth near the tip of Coron Island, the channel in the northwest where the Culion and Busuanga Islands are closest and the pass between the Tampel and Bulalacao Islands called the Tampel Pass. The presence of this along bay flow (mouth to northwest channel) limits exchange between the northern and southern coasts of the bay and connectivities as inferred from larval dispersal simulations may be stronger in the alongshore direction rather than across the Bay. Three clusters were identified and include the northern coast of the Bay as the first cluster, the southern coast as the second cluster and Coron Island (particularly the western and southern coast) as the third. The effect of the tides is consistent with the seasonal patterns in terms of dispersal except the more wide spread dispersal of particles released in the vicinity of Tampel Pass.

5 REFERENCES

Magno MM, 2005. Estimation of entrainment potential in Philippine Coastal Waters: The physical consequence of island wakes and eddies. MSc Thesis. College of Science, University of the Philippines, Diliman, Quezon City.

Mellor, G. L., 2003. Users guide for a three-dimensional, primitive equation, numerical ocean model (June 2003 version), 53 pp., Prog. in Atmos. and Ocean. Sci, Princeton University.

NAMRIA, 2005. Tide and Current Tables Philippines 2005. The Coast and Geodetic Survey Department, National Mapping and Resource Information Authority. Department of Environment and Natural Resources.

Polovina JJ, Kleiber P, Kobayashi DR. 1999. Application of TOPEX-POSEIDON satellite altimetry to simulate transport dynamics of larvae of spiny lobster, *Panulirus marginatus*, in the northeastern Hawaiian Islands, 1993-1996. Fish. Buyll. 97:132-143.

Sauers KA, Klinger T, Coomes C, Ebbesmeyer CC. 2003. Synthesis of 41,300 Drift Cards Released in Juan de Fuca Strait (1975-2002). Proceedings of the 2003 Georgia Basin/Puget Sound Research Conference. http://www.psat.wa.gov/Publications/01_proceedings/sessions/oral/7c_sauer.pdf

Figure 14 Source areas and relative amounts of dispersed particles settling in each of the areas marked by the colored boxes. Colored bars within each box represent where the sources of the particles that settled in a particular box. Top row represents April dispersal, middle rowfor August dispersal and the last row for Jan Dispersal. First column is the 10 day dispersal, 2nd column for 20 day dispersal and the third column for 30 day

Figure 15. Sink areas and relative amounts of particles dispersed from each of the area marked by the colored boxes. Colored bars within each box represent where the particles released from a source box ended up.

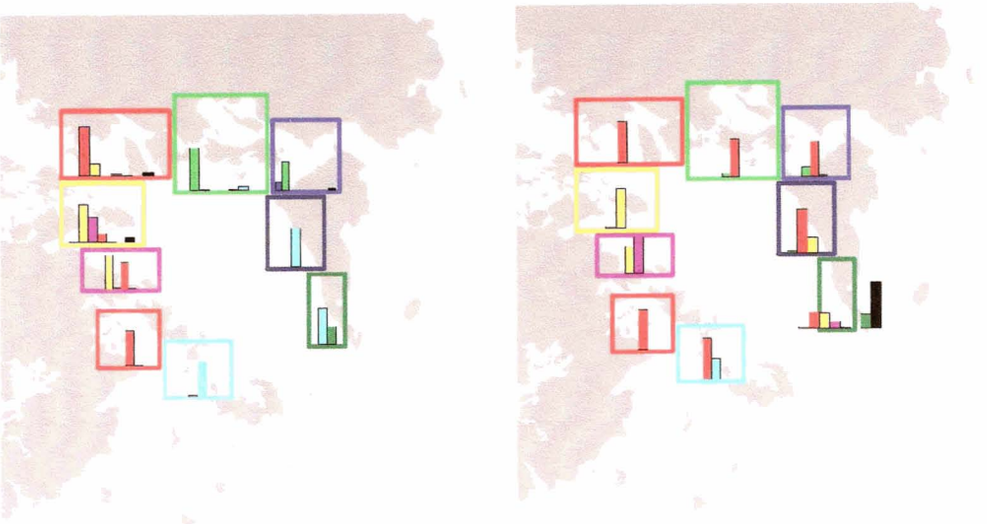

Figure 16. *Same as in Figure 14 and 15 but for dispersal driven by the tidal circulation. Left panel is for particle sources and right panel for particle sinks*

NUMERICAL SIMULATIONS OF LARVAL DISPERSAL PATTERNS IN SURIGAO DEL SUR

1 INTRODUCTION

Surigao Del Sur is one of the four focal sites of the USAID funded Fisheries Improvements for Sustainable Harvests (FISH) Project. The goal of the project is to improve fish stocks by as much as 10% over a 5-year project. One of the interventions to address this goal is the establishment of fish sanctuaries. Studies (Ward et al., 2001) have suggested that synergistic effects of sanctuary or MPA networks will be more beneficial to the fisheries through larval spillover than just by adult spillover. It is assumed that these networks are established on the basis of larval connectivities and dispersal. The aim of this study is to determine, using numerical models, the potential dispersal patterns of larvae of fish, which may help in selecting locations of future MPAs, and MPA networks.

1.1 Description of Study Site

The study site is composed of two embayments, namely Carrascal Bay and Lanuza Bay that are both characterized by relatively extensive reefs, particularly along their northwest margins. These bays are geographically located in the northeastern coast of Surigao del Sur, directly facing the Pacific (

Figure 1). Carrascal Bay is separated from Lanuza Bay by a headland and is surrounded by several small islands that make its coastline morphology highly complex. Such complex configurations are important factors in the development of features in the circulation of the area that can influence dispersal patterns of larvae (e.g., may increase dispersal or enhance entrainment/retention of larvae from source). It is for this reason that physical circulation patterns are deemed important in selecting sites for the establishment of fish sanctuaries and protected area networks.

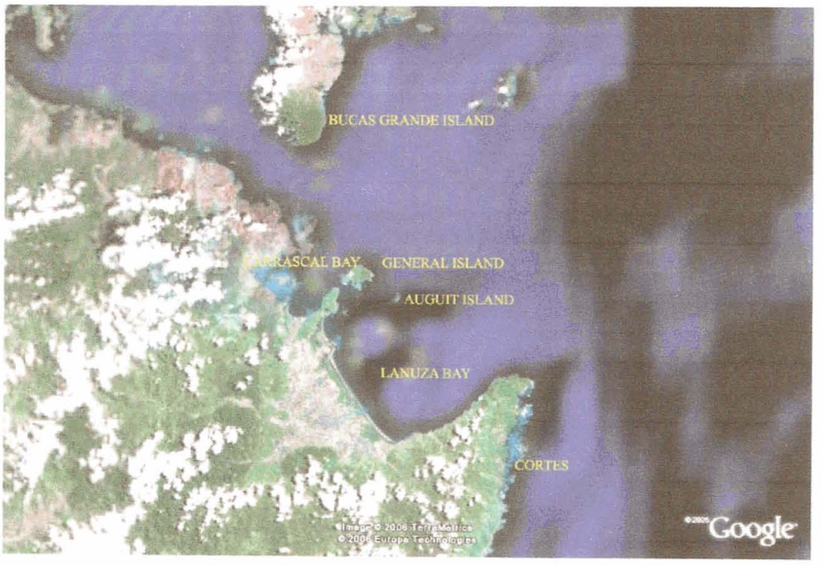

Figure 1. Map showing study area.

In terms of bathymetry, Carascal and Lanuza bays are very shallow with depths not exceeding 100m (Figure 2). The shelf is narrowest at the eastern side of the Lanuza Bay mouth near the municipality of Cortez. The shelf facing Carrascal bay extends for more than 20km beyond the bay mouth. Northwest of Carrascal Bay is a narrow passage between the mainland and Bucas Grande Island and a shallow 20m sill. The limited opening to the area northwest of Carrascal Bay suggests limited exchange with the waters there.

1.2 Specific Objectives

The objectives of this study are:

- Characterize circulation patterns in Carascal and Lanuza Bays in scales relevant to the dispersal of larvae
- Simulate larval dispersal patterns from different areas in Carascal and Lanuza Bays and to characterize potential larval exchange between these areas

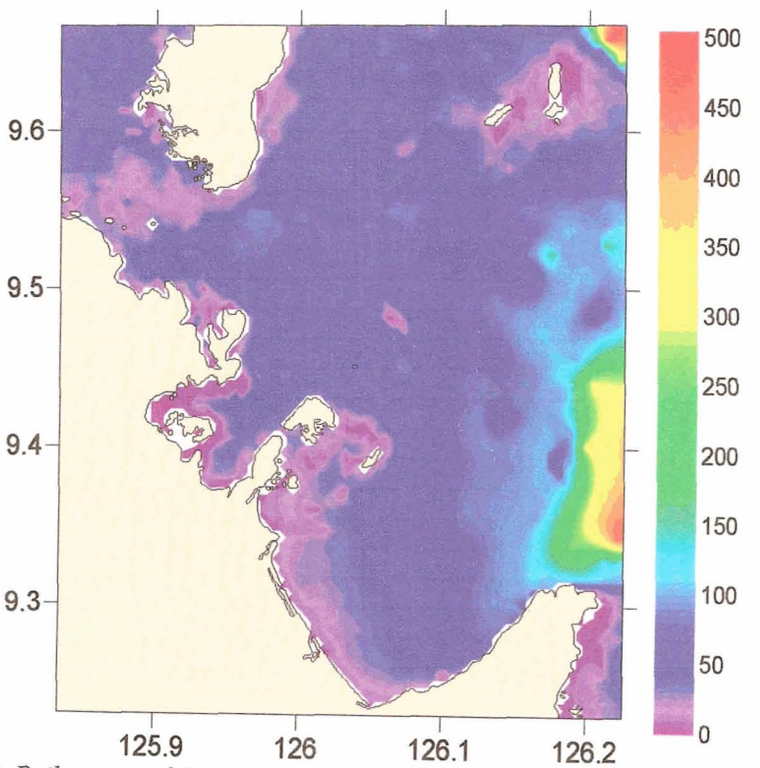

Figure 2. Bathymetry of Carascal and Lanuza Bays and vicinity. Contours in meters.

2 METHODOLOGY

2.1 Field Survey

A field survey was conducted last August 14-18, 2005 to collect baseline information on the distribution of temperature, salinity, chlorophyll and surface currents. The stations occupied during the survey are shown in Figure 3. At each station, the

temperature, salinity and chlorophyll profiles were obtained using a Seabird SBE19 CTD with a Turner SCUFA Fluorometer. The surface currents were measured using a 0.5m diameter holey-sock drogue. A handheld GPS in tracking mode was attached to the drogue and measures the position of the drogue as it drifts with the currents. A handheld anemometer and an electronic compass were used to measure wind speed and direction, respectively.

2.2 Hydrodynamic Modeling

The three-dimensional circulation of the waters in Surigao del Sur was modeled using the Princeton Ocean Model (Mellor, 2003). This model is a three-dimensional primitive-equation sigma coordinate model and is used in numerous applications ranging from estuarine to global ocean models. The model domain for Surigao del Sur model covers the area shown in Figure 2. The model grid resolution is 500m x 500m. At the boundaries, the model is forced by the tides and offshore currents and at the surface by the wind. The tidal forcing prescribed at the open boundaries was derived from the Oregon State University Tidal Inversion Software (OTIS) model applied to Philippine waters by Magno (2005). Open ocean currents at the model open boundaries were obtained from the monthly mean barotropic velocities computed by the Pacific HYCOM Simulations (http://hycom.rsmas.miami.edu/data/information.html#pacific). Separate runs were made to represent seasonal circulation patterns. Each run was allowed to run for 30 days of model time for each seasonal boundary forcing. The model is also forced at the surface by winds derived from satellite altimetry (http://manati.orbit.nesdis.noaa.gov/hires/).

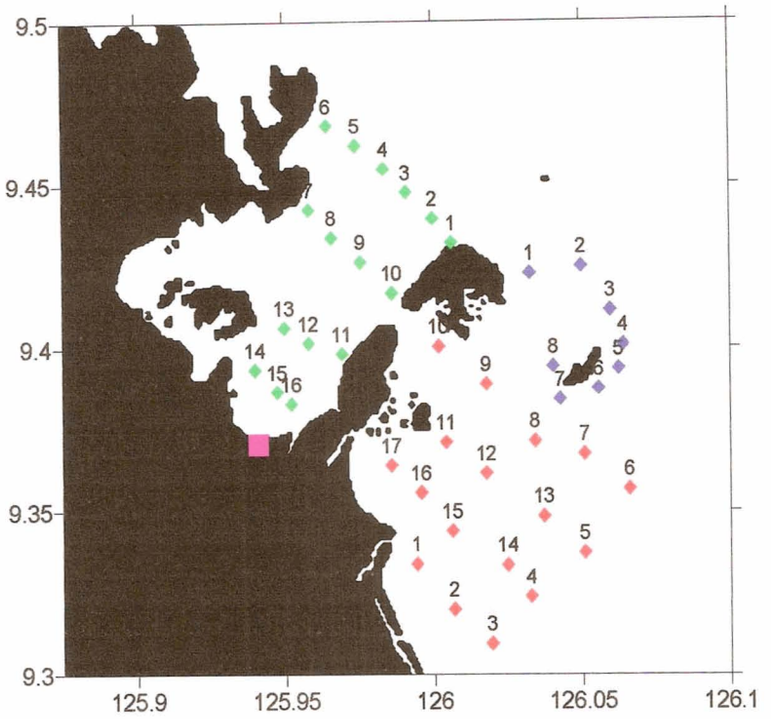

Figure 3. Map showing the location of stations occupied during the field survey (diamonds) and the location where the winds were continuously measured for three days (square). Color of the diamonds denotes different sampling days.

The parameters for the simulation experiments conducted for this study are listed in Table 1. Three seasons were considered, northeast monsoon season (January 2003 forcing), southwest monsoon season (August 2003 forcing) and the spring monsoon transition (April 2003 forcing).

Table 1. Summary of hydrodynamic simulations

Run No	Tides	HYCOM Boundary forcing	Winds
1	√		
2		√ August 2003 data	
3		√ August 2003 data	√
4		√ April 2003 data	
5		√ April 2003 data	√
6		√ January 2003 data	
7		√ January 2003 data	√

2.3 Lagrangian dispersal model

The dispersal model is adapted from the model of Polovina et al. (1999). In this model, the larvae are represented as neutrally buoyant passive particles and their position over time is tracked using the following equations:

$$x_{t+\Delta t} = x_t + \left(u_{x,y,t}\Delta t + \varepsilon\sqrt{D\Delta t}\right)$$
$$y_{t+\Delta t} = y_t + \left(v_{x,y,t}\Delta t + \varepsilon\sqrt{D\Delta t}\right) \quad (1)$$

where x and y are the coordinates of a particle; u and v are the advection velocities from the hydrodynamic model, Δt is the integration time step, ε is a randomly generated number ranging from -1 to 1, and D is the eddy diffusion rate (m^2s^{-1}). Each particle when released has attributes, which identifies it individually from the other particles. These attributes include age from release, location of release, date and time of release. These attributes will enable us to estimate the degree of exchange of simulated particles between areas based on the method used by Sauers et al. (2003) in analyzing drifter card data.

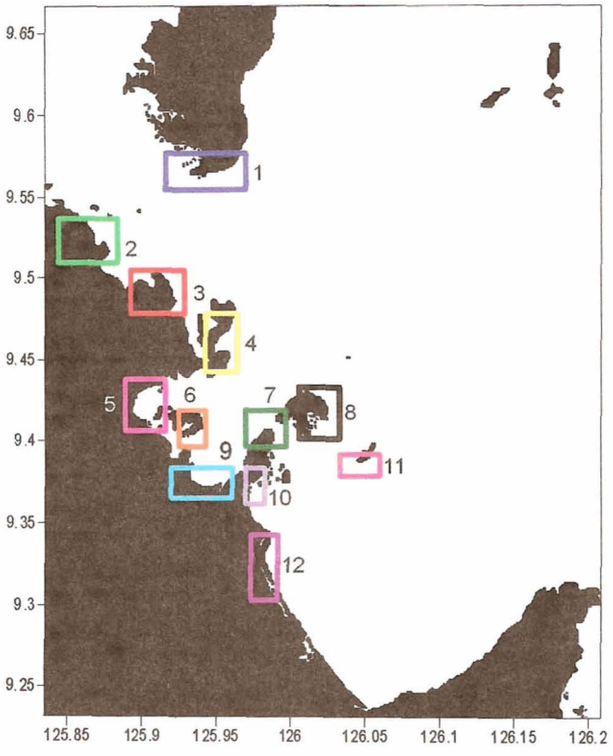

Figure 4. Areas used for dispersal simulation as larval source or sink areas.

To determine the exchange between areas, several areas were designated as source and sink areas around the two bays. The sizes and locations of these areas, shown in Figure 4, vary in size and were chosen to represent different areas all around Carascal and Lanuza Bays as closely as possible. The dispersal model was used to simulate the dispersal of particles released from these boxes. Separate runs were used for dispersal periods of 10, 20 and 30 days duration to represent short, medium, and long-range dispersal. Dispersal simulations based on the tidal component of the circulation was also conducted. After each of these simulations, the location of the particles and where they were released were noted and used in the analysis.

3 RESULTS AND DISCUSSION

3.1 Field Survey

It is important to note that the field survey was designed to provide initial insights into prevailing hydrodynamic conditions in the study site during the duration of the survey. It does not provide information on how such conditions vary during different seasons or time of the year describes the conditions prevailing. The comparison of field data with model results is at best qualitative because resolving variability at different temporal and spatial scales requires much more observations which can not be acquired due to limited resources. Nevertheless, it is interesting to note that the observed velocities were generally consistent with model simulations. This will be described in greater detail in the succeeding paragraphs.

Despite the being the peak of the Southwest Monsoon, prevailing winds during the field survey were from the northeast (Figure 5). The strongest winds were measured on the noon of August 15 where maximum wind speed was around 16 knots. However, winds were very weak (<0.5ms^{-1}) more than 50% of the time, mainly during the evening and early morning. As such, the measurements were conducted with very weak winds except in the inner part of Carrascal Bay and most of the measurements most likely reflect the circulation forced by the tides and offshore currents.

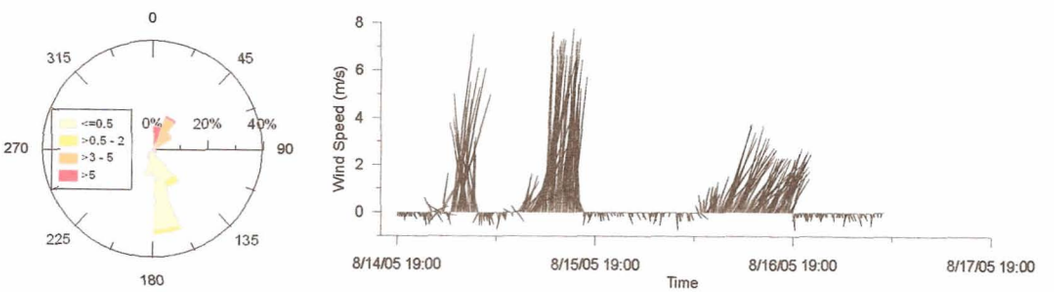

Figure 5. Measured wind velocities during the field survey period at a stationary location along the coast of Carascal Bay

The tides during the survey period were mainly diurnal with flooding in the morning and ebbing in the afternoon (Table 2). Since the tide phases for the three day survey were similar, the measurements can be combined to produce a composite picture of the surface circulation in Carrascal and the western part of Lanuza Bay.

Table 2. Predicted tides for the survey period from August 15-17, 2005 (source: NAMRIA, 2005)

Date	Time	Height
15	0412	1.12
	1527	0.13
16	0531	1.17
	1639	-0.05
17	0718	1.26
	1723	-0.18

Temperature/Salinity and chlorophyll

The surface current measurements conducted during the field survey are shown in Figure 6. At the mouth of Carrascal Bay, surface currents were flowing into the Bay and exiting through the chennel southwest of General Island. In the interior of the Bay, strong currents were observed flowing landward. When these stations were sampled, a squall was approaching Carrascal with very strong winds from the northeast resulting in very strong southwestward currents in the inner part of the Bay.

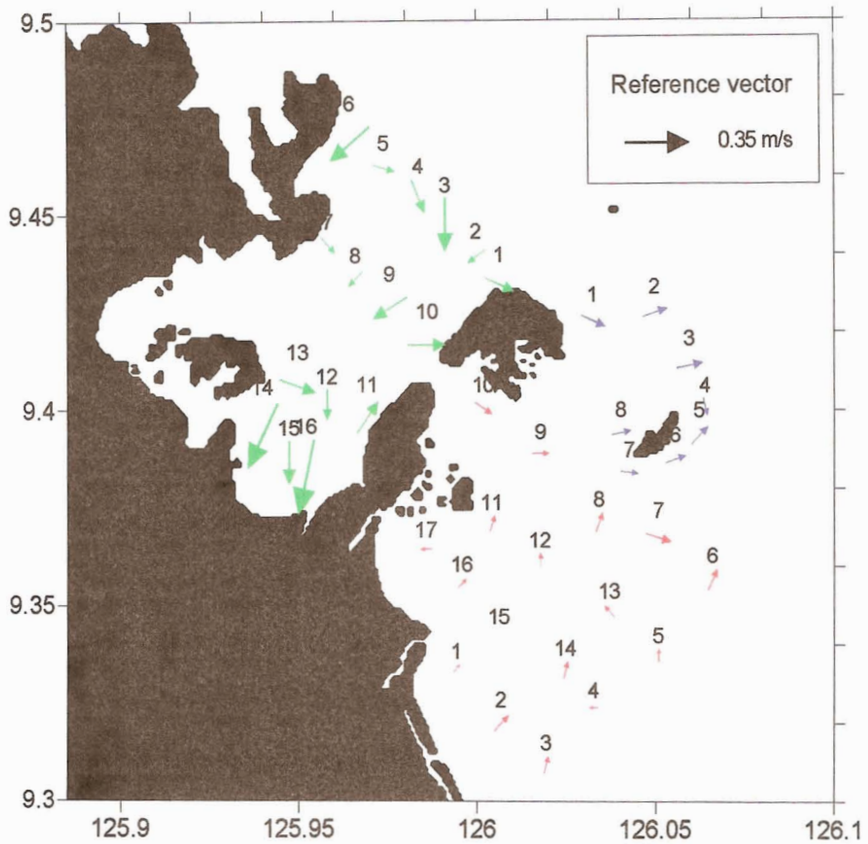

Figure 6. Measured surface currents from surface drogue. Colors of arrow denote different sampling days.

3.2 Hydrodynamic Model Results

The hycom-forced current patterns are very similar for the different seasons considered (Figure 7). The only noticeable difference is the direction of the currents in the channel between the mainland and Bucas Grande Island on the northeast corner of the model domain. Within this area, the flow is towards the south during January and April but reverses during August. The presence of the shallow sill between Bucas Grande Island and the mainland limits the volume of water flowing through this passage.

For the rest of the area, the flow is predominantly along the coast towards the southeast. The strongest currents are found along the passage between General Island and the mainland. Currents are also stronger in the shallow areas of western Lanuza Bay and along the coast of Cortes.

The results from the hydrodynamic model are qualitatively similar to that observed during April. The dominance of the southward flow is evident. Strong velocities are also found on the northwestern side of Lanuza Bay between General Island and Auguit Island and are most likely associated with the shallow ridge connecting these two islands. The bathymetry and coastline configuration is much more complex in this area compared to the other side of Lanuza Bay. The strongest velocities are found in the channel between General Island and the mainland. It is also through this channel where most of the outflow from Carrascal Bay occurs. Most of the time, the southeastern coast of General Island forms the leeward side of the island. It is interesting to note that the headlands of Carrascal/Cantillan and Cortes show more complex coastlines and more extensive reef areas on the southeastern sides or leeward side of these promontories. This feature together with the fact that the southern coast contains several embayments and promontories may make it ideal as a larval settlement area. Looking at the Carrascal and Lanuza Bay in more detail, inflow into these bays are concentrated on the northwestern boundaries as is expected if the dominant flow off the mouth of the bay is towards the southeast.

The other interesting area but is outside the focal area is the cape between the Municipalities of Lanuza and Cortes. The southeastward flowing currents as it moves around the cape is compressed and current velocities increase such that at the tip of the cape, currents are very strong. The sharp curve at the tip of the headland makes the current turn sharply to the south. It is possible that headland wakes may be generated in this region. The presence of a more extensive reef flat system on the leeward side of the cape may be influenced by the dominant southward flow past the cape.

The simulations forced by both HYCOM and winds show basically the same pattern except that current velocities are slightly stronger in the shallow areas (Figure 8). Off the coast of Madrelino of the Municipality of Cortes, the wind driven circulation resulted in a recirculation which may be an artifact of the prescribed boundary flow in an area with very steep bathymetry and applies only to the surface layer.

The tidal flow patterns are shown in Figure 9. Ebb flow is towards the south while flood is towards the north. North of this area is Surigao Strait which is one of the two connections between the Pacific and internal seas of the Visayas. The strong tidal difference between the South China Sea and the Pacific (source) results in very strong pressure gradients across these straits that the tidal component of the flow dominates. However, further south of Surigao Straits, the tide are much weaker owing to the fact that the area opens to the wide and deep Pacific. The strongest tidal current velocities are mostly found is shallow passages like the passage between Bucas Grande Island and the mainland, the southeast of General island which forms the shallow entrance to Lanuza Bay and the easter coast of Cortes.

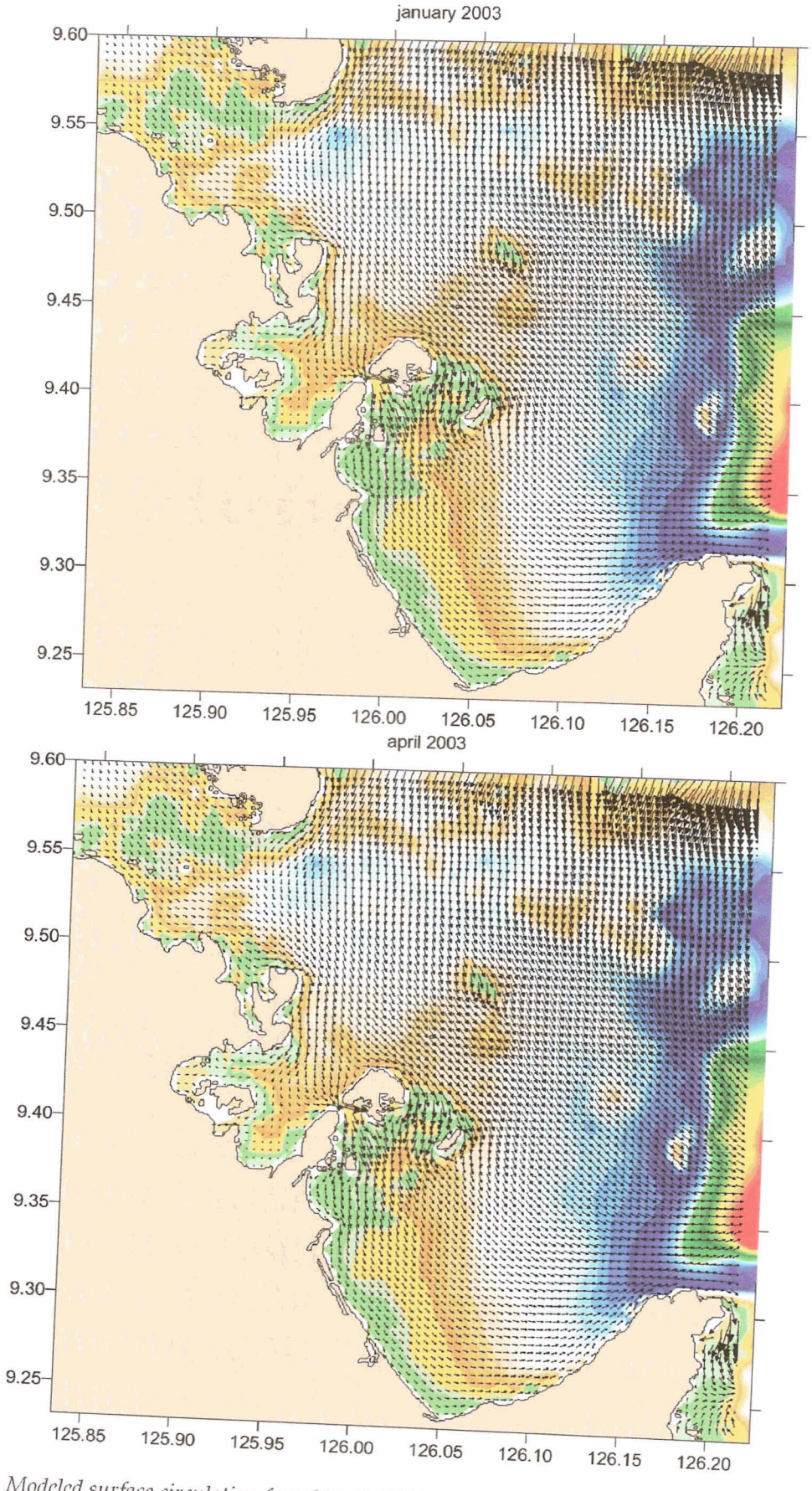

Figure 7. Modeled surface circulation forced by HYCOM barotropic velocities at the open boundaries.

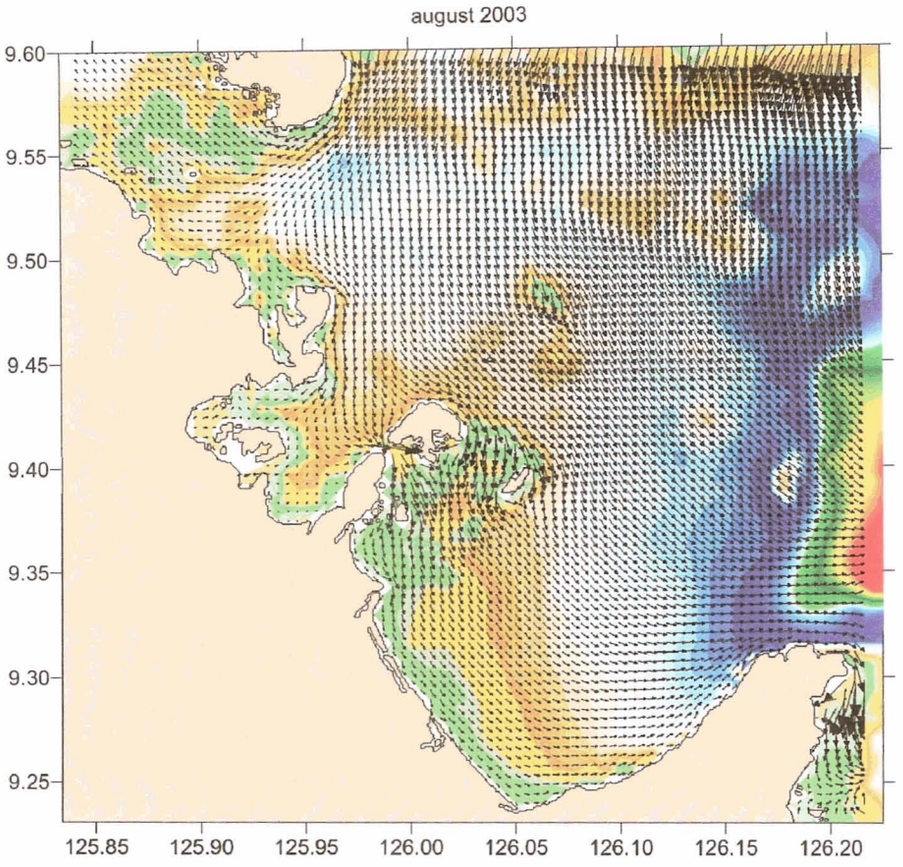

Figure 7. (continued)

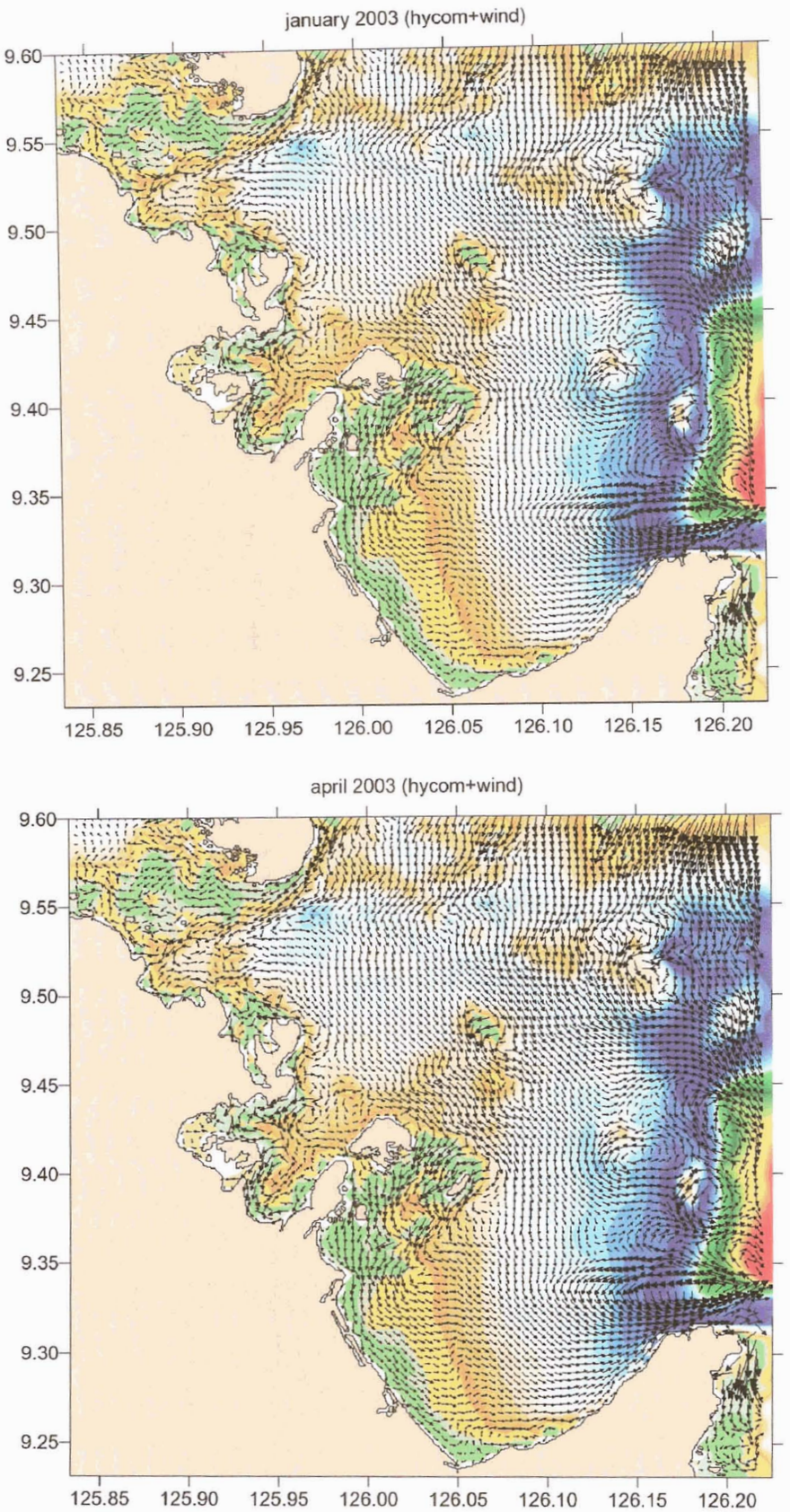

Figure 8. Modeled surface circulation forced by HYCOM at the open boundaries and monthly climatological winds

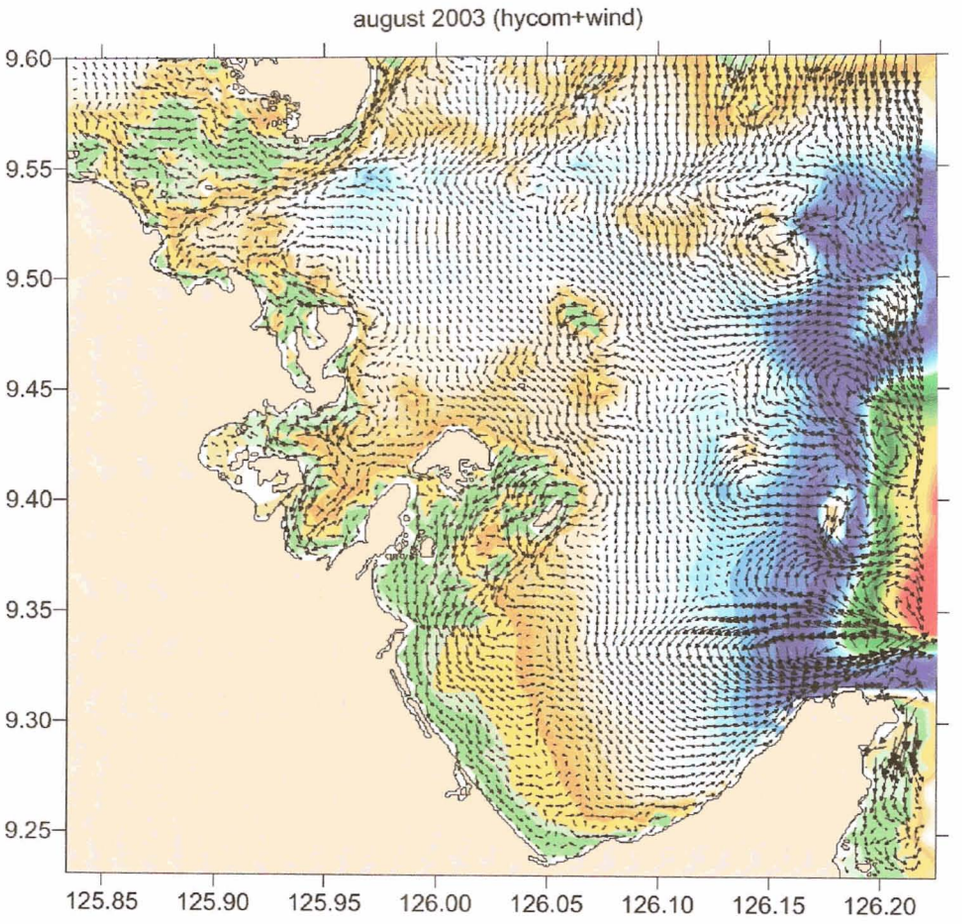

Figure 8. (continued)

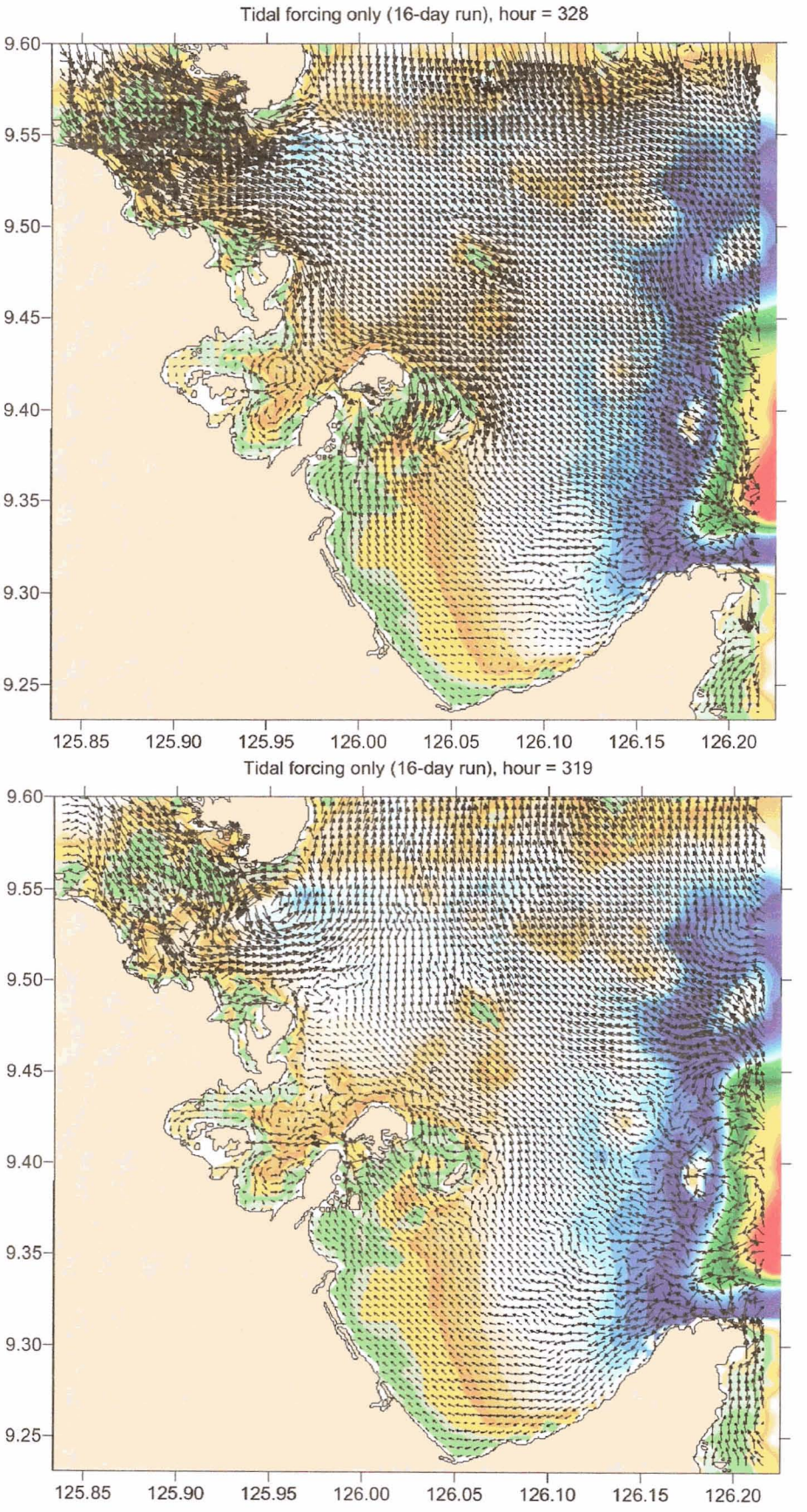

Figure 9. Modeled tidal velocities during ebb (top) and flood (bottom) conditions.

3.3 Larval Dispersal Patterns

Figure 10-Figure 12 shows the dispersal patterns from specific areas (defined by the colored boxes) and the degree to which particles released from a box can end up in another box. There does not seem to be significant differences between the 10-day, 20-day and 30-day simulations. Only a small percentage of released particles remain within the boundaries of the defined boxes and the colored bars shown in the dispersal figures the relative distribution of those found within the boxes. The minimal difference between the 10, 20 and 30-day simulations suggest that most of the particles are advected out of the domain in less than ten days and the remaining particles are those which are entrained in small embayments along the coast.

Particles released from the southern tip of Bucas Grande Island (blue box) ended up in areas along the coast northeast of Carrascal but most remained within the boundaries of the Blue Box (Figure 10). The areas opposite Bucas Gande Island (green box) did not show any exchange with the neighboring boxes. Moving southwards along the coast, the succeeding boxes show some degree of exchange between boxes.

The weaker velocities during April resulted in a relatively higher degree of exchange between boxes (Figure 11). For instance, the particles from the green box did not end up in any of the other boxes during January but was found in 3-4 other boxes during April and August (Figure 12).

For most of the boxes particularly along the southeastern side of Carrascal Bay and the western side of Lanuza Bay, the particles released from these boxes did not end up in the other boxes. This suggests that most of the particles were advected out of the model domain within a 10-day period with some particles remaining within the source area. This is expected as the southward flowing Mindanao Current dominates the coastal currents.

To identify which of the areas are good candidates for larval settlement areas, one can determine the origin of particles settling into an area. The assumption is that the ideal settlement areas are those which receive particles from the most boxes. For the boxes considered, this is shown in Figure 13-Figure *15*.

The boxes shown in Figure 13-Figure *15* containing the most colored bars are found mostly in Carrascal Bay and based on the simulated dispersal patterns, these areas appear to be ideal settlement sites. Areas facing Lanuza Bay contain only bars of the same color indicating settled particles originating from the same box.

Perhaps, a very interesting feature of the dispersal patterns is that most of the particles from all the boxes used in the simulations eventually passed just off the easternmost coast of Lanuza and the coast of Cortes (Figure 16). These two municipalities form the Cape forming the eastern side of Lanuza Bay. Along this stretch of coastline, the shelf is narrowest at the tip of this Cape and the offshore currents tend be closest to land at this location. As discussed in the previous section, the strong current passing past this headland makes a sharp turn towards the south flowing along the extensive reef flats of Cortes. The reef areas of Cortes appear to be at the receiving end of the potential larval dispersal from the reef systems of Lanuza, Cantillan and Carrascal.

4 SUMMARY AND CONCLUSIONS

Owing to the dominance of the Mindanao Current in the circulation off Carrascal and Lanuza Bays, the larval dispersal patterns in this area are probably unidirectional. The Mindanao Current is a strong current, which flows close to the coast and persists throughout the year. In fact, a simple examination of coastline configuration and reef distribution in this area show that the reefs are more extensive on the leeward sides of Carrascal and Lanuza Bays. Even the headland forming the southeastern side of Lanuza Bay shows a wider reef flat on the leeward (southeast) side of the headland.

The modeling of the dispersal of larvae also revealed similar results. Particles from selected areas were tracked and their source and location noted at the end of the simulation. Of the released particles, those that ended up within the boundaries of the defined boxes almost always ended up in downstream boxes. The only area where some degree of exchange was apparent is in Carrascal Bay. In Lanuza Bay most of the particles were advected southwards around the cape on the southeastern side of Lanuza Bay. However, the area of Cortez appears to be receiving particles released in Lanuza and Carrascal Bays but chances are slim that particles released from Cortes will be able to move northwards to Lanuza and Carrascal.

These results highlight the importance of MPA networks in an area where larval dispersal is along a "one-way street". The strong alongshore currents also mean that larval dispersal scales are larger and that in order to benefit from MPA networks, one has to take into consideration these scales.

5 REFERENCES

Magno MM, 2005. Estimation of entrainment potential in Philippine Coastal Waters: The physical consequence of island wakes and eddies. MSc Thesis. College of Science, University of the Philippines, Diliman, Quezon City.

Mellor, G. L., 2003. Users guide for a three-dimensional, primitive equation, numerical ocean model (June 2003 version), 53 pp., Prog. in Atmos. and Ocean. Sci, Princeton University.

NAMRIA, 2005. Tide and Current Tables Philippines 2005. The Coast and Geodetic Survey Department, National Mapping and Resource Information Authority. Department of Environment and Natural Resources.

Polovina JJ, Kleiber P, Kobayashi DR. 1999. Application of TOPEX-POSEIDON satellite altimetry to simulate transport dynamics of larvae of spiny lobster, *Panulirus marginatus*, in the northeastern Hawaiian Islands, 1993-1996. Fish. Buyll. 97:132-143.

Sauers KA, Klinger T, Coomes C, Ebbesmeyer CC. 2003. Synthesis of 41,300 Drift Cards Released in Juan de Fuca Strait (1975-2002). Proceedings of the 2003 Georgia Basin/Puget Sound Research Conference. http://www.psat.wa.gov/Publications/01_proceedings/sessions/oral/7c_sauer.pdf

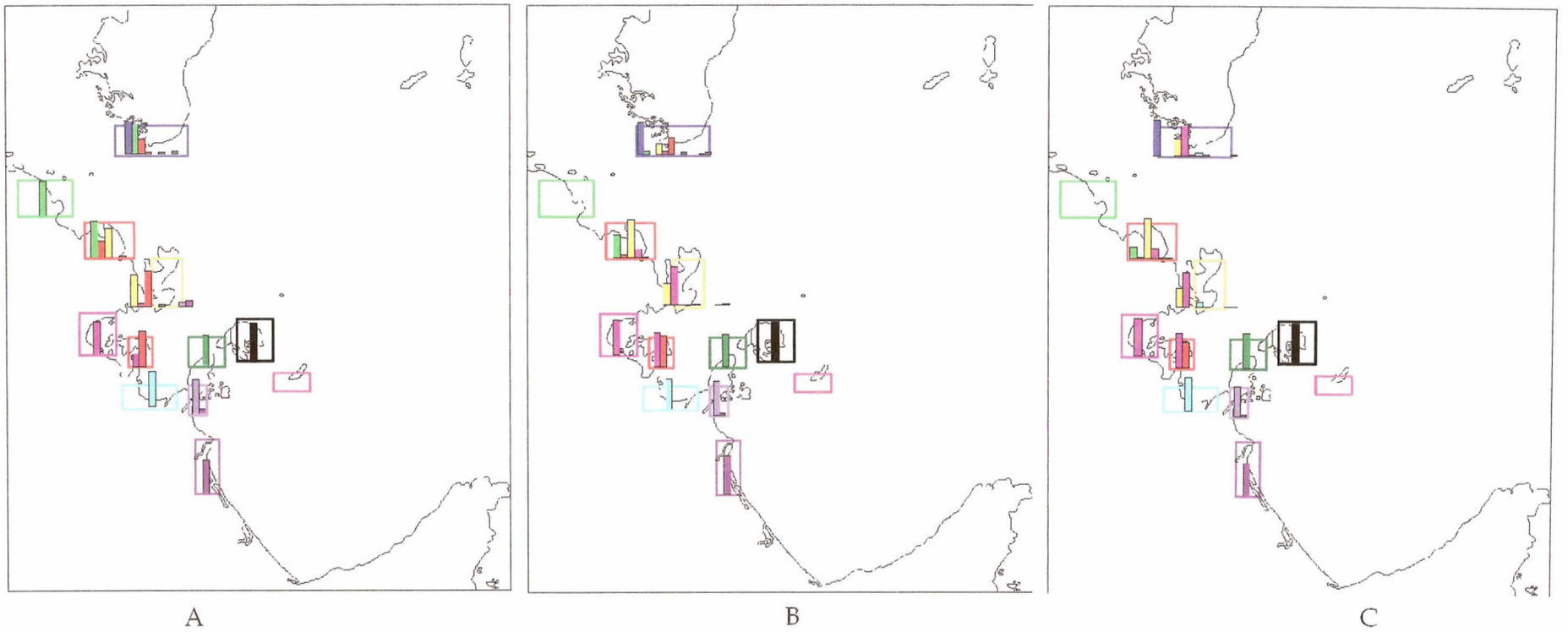

Figure 10. Relative distribution of sink areas during January for 10-day (A), 20-day (B) and 30-day (C) dispersal simulations. The colored boxes represent release areas for dispersed particles. Colored bars represent where particles from a specific box ended up after the simulation period. The colors of the bars identify which boxes the particles ended up.

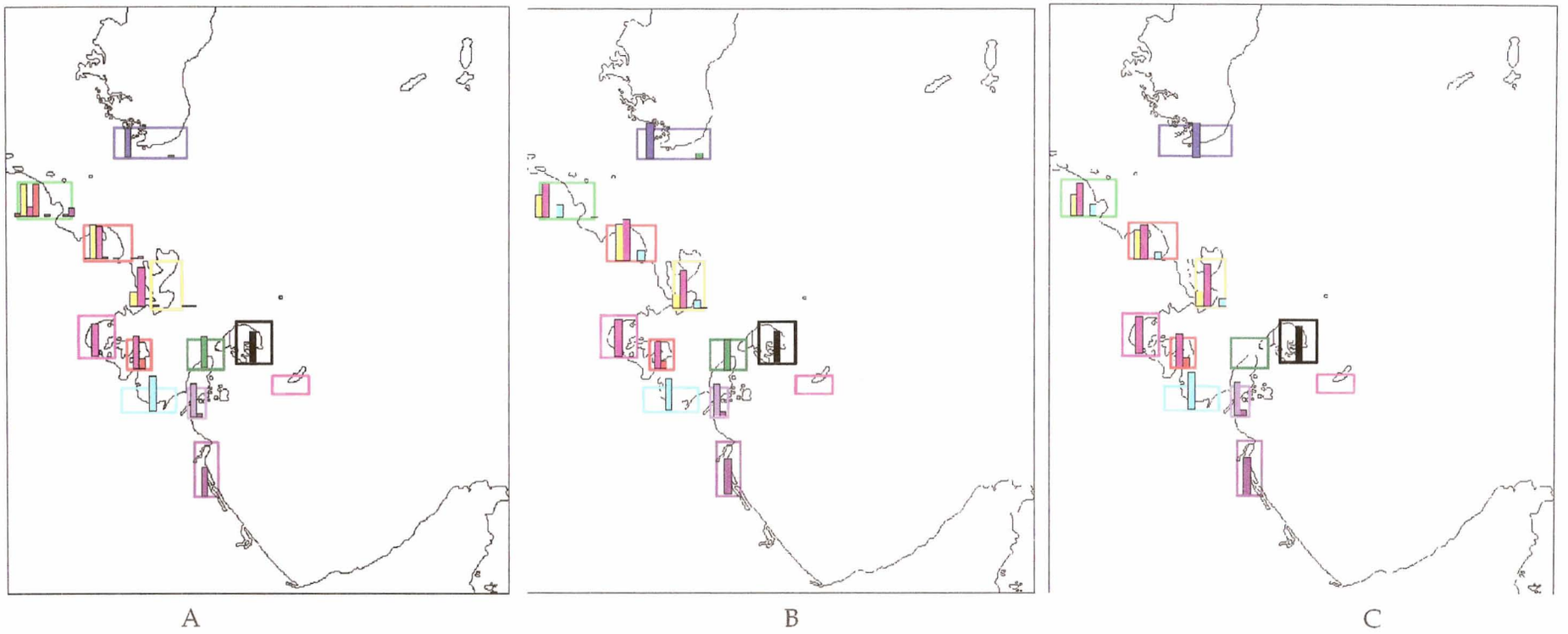

Figure 11 Relative distribution of sink areas during April for 10-day (A), 20-day (B) and 30-day (C) dispersal simulations. The colored boxes represent release areas for dispersed particles. Colored bars represent where particles from a specific box ended up after the simulation period. The colors of the bars identify which boxes the particles ended up.

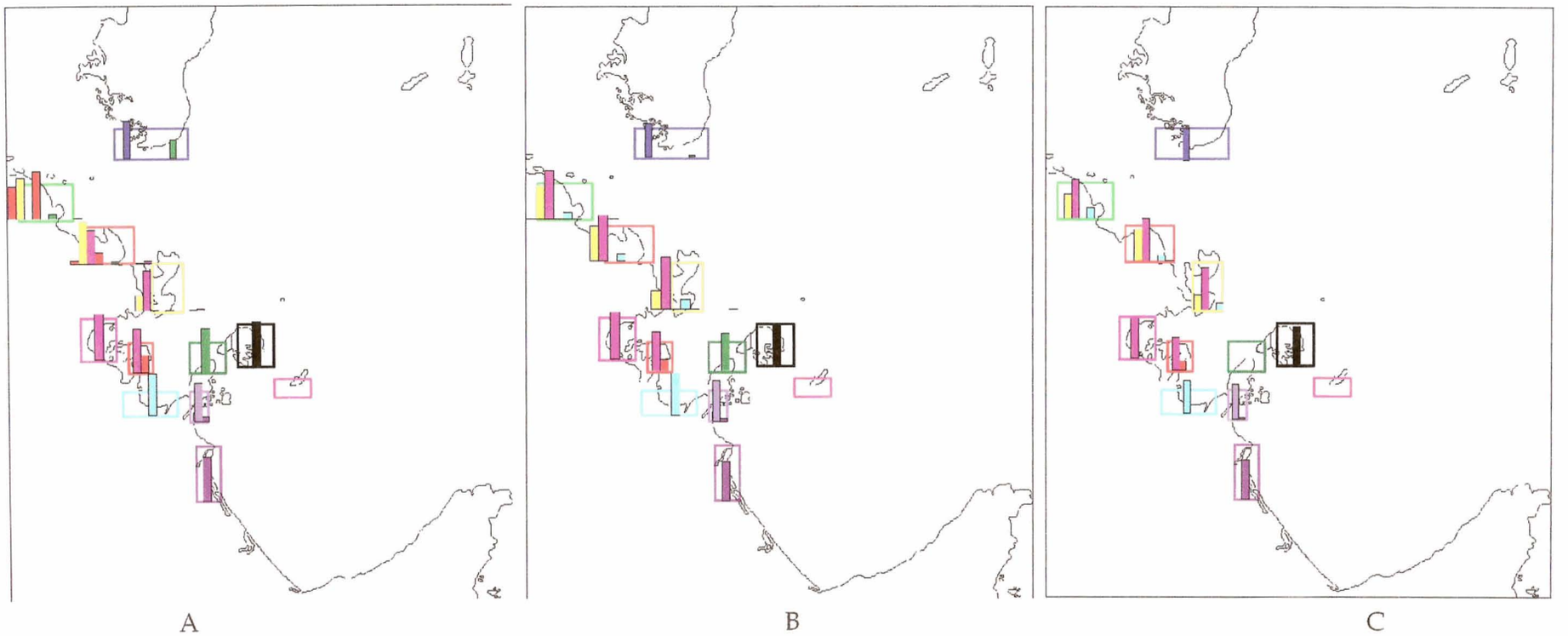

Figure 12. Relative distribution of sink areas during August for 10-day (A), 20-day (B) and 30-day (C) dispersal simulations. The colored boxes represent release areas for dispersed particles. Colored bars represent where particles from a specific box ended up after the simulation period. The colors of the bars identify which boxes the particles ended up.

Figure 13 Relative distribution of source areas during January for 10-day (A), 20-day (B) and 30-day (C) dispersal simulations. The colored boxes represent release areas for dispersed particles. Colored bars represent sources of particles that settled at a particular box after the simulation period.

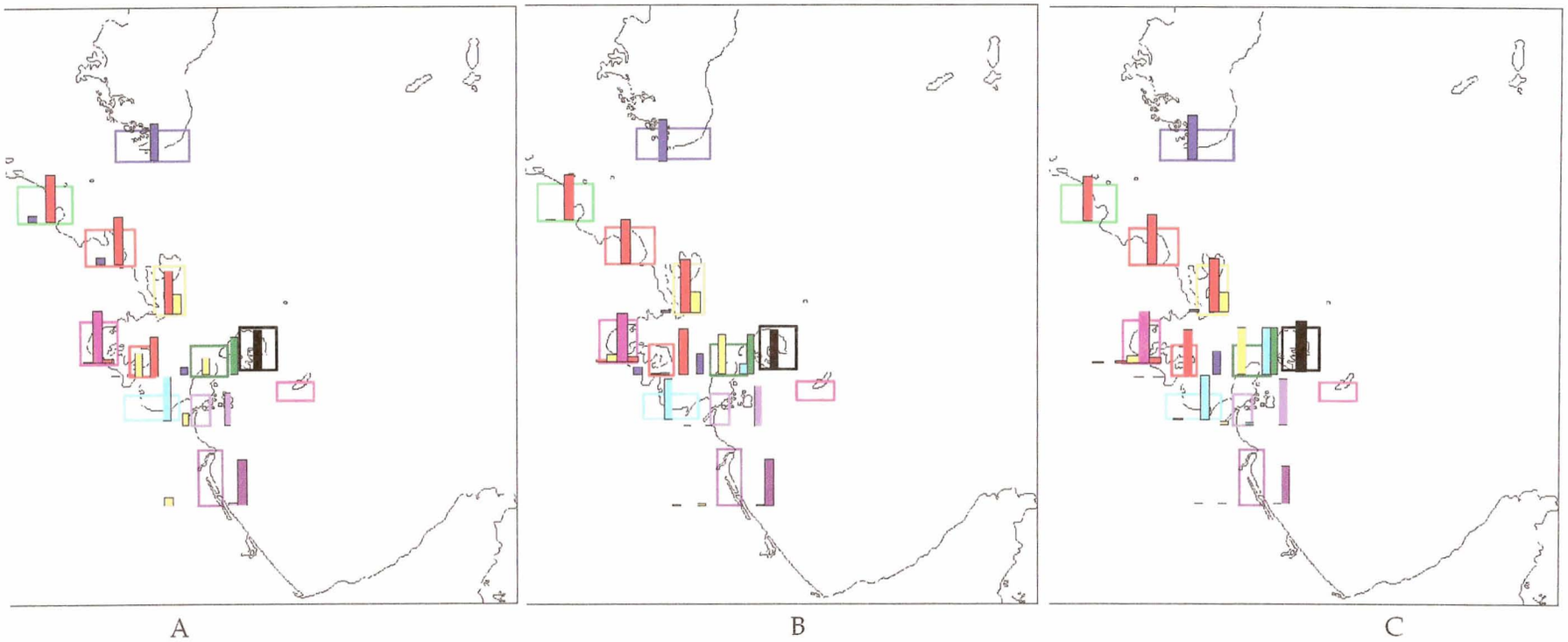

Figure 14 Relative distribution of source areas during April for 10-day (A), 20-day (B) and 30-day (C) dispersal simulations. The colored boxes represent release areas for dispersed particles. Colored bars represent sources of particles that settled at a particular box after the simulation period.

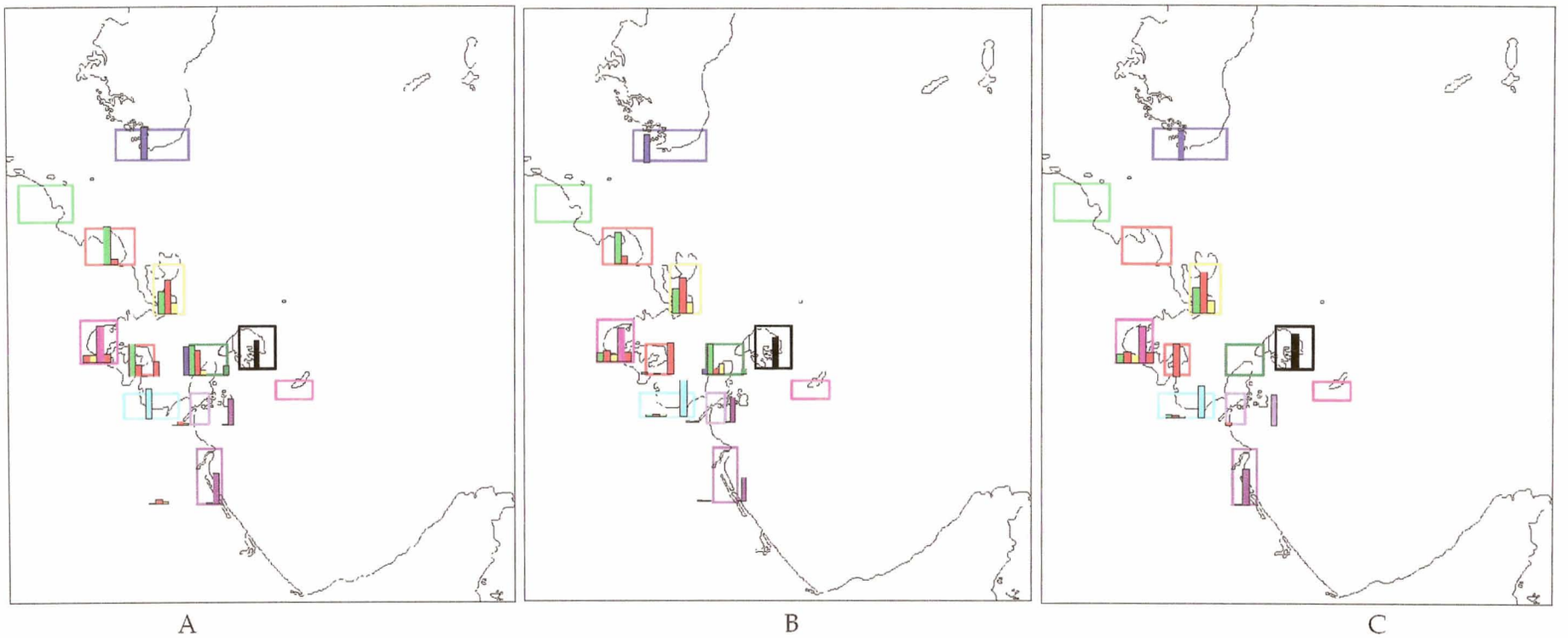

Figure 15. Relative distribution of source areas during August for 10-day (A), 20-day (B) and 30-day (C) dispersal simulations. The colored boxes represent release areas for dispersed particles. Colored bars represent sources of particles that settled at a particular box after the simulation period.

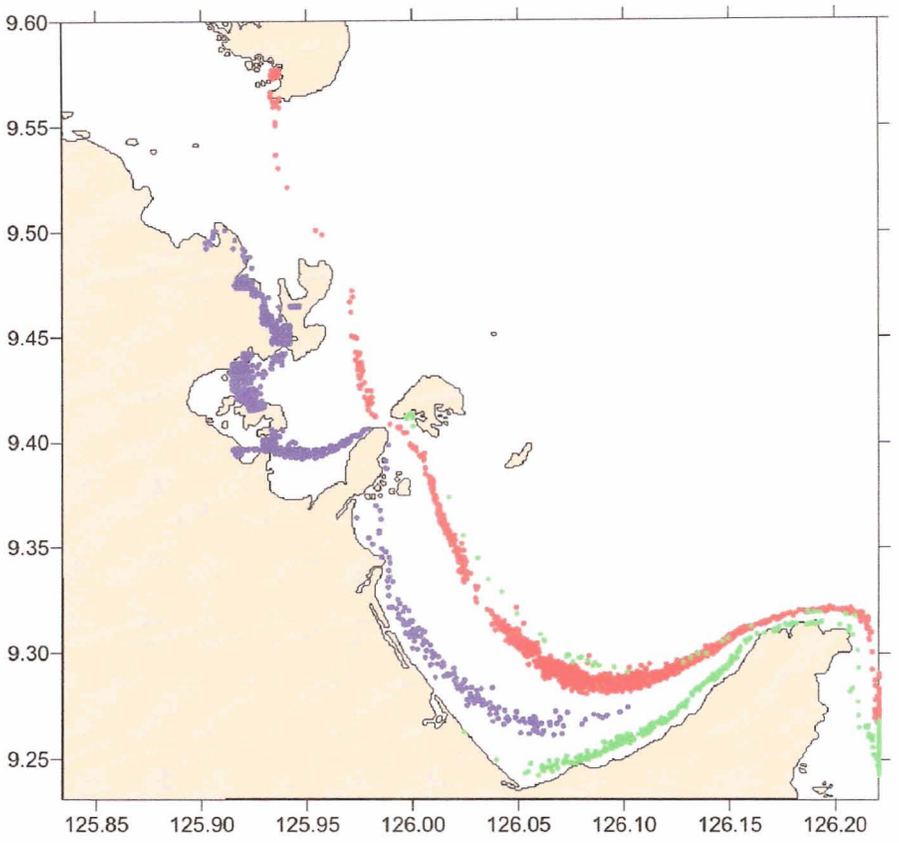

Figure 16 Dispersal of particles released from different locations but following the same downstream pattern in Lanuza Bay and further southwest.

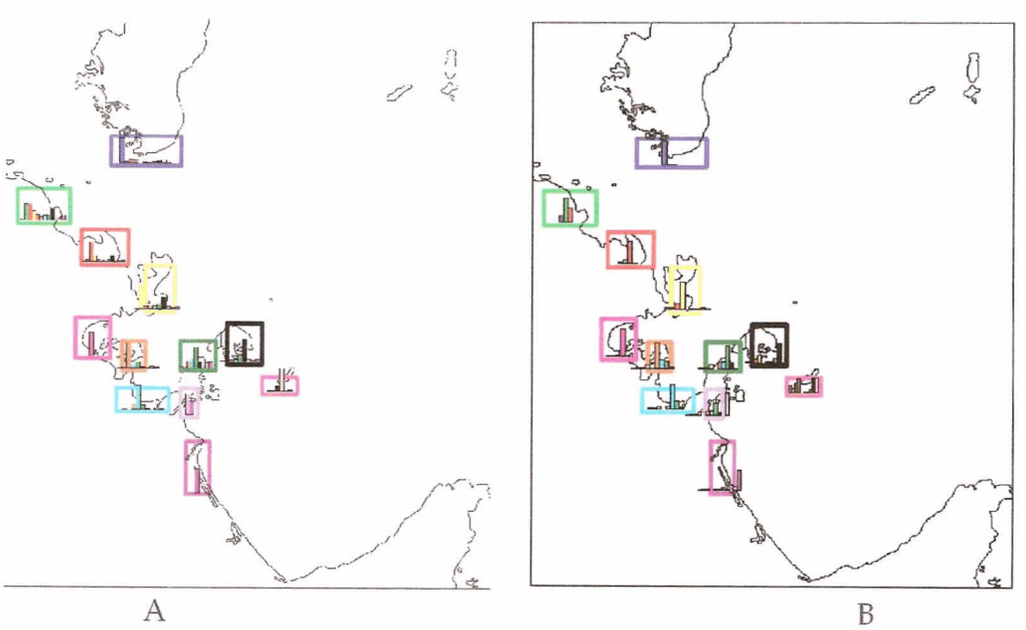

Figure 17 Relative distribution of (A) source and (B) sink areas for 30- dispersal simulations. The colored boxes represent release areas for dispersed particles.

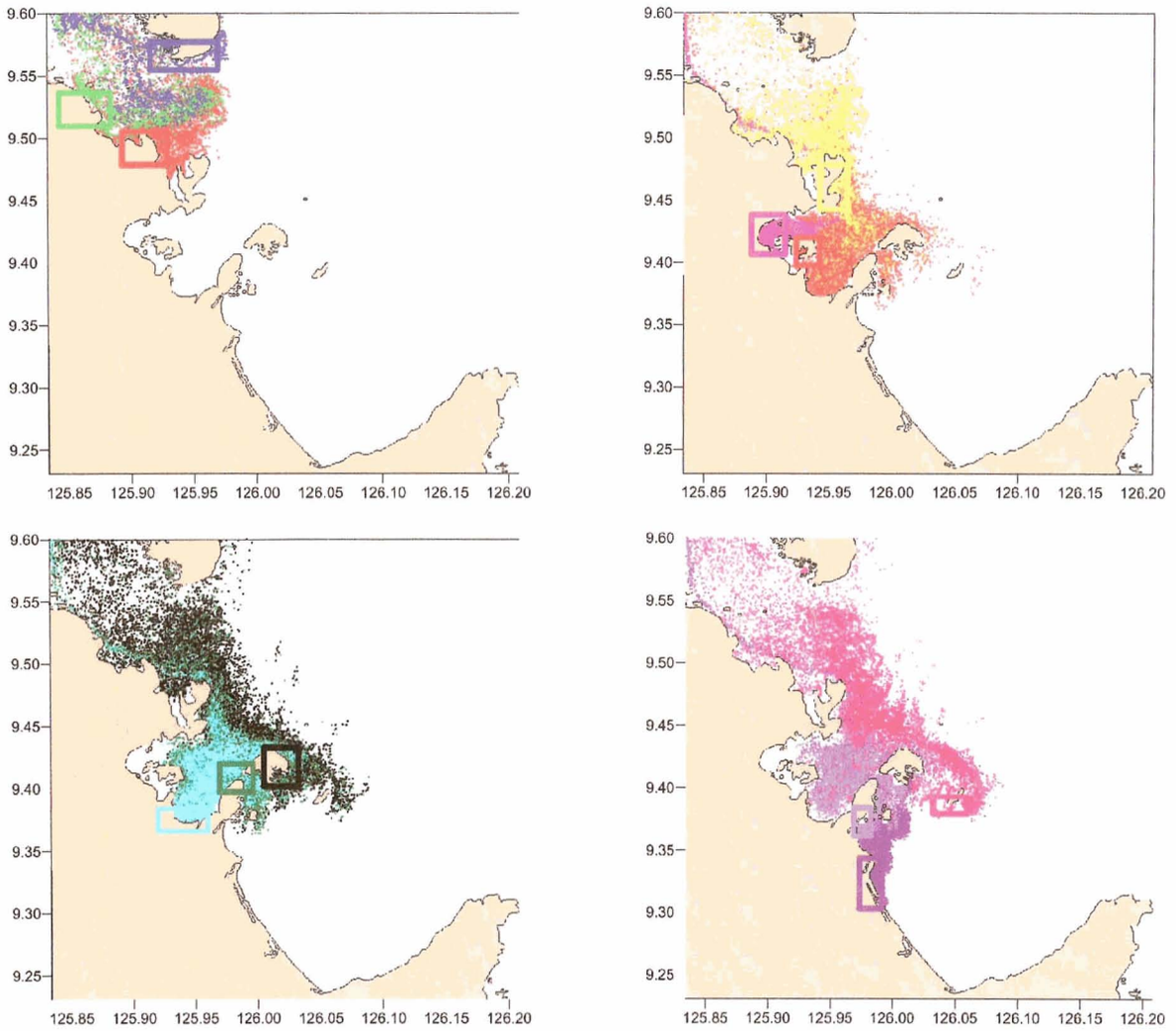

Figure 18 Dispersal of particles released from different locations but following the same downstream pattern in Lanuza Bay and further southwest forced by tidal velocities

NUMERICAL SIMULATIONS OF LARVAL DISPERSAL PATTERNS IN TAWI-TAWI

1 INTRODUCTION

Tawi-tawi is one of the four focal sites of the USAID funded Fisheries Improvements for Sustainable Harvests (FISH) Project. The goal of the project is to improve fish stocks by as much as 10% over a 5-year project. One of the interventions to address this goal is the establishment of networks of fish sanctuaries. Studies (Ward et al., 2001) have suggested that synergistic effects of sanctuary or MPA networks will be more beneficial to the fisheries through larval spillover than just by adult spillover. It is assumed that these networks are established on the basis of larval connectivities and dispersal. The aim of this study is to determine, using numerical models, the potential dispersal patterns of larvae of fish, which may help in selecting locations of future MPAs, and MPA networks.

1.1 Description of Study Site

Tawi-tawi is a group of islands located in the far southwestern portion of the Philippines (***Figure 1***). It is found southwest of Jolo and northeast of the Sibutu island group separated from each other by the relatively narrow Sibutu Passage. Tawi-tawi is also sandwiched between two important but hydrographically distinct basins, the Sulu Sea in the north and the Sulawesi Sea in the south. Among the water channels that connect these two basins, the Sibutu Passage is the deepest with a threshold or sill depth of 275m (Meñez 2004) located on the southern end of the Passage between Sibutu and Simunul islands. The presence of this sill limits the exchange of water properties from both sides of the sill. Nevertheless, this passage is the only connection through which net transport from the Sulu Sea to Celebes Sea takes place.

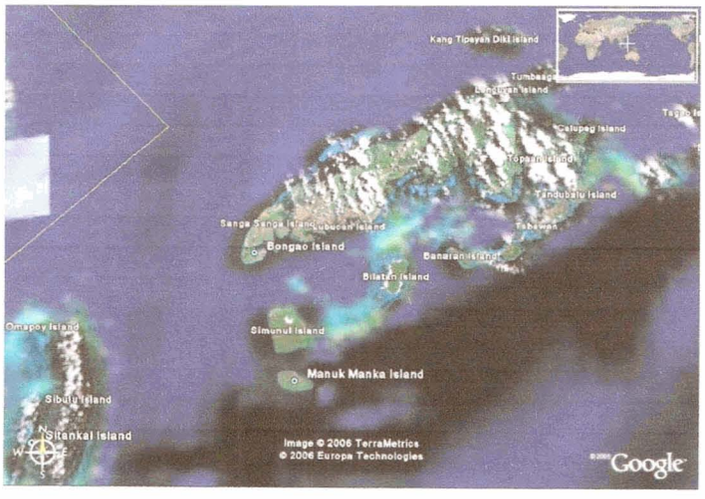

Figure 1. Image showing the study area and surrounding waters

While most of the coral reefs in the Philippines are mainly of fringing reef type, Tawi-tawi has a barrier reef system where coral reefs develop parallel to the coast separated from it by a lagoon. The Bongao lagoon (enclosed area between southern Tawi-tawi and Simunul and TIji-tiji coral reefs) has a meridional diameter of at least 16.5 km. The lagoon is connected to outside waters in the southwest between Bongao and Simunul islands which is about 11 km wide and less than a hundred meters in depth. From here, bathymetry gradually deepens to at least 300m westward (***Figure*** 2). Inside the lagoon, maximum bathymetry is only about 30 meters. At the eastern boundary, the narrow Balimbing Channel connects the lagoon to Tawi-tawi Bay. This area is characterized by extensive coral reefs and even shallower bathymetry and may limit the exchange of water properties between the lagoon and the bay. Overall, the lagoon configuration is akin to an inverted and slightly right-tilted horseshoe with its opening facing the Sibutu Passage and is only partially connected to the Tawi-tawi Bay in the east.

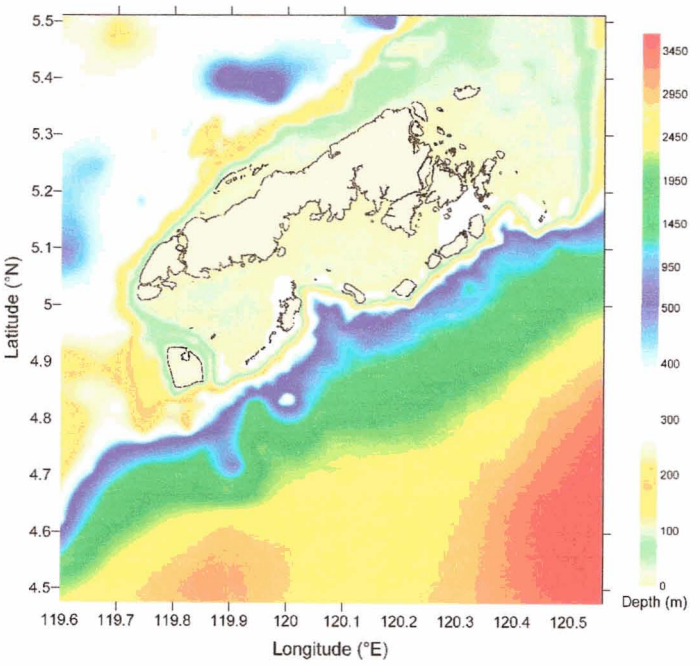

Figure 2. Bathymetry of Tawi-tawi and surrounding waters

1.2 Specific Objectives

The objectives of this study are:

- Characterize circulation patterns in Tawi-tawi in scales relevant to the dispersal of larvae
- Simulate larval dispersal patterns from different areas in Bongao lagoon and to characterize potential larval exchange between these areas

2 METHODOLOGY

2.1 Field Survey

A field survey was conducted last February 8-12, 2006 to collect baseline information on the distribution of temperature, salinity, chlorophyll and surface currents. The stations occupied during the survey are shown in ***Figure*** 3. At each station, the temperature, salinity and chlorophyll profiles were obtained using a Seabird SBE19 CTD with a Turner SCUFA Fluorometer. The surface currents were measured using a 0.5m diameter holey-sock drogue. A handheld GPS in tracking mode was attached to the drogue and measures the position of the drogue as it drifts with the currents. A handheld anemometer and an electronic compass were used to measure wind speed and direction, respectively.

2.2 Hydrodynamic Modeling

The three-dimensional circulation of the waters in Tawi-tawi was modeled using the Princeton Ocean Model (Mellor, 2003). This model is a three-dimensional primitive-equation sigma coordinate model and is used in numerous applications ranging from estuarine to global ocean models. The model domain for the Tawi-tawi model covers the area shown in ***Figure*** 2. The model grid resolution is 550m x 550m. At the boundaries, the model is forced by the tides and offshore currents and at the surface by the wind. The tidal forcing prescribed at the open boundaries was derived from the Oregon State University Tidal Inversion Software (OTIS) model applied to Philippine waters by Magno (2005). Open ocean currents at the model open boundaries were obtained from the monthly mean barotropic velocities computed by the Pacific HYCOM Simulations (http://hycom.rsmas.miami.edu/data/information.html#pacific). Separate runs were made to represent seasonal circulation patterns. Each run was allowed to run for 30 days of model time for each seasonal boundary forcing. The model is also forced at the surface by winds derived from satellite altimetry (http://manati.orbit.nesdis.noaa.gov/hires/).

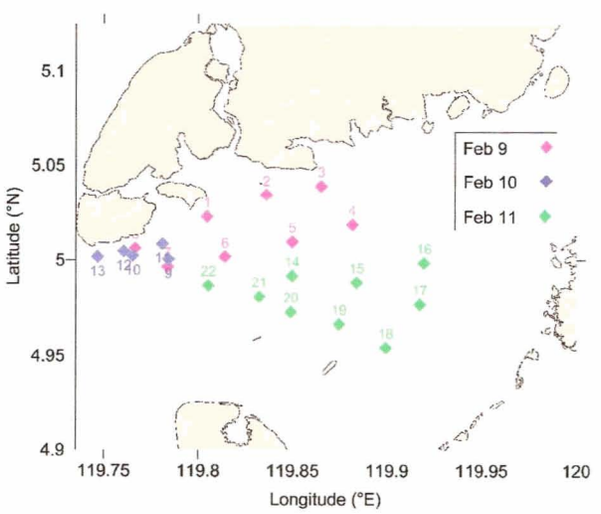

Figure 3. Map showing the location of stations occupied during the field survey. Colors denote different days the stations were occupied.

The parameters for the simulation experiments conducted for this study are listed in ***Table 1***. Three seasons were considered, northeast monsoon season (January 2003 forcing), southwest monsoon season (August 2003 forcing) and the spring monsoon transition (April 2003 forcing).

Table 1. Summary of hydrodynamic simulations

Run No	Tides	HYCOM Boundary forcing	Winds
1	√		
2		√ August 2003 data	
3		√ August 2003 data	√
4		√ April 2003 data	
5		√ April 2003 data	√
6		√ January 2003 data	
7		√ January 2003 data	√

2.3 Lagrangian dispersal model

The dispersal model is adapted from the model of Polovina et al. (1999). In this model, the larvae are represented as neutrally buoyant passive particles and their position over time is tracked using the following equations:

$$x_{t+\Delta t} = x_t + \left(u_{x,y,t}\Delta t + \varepsilon\sqrt{D\Delta t}\right)$$
$$y_{t+\Delta t} = y_t + \left(v_{x,y,t}\Delta t + \varepsilon\sqrt{D\Delta t}\right) \quad (1)$$

where x and y are the coordinates of a particle; u and v are the advection velocities from the hydrodynamic model, Δt is the integration time step, ε is a randomly generated number ranging from –1 to 1, and D is the eddy diffusion rate (m^2s^{-1}). Each particle when released has attributes, which identifies it individually from the other particles. These attributes include age from release, location of release, date and time of release. These attributes will enable us to estimate the degree of exchange of simulated particles between areas based on the method used by Sauers et al. (2003) in analyzing drifter card data.

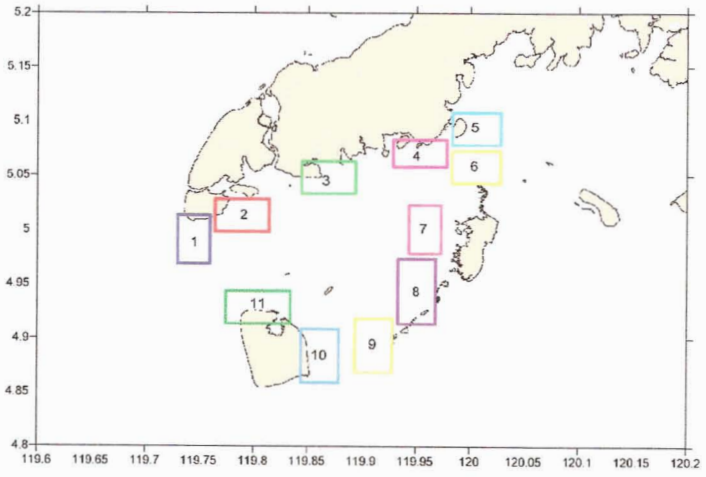

Figure 4. Areas used for dispersal simulation as larval source or sink areas.

To determine the exchange between areas, several areas were designated as source and sink areas around the study area. The sizes and locations of these areas, shown in ***Figure 4***, vary and were chosen to represent different areas all around the Bongao lagoon. The dispersal model was used to simulate the dispersal of particles released from these boxes. The model was allowed to run for 10 days but the output dispersal was written to a file at two-day intervals to represent short, medium, and long-range dispersal. Dispersal simulations based on the tidal component of the circulation was also conducted. After each of these simulations, the location of the particles and where they were released were noted and used in the analysis.

3 RESULTS AND DISCUSSION

3.1 Field Survey

Prevailing winds during the field survey were from the northwest (***Figure 5***). The strongest winds were measured during the noon of February 9 where the maximum wind speed is about 6 knots. Winds were relatively weaker along the coast for the succeeding two days of measurement and came from different directions. It was apparent that although mean winds in the area were coming from the northeast, within the Tawi-tawi lagoon, winds were modified by local topography, particularly Bongao Peak. As a result, winds to the south of Bongao Island were blowing from the northwest.

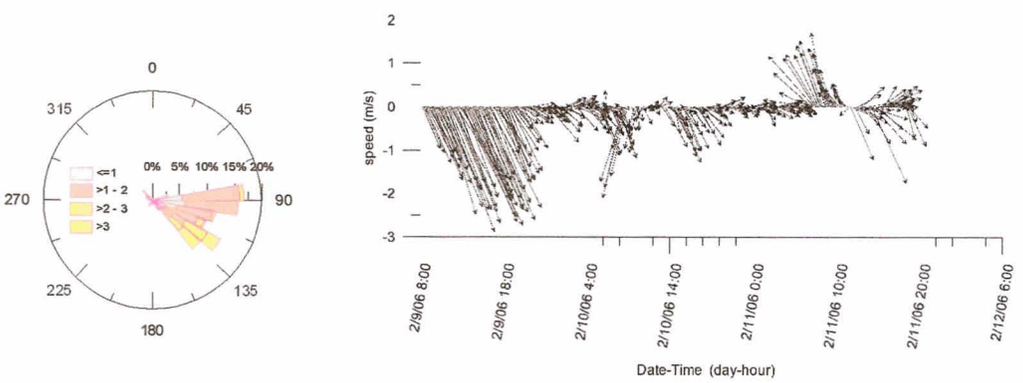

Figure 5. Measured wind velocities during the field survey period at a stationary location along the coast of Bongao.

The tides during the survey period were mainly diurnal with flooding in the morning and ebbing in the evening (***Table 2***). Since the tide phases for the three day survey were similar, the measurements can be combined to produce a composite picture of the surface circulation in Tawi-tawi.

Table 2. Predicted tides for the survey period from February 9-11, 2006 (source: NAMRIA, 2006)

Date	Time	Height
9	0418	-0.22
	1836	0.85
10	0426	-0.22
	1931	0.91
11	0425	-0.19
	2016	0.95

The spatial surface current and wind measurements conducted during the field survey are shown in ***Figure 6***. During the first two days of sampling, directions of the surface currents are generally consistent with the wind directions. Weakest surface currents moving southward into the inner lagoon were observed during the first day of sampling while relatively stronger currents measured along the two transect in the inner lagoon shows an eddy flowing counterclockwise consistent with the wind. Meanwhile, strong headland currents moving out of the lagoon and in opposite direction of the wind were observed just off the southern tip of Bongao Island during the second day of sampling.

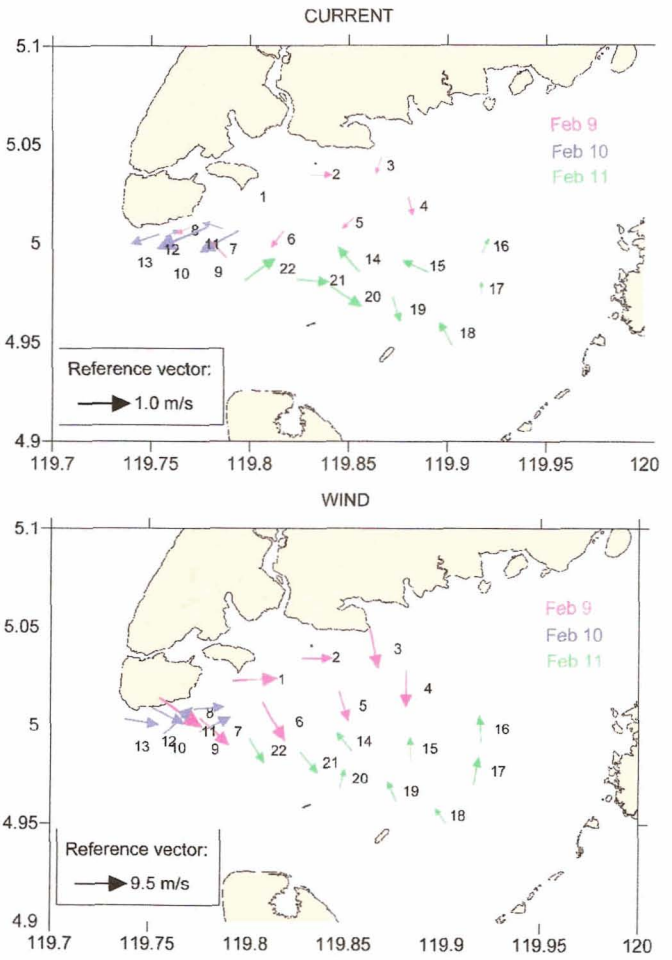

Figure 6. Measured surface currents from surface drogue and wind. Colors of arrow denote different sampling days

Temperature, Salinity and Chlorophyll

The observed variable atmospheric conditions during the three days of sampling shown in ***Figure 5*** and ***Figure 6*** could also be seen in the vertical profiles of the hydrographic parameters surveyed. Most of the stations sampled show vertically homogenous profiles extending to about 20 meters (***Figure 7***). Among the stations, those that were surveyed during Feb 11 showed the widest range of temperature and salinity at the surface, which actually coincided with the weakest winds measured.

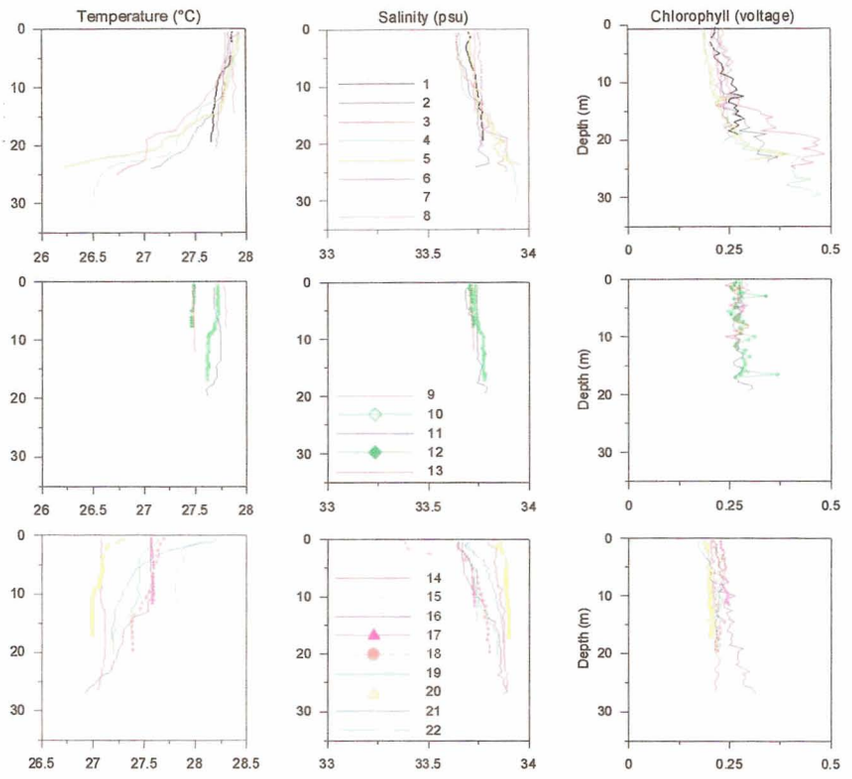

Figure 7. Vertical profiles of temperature, salinity and chlorophyll

3.2 Hydrodynamic Model Results

The HYCOM-forced current patterns are generally similar in direction for the different seasons considered (***Figure 8***). The only conceivable difference is the presence of the southward moving currents at the base of the Tiji-tiji reef system emanating from east of the model domain during August and which converge with the currents coming from the Sibutu Passage before continuing further south. Regardless of season, currents move southward through the Sibutu Passage from Sulu Sea although part of this current flow into the Bongao lagoon through the Simunul channel. From this point, a segment of this current continues as a strong coastal jet along the eastern coast of Simunul Island during January but weakens during April and picks up in magnitude again during August. The other and relatively weaker segment, however, flows along the northern coast of the lagoon and eastward through the Balimbing Channel into the Tawi-tawi Bay. Within the lagoon, clockwise rotating currents are also evident which exit as swift currents through the southern portion of the Simunul Channel or through the Balseyro Channel which is a narrow break in southern Tiji-tiji coral reefs.

The simulations forced by both HYCOM and winds show basically the same pattern except inside the lagoon and Tawi-tawi Bay (***Figure 9***). During the northeast monsoon and transition months, the currents that used to move eastward through the Balimbing Channel is now deflected southward and continues as an alongshore flow west of Tiji-tiji coral reefs and again exits through the Simunul or Balseyro Channels. Currents inside the Tawi-tawi Bay also flow westward through the

Balimbing Channel and ultimately join this southward current. During August, however, this alongshore flow is not evident but is instead replaced by a weak circulation with a small eddy in the northeastern end of the lagoon. It also appears that the lagoon circulation is barely connected with the circulation inside Tawi-tawi Bay during the southwest monsoon since currents seems to flow out of the bay through another narrow opening north of Tiji-tiji reef instead of flowing as a usual alongshore current west of Tiji-tiji reef. Nonetheless, similar to the results of HYCOM forced model, currents for the combined HYCOM and wind forcings (particularly along the Sibutu Passage and Simunul Channel) show maximum magnitude during the northeast monsoon, slightly weaken during the April transition period and appears to gain momentum again when monsoon is from southwest. Inside the lagoon and in Tawi-tawi Bay, southwest monsoon months showed the weakest currents.

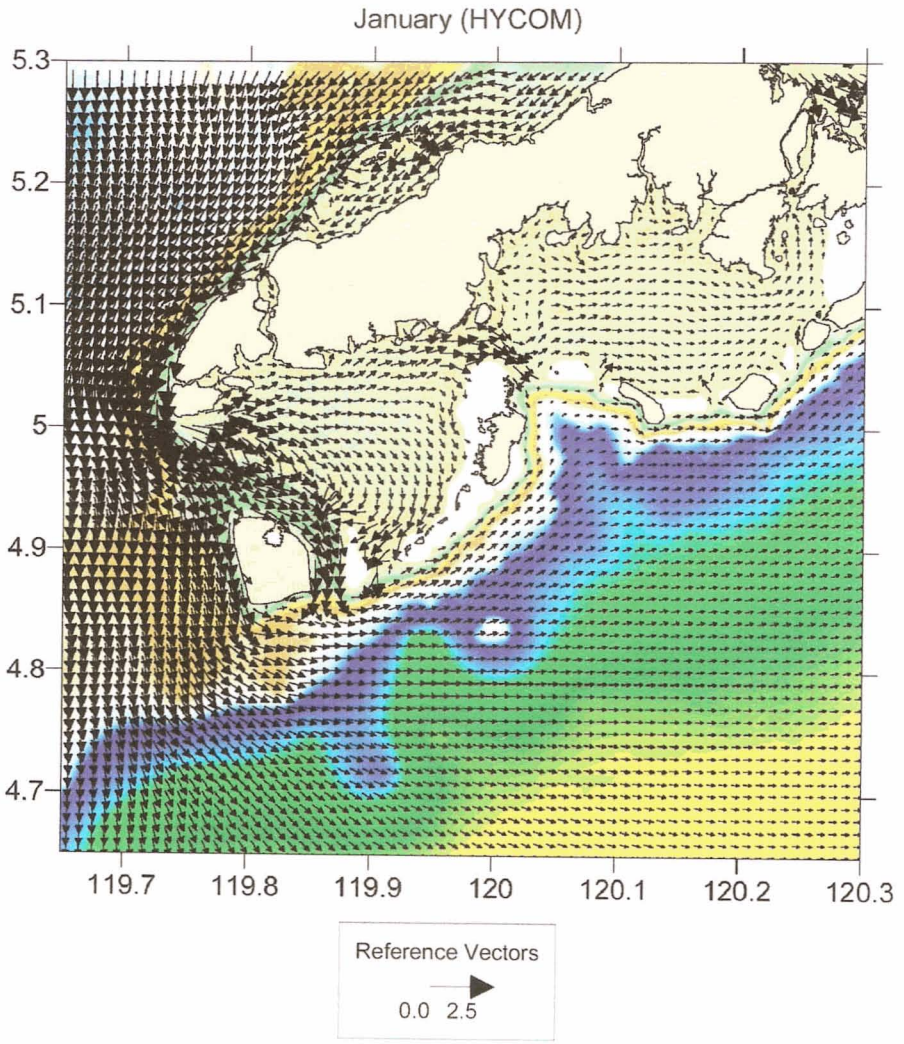

Figure 8. Modeled surface circulation forced by HYCOM barotropic velocities at the open boundaries.

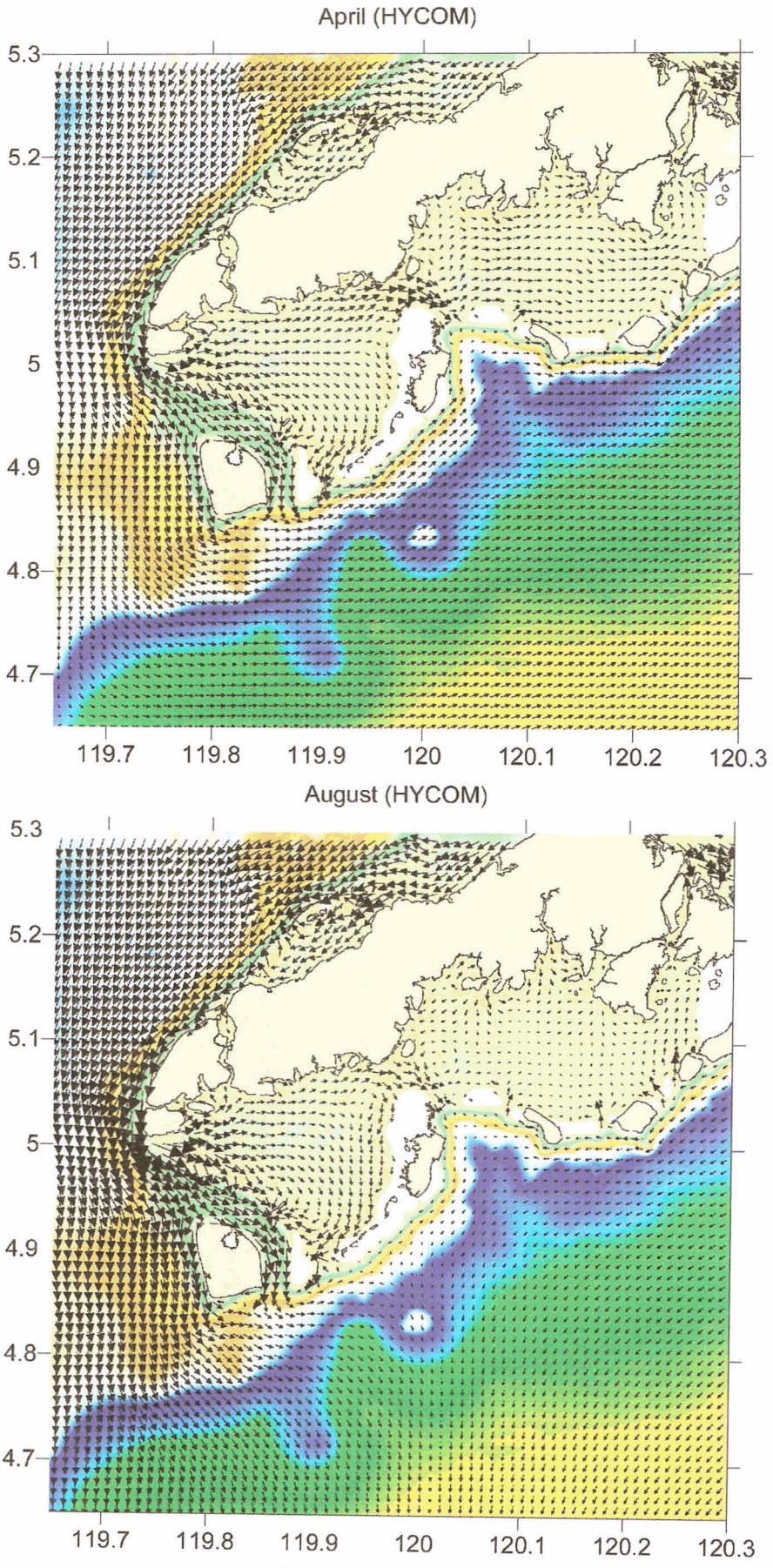

Figure 8. (continued)

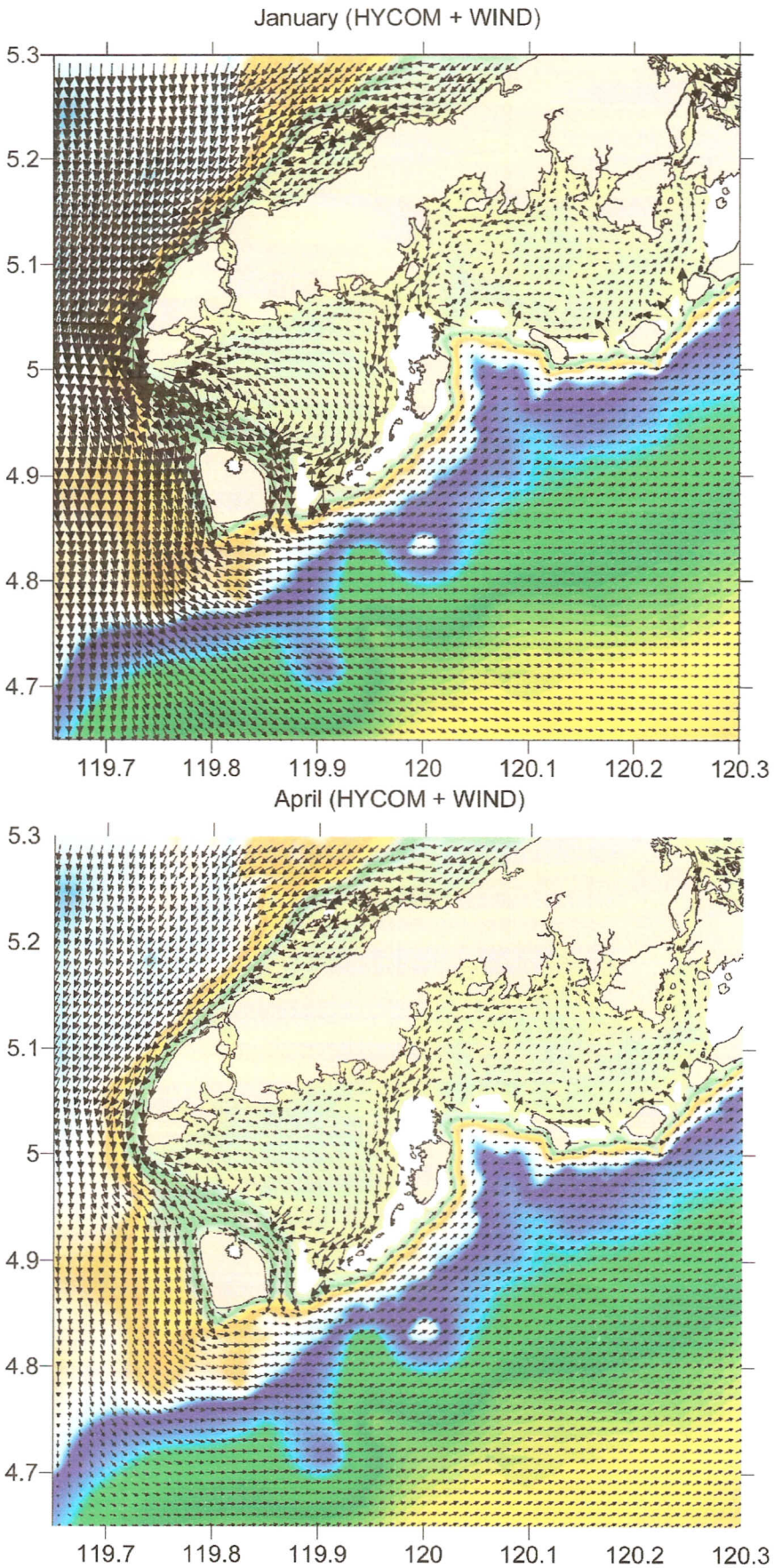

Figure 9. Modeled surface circulation forced by HYCOM at the open boundaries and monthly climatological winds

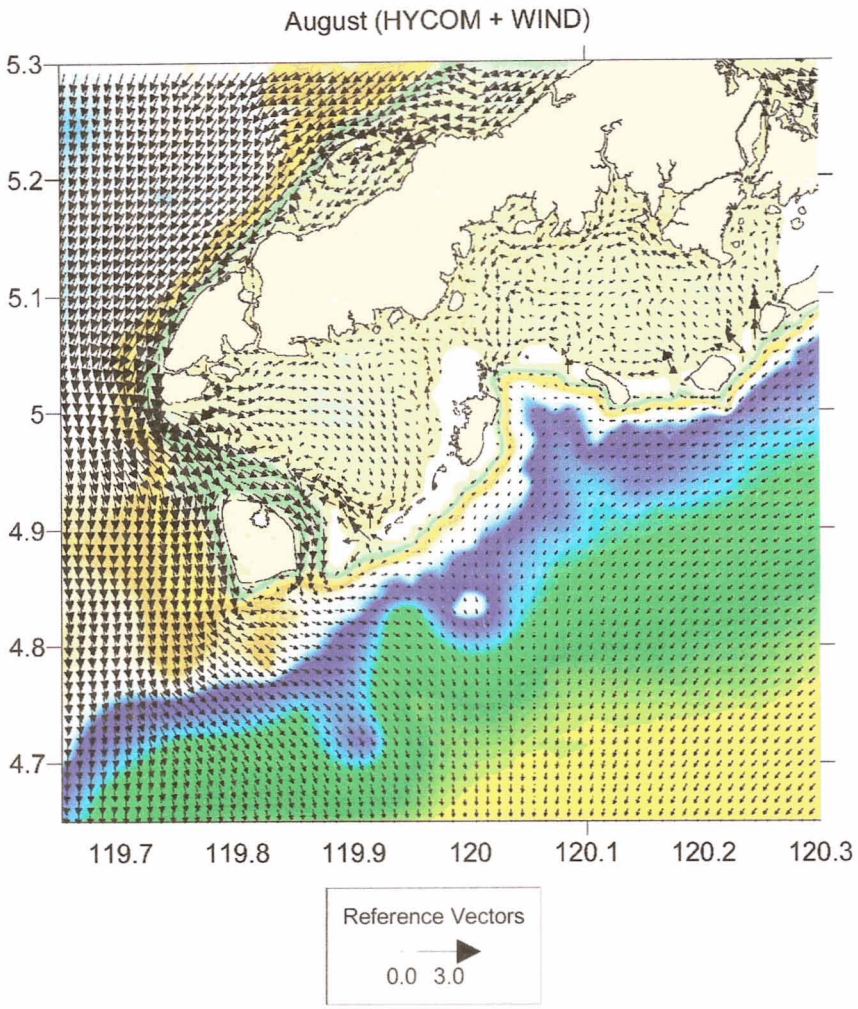

Figure 9. (continued)

Comparison of the model circulation and observed currents during the field survey show an important difference in the circulation at the portion of the Lagoon mouth immediately south of Bongao Island. The model results show a consistent flow into (i.e. eastward) the Lagoon apparently forced by the strong net transport from the Sulu Sea to the Sulawesi Sea. However, observed surface currents during the survey showed westward flow, at times moving opposite to the wind. It is apparent that an aspect of the Lagoon circulation may not be captured properly by the circulation model. For instance the flow between the Sulu Sea and the Sulawesi Sea via the Sibutu Passage is highly modulated by the tides. In fact, the interaction of the tides with sills in the vicinity induce the formation of non-linear internal waves which propagate towards Palawan (Liu et al., 1985). Tidal current information from the NAMRIA tide tables indicate flow towards the Sulawesi Sea from the Sulu Sea during flood tides. It is therefore likely that in the Sibutu Passage, flow reverses with the tides while net flow may be towards the Sulawesi Sea. The simulated flood and ebb currents are shown in ***Figure 10***. With reversing tidal currents in Sibutu Passage, it can be seen that the flow to the south of Bongao Island is predominantly westwards, similar to the observed surface currents during the survey.

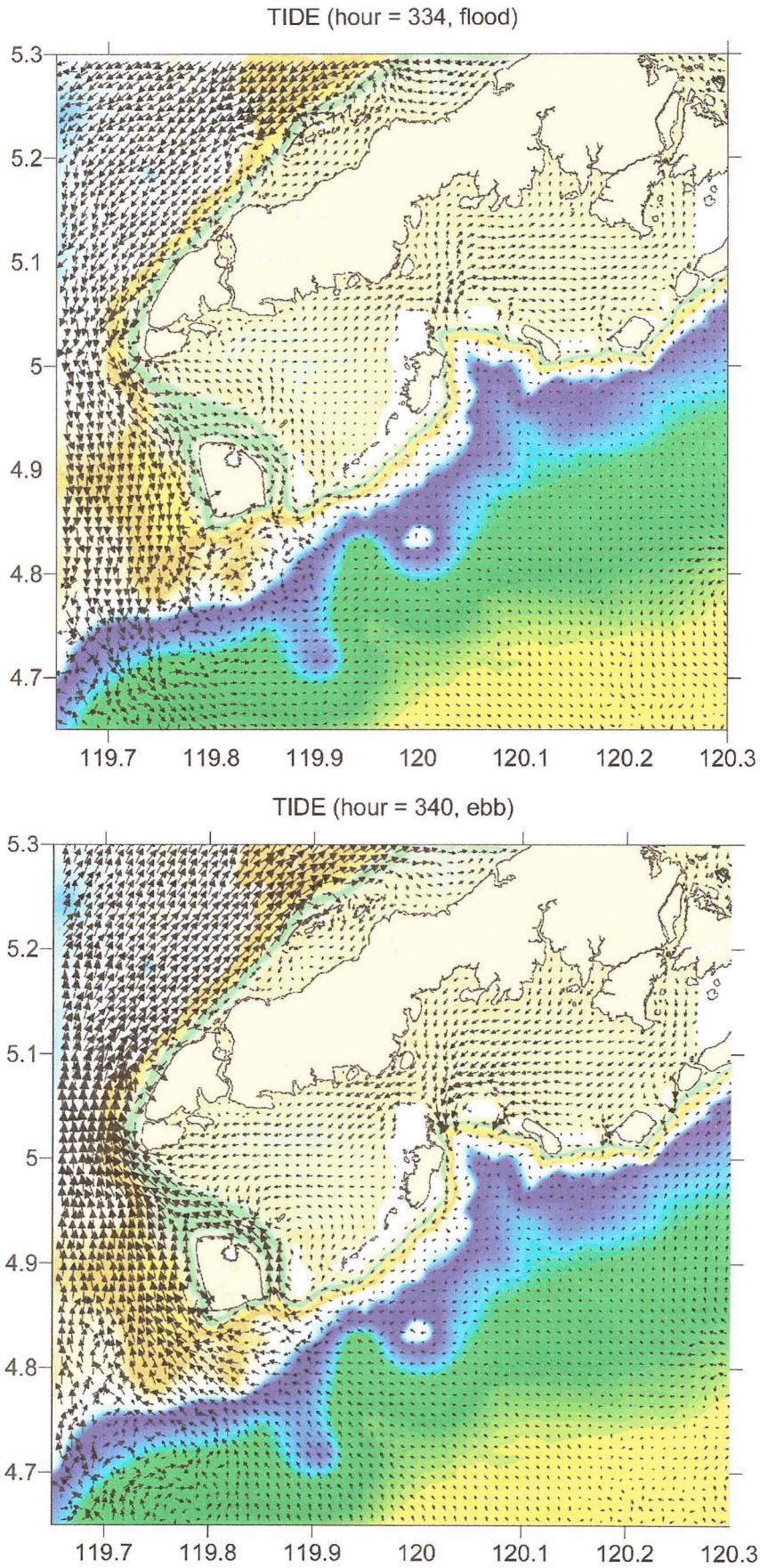

Figure 10. Modeled tidal circulation in Tawi-tawi

3.3 Larval Dispersal Patterns

The almost unidirectional flow inside the lagoon from the Sibutu Passage for the HYCOM forced simulations will definitely have some implications on the patterns of larval dispersal in the area. The results of the dispersal simulations are shown in ***Figure 11*** to ***Figure 13*** representing dispersal patterns for the month of January, April and August, respectively. The two plots for each month stand for dispersal of particles released from boxes located in the northern coast and the other from southern coast of the lagoon. The colored dots represent the location of dispersed particles and the box of the same color indicates the source of these dots. The stepwise pattern in the dispersal represents dispersal of the particles every two days for ten days.

The net southward dispersal through the Simunul and Balseyro Channels is the most evident and consistent feature in the figures. However, interesting seasonal differences in the dispersal can be observed in several locations as well. For instance, during January, particles released from the northern portion of the lagoon from Bongao to Parangan Island (four boxes from Bongao) were initially advected eastward within the lagoon before being ultimately advected southward. In April, however, particles released from the same four northern boxes at first appear to be highly entrained within the lagoon before being advected southward. During August, particles released from the first three northern boxes are limited in the middle of the lagoon and reaches the southern half of Tiji-tiji reefs at the end of the simulation while particles from the fourth northern box is advected to the boundary of the lagoon and Tawi-tawi Bay.

Particles released from boxes 5 and 6 (along the Balimbing Channel) are always advected eastward into the Tawi-tawi Bay except for August. For the boxes located south of the lagoon, particles are always advected southward by the alongshore flow west of Tiji-tiji reefs except for those that were released from boxes 7 and 8 during August which are rather advected northward towards the eastern boundary of the lagoon. Particles released from box 10 and 11 along the eastern and northern coast of Simunul Island, respectively, are always advected southward by the strong coastal jet in the area leaving no connection between Simunul and the lagoon.

Figure 15 to ***Figure 17*** gives the proportion of the particles settling in a particular box for the different seasons considered. For January, there are three boxes (3, 5, and 6) where at least 50% of their particles successfully settled in one of the boxes used while the rest of the boxes have at least 75% of their particles lost in the system. In the transition monsoon, only boxes 3 and 6 have at least half of their particles entrained in one of the boxes while boxes 4 and 5 also have significant proportions of particles that settled. The abovementioned boxes are either located in the northern coast of the lagoon or in the boundary between the lagoon and the Tawi-tawi Bay. For the southwest monsoon, box 4 showed a large proportion of particles settling within the boxes (80%), in fact the largest for all three seasons. Two boxes, 7 and 8, located in the southern coast of the lagoon also had relatively high proportion with at least 40% of their particles found in one or more other locations.

The results of the particle simulation can provide information on the potential of different areas to function as either a larval source or sink. For instance, an area could

be considered as a good or potential larval source if particles released from this area ends up in the most number of neighboring areas. For this study, this means that the higher the proportion of the particles found within a box (as described above) and the most number of boxes that contain the same particles indicates that the release box is an important larval source.

The interaction between selected areas or boxes can be shown in the sink matrix shown in ***Table 3*** to ***Table 5***. The numbers in the first row and the first column represent the box numbers shown in ***Figure 4***. The source boxes are represented in columns and the sink areas represented as rows. The numbers within a sink matrix represents the proportion of particles released from a source and distributed over 1 or more sink areas. The total of each column equals 100%. Boxes located along the southern and eastern coast of Bongao (2 to 6) act as the potential source areas for both the northeast (***Table 3***) and transition monsoons (***Table 4***) and boxes 1-3 and 7-8 during the southwest monsoon.

Similarly, the potential of an area to be a larval sink can also be evaluated using a similar matrix referred to as source matrix shown in ***Table 6*** to ***Table 8***. The total of each row equals 100%. For the northeast and transition monsoons, boxes 8 and 9 receives from the most number of particles from different boxes while boxes 9 and 10 appear to be the potential sink areas for the southwest monsoon.

The sink and source matrices for the tidal-forced dispersal scenarios show similar results (Table 9 and Table 10, respectively). The areas south of Bongao Island are potentially good source areas since particles from these areas reach the eastern and southern parts of the Lagoon while the areas in the southern part of the lagoon represent good sink areas since it receives particles released from along the northern and eastern parts of the lagoon.

4 SUMMARY AND CONCLUSIONS

Hydrodynamic and larval dispersal models of the Tawi-tawi area show insights on the potential larval dispersal patterns in the area. The strong net flow from the Sulu to the Sulawesi results in a strong dispersal from Bongao southwards to Simunul and along the southern part of the lagoon, and eastwards towards the eastern and southern fringes of the lagoon. Some variations occur with seasons and with the tides but the general patterns remain similar. The reefs in the southern and eastern coasts of Bongao appear to be good larval sources based primarily on passive larval dispersal patterns while the eastern and southern parts of the lagoon appear to be candidate sites for larval sinks. Other factors other than physical advection and diffusion may influence dispersal, settlement and eventual recruitment of fish populations but the results presented here represent estimates based on the assumption that the dispersed larvae are passive all throughout the planktonic larval duration.

5 REFERENCES

Liu AK, Holbrook JR, Apel JR 1985. Nonlinear Internal Wave Evolution in the Sulu Sea. Journal of Physical Oceanography 15(12):1613-1624.

Magno MM, 2005. Estimation of entrainment potential in Philippine Coastal Waters: The physical consequence of island wakes and eddies. MSc Thesis. College of Science, University of the Philippines, Diliman, Quezon City.

Mellor, G. L., 2003. Users guide for a three-dimensional, primitive equation, numerical ocean model (June 2003 version), 53 pp., Prog. in Atmos. and Ocean. Sci, Princeton University.

Meñez LA B., 2004. Influence of surface and deep-water mass sources on the hydrographic character of Philippine inland seas. MSc Thesis. College of Science, University of the Philippines, Diliman, Quezon City.

NAMRIA, 2005. Tide and Current Tables Philippines 2005. The Coast and Geodetic Survey Department, National Mapping and Resource Information Authority. Department of Environment and Natural Resources.

Polovina JJ, Kleiber P, Kobayashi DR. 1999. Application of TOPEX-POSEIDON satellite altimetry to simulate transport dynamics of larvae of spiny lobster, *Panulirus marginatus*, in the northeastern Hawaiian Islands, 1993-1996. Fish. Buyll. 97:132-143.

Sauers KA, Klinger T, Coomes C, Ebbesmeyer CC. 2003. Synthesis of 41,300 Drift Cards Released in Juan de Fuca Strait (1975-2002). Proceedings of the 2003 Georgia Basin/Puget Sound Research Conference. http://www.psat.wa.gov/Publications/01_proceedings/sessions/oral/7c_sauer.pdf

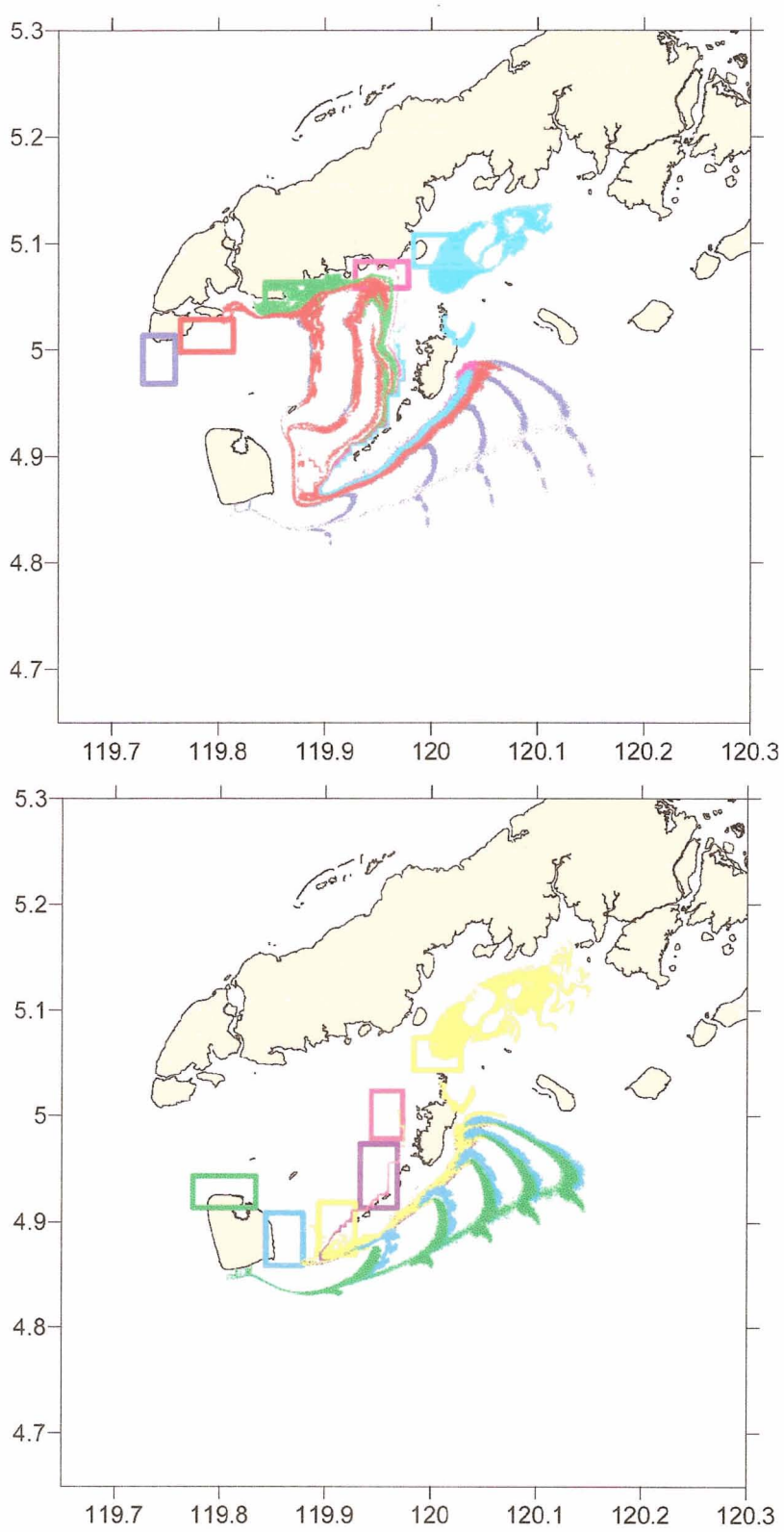

Figure 11. Dispersal of particles released from different locations for January 2003

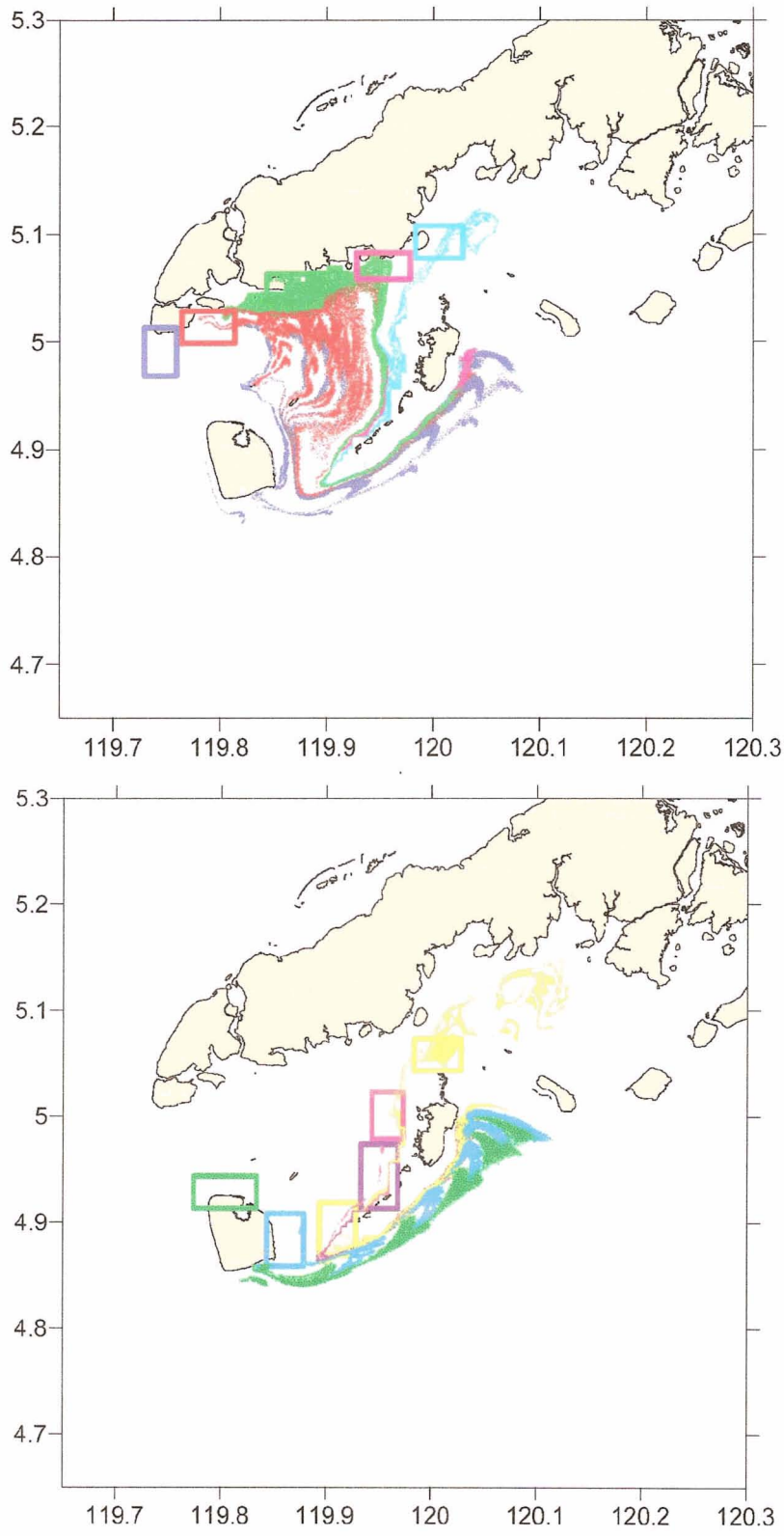

Figure 12. Dispersal of particles released from different locations for April 2003

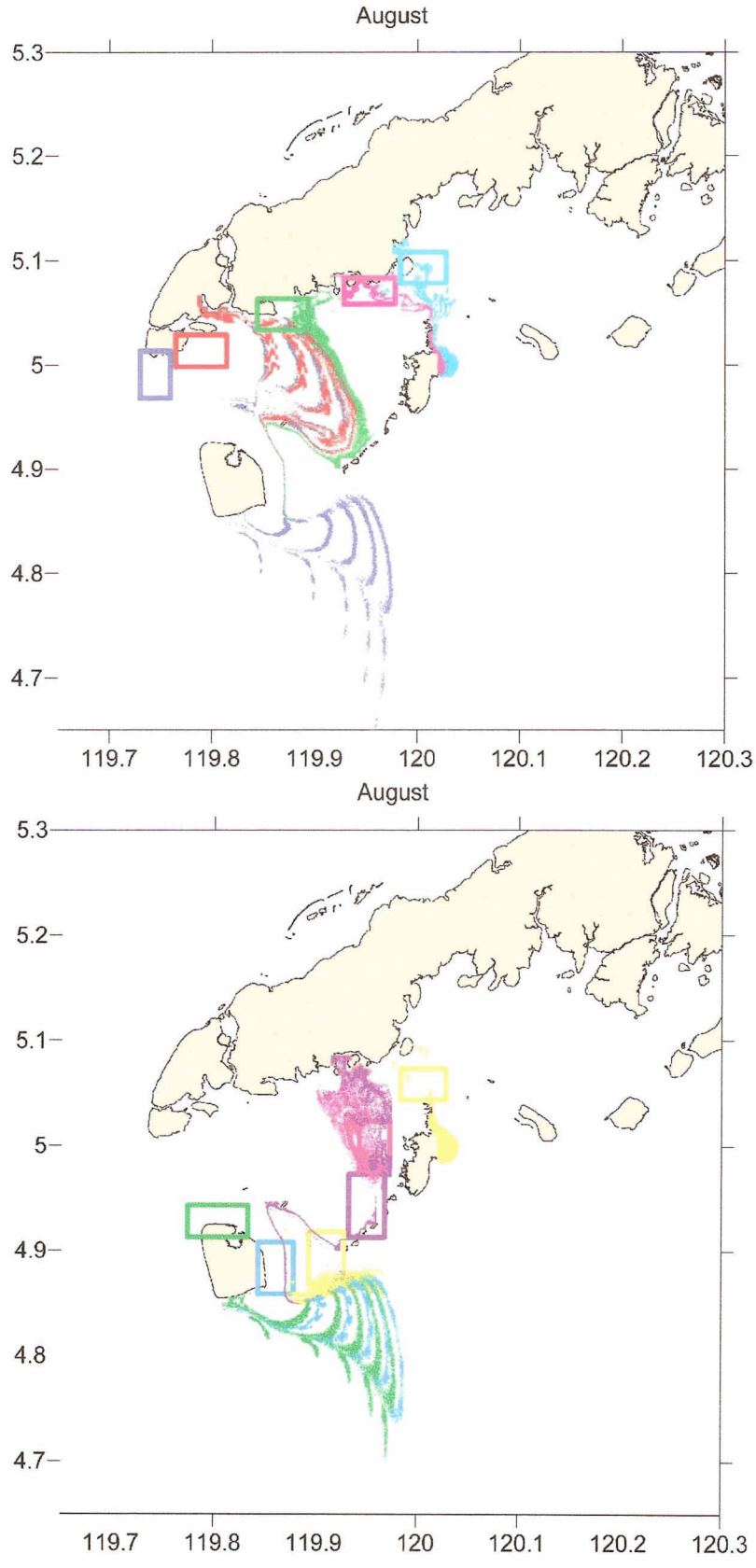

Figure 13. Dispersal of particles released from different locations for August 2003

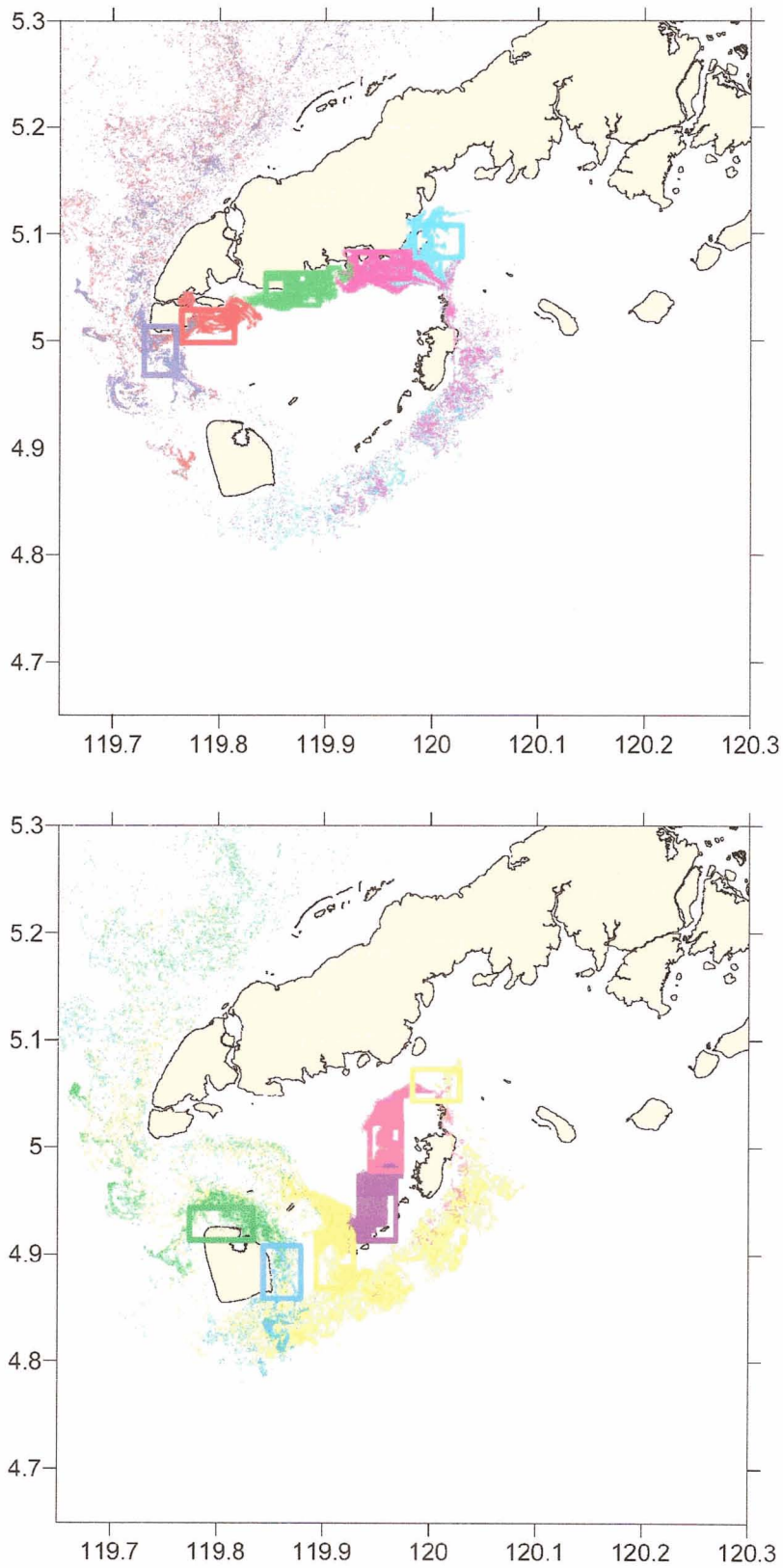

Figure 14 Dispersal of particles released from different locations forced by tides

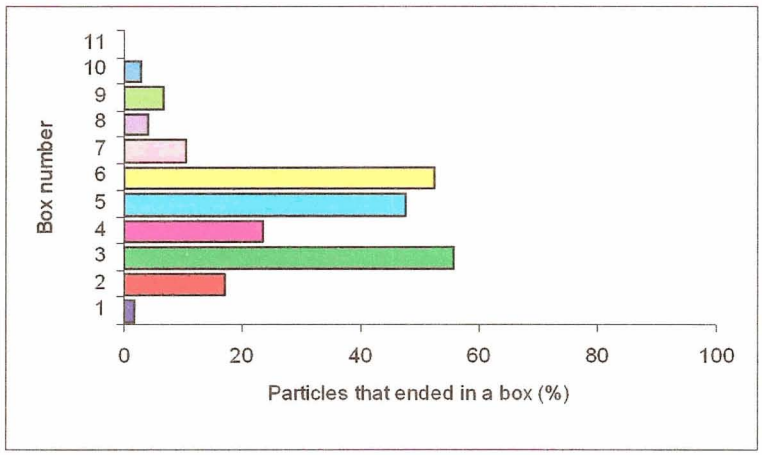

Figure 15 Proportion of particles settling within boxes in NE monsoon experiment

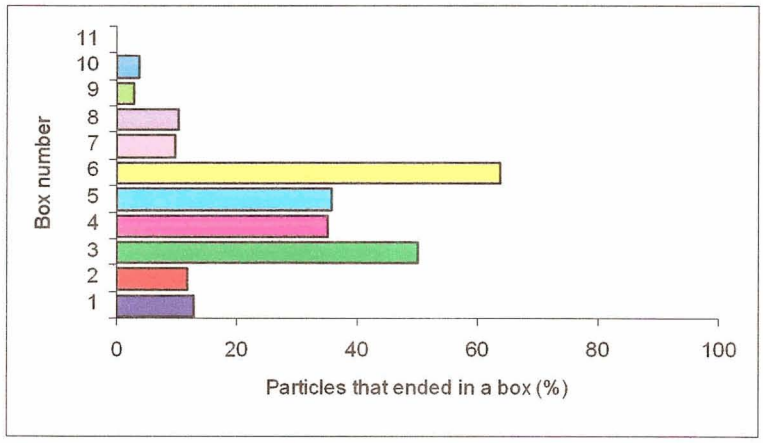

Figure 16 Proportion of particles settling within boxes in transition monsoon experiment

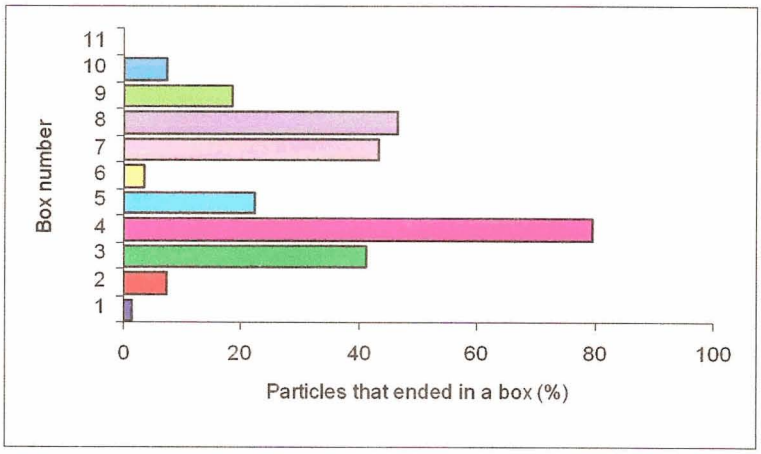

Figure 17 Proportion of particles settling within boxes in SW monsoon experiment

Table 3 Sink matrix for the northeast monsoon

Particle Sink \ Particle Source	1	2	3	4	5	6	7	8	9	10	11
1											
2		1.6									
3		18.5	79.0								
4		3.9	1.6	4.0							
5					32.5	15.4					
6					51.6	83.3					
7	15.5	17.0	7.9	2.4	2.7	0.5					
8	19.4	18.5	5.4	51.5	9.3	0.5	21.3				
9	33.6	31.8	6.1	42.1	3.9	0.3	78.7	96.6	97.2	2.4	
10	31.4	8.8						3.4	2.8	97.6	
11											

Table 4. Sink matrix for the transition monsoon

Particle Sink \ Particle Source	1	2	3	4	5	6	7	8	9	10	11
1											
2	0.1	18.3	4.0								
3		1.6	58.9								
4		0.3	16.1	25.4	0.1						
5					8.4	5.0					
6					2.3	73.2					
7		0.2	11.4	24.6	19.9	3.3					
8		13.8	5.4	23.7	36.8	11.7	26.7	0.1			
9	6.3	21.4	4.2	26.3	32.5	6.8	73.3	99.9	97.5	58.6	
10	92.0	44.5							2.5	41.4	100
11	1.6										

Table 5. Sink matrix for the southwest monsoon

Particle Sink \ Particle Source	1	2	3	4	5	6	7	8	9	10	11
1											
2											
3	29.9	53.9	44.5				0.0				
4				95.2	25.2	29.8	37.0	10.9			
5				0.0	21.8	21.7					
6				4.8	53.0	48.4					
7							43.8	22.5			
8	4.4	18.5	39.1				19.2	29.1			
9	49.7	25.8	12.7					28.8	61.5	48.3	44.4
10	16.0	1.8	3.7					8.6	38.5	51.7	55.6
11											

Table 6. Source matrix for the northeast monsoon

Particle Sink \ Particle Source	1	2	3	4	5	6	7	8	9	10	11
1											
2		100									
3		8.4	91.6								
4		33.5	33.8	32.7							
5					65.6	34.4					
6					36.0	64.0					
7	2.5	34.0	40.7	4.7	15.1	3.0					
8	1.3	15.2	11.4	41.3	21.4	1.1	8.3				
9	1.3	15.3	7.5	19.7	5.2	0.4	18.0	12.1	20.3	0.2	
10	8.6	29.8						3.0	4.1	54.4	
11											

Table 7. Source matrix for the transition monsoon

Particle Sink \ Particle Source	1	2	3	4	5	6	7	8	9	10	11
1											
2	0.3	57.4	42.3								
3		0.8	99.2								
4		0.2	49.7	49.8	0.3						
5					48.6	51.4					
6					1.7	98.3					
7		0.1	22.7	30.9	35.7	10.6					
8		5.0	6.5	18.4	40.6	23.1	6.4	0.0			
9	1.3	5.1	3.3	13.2	23.3	8.8	11.3	22.9	6.5	4.3	
10	58.6	31.4							0.5	9.0	0.5
11	100										

Table 8. Source matrix for the southwest monsoon

Particle Sink \ Particle Source	1	2	3	4	5	6	7	8	9	10	11
1											
2											
3	2.1	21.2	76.7				0.0				
4				68.5	7.2	1.3	16.0	7.1			
5				0.2	86.7	13.1					
6				16.6	73.2	10.2					
7							56.7	43.3			
8	0.2	3.9	35.8				18.5	41.7			
9	1.7	5.1	11.0					39.0	33.7	9.5	0.0
10	1.2	0.8	6.9					24.7	44.9	21.5	0.1
11											

Table 9. Sink matrix for tidally forced dispersal.

Particle Sink	Particle Source										
	1	2	3	4	5	6	7	8	9	10	11
1	81.4	13.3		0.0	0.3	5.2			1.7	4.9	2.9
2	15.4	85.1	0.2						1.4	2.1	4.3
3			99.7								
4			0.1	72.7	29.5						
5				1.4	35.5	0.9	0.0				
6				24.1	28.9	26.3	4.9				
7							92.0	2.9			
8							3.0	92.1			
9				0.7	2.0	7.9	0.0	5.0	86.8		
10		0.0		0.6	2.0	34.6			4.5	71.1	11.7
11	3.2	1.6		0.6	1.8	25.1			5.6	21.8	81.2

Table 10. Source matrix for tidally-forced dispersal.

Particle Sink	Particle Source										
	1	2	3	4	5	6	7	8	9	10	11
1	53.6	28.1		0.1	0.9	2.5			4.9	4.9	5.1
2	5.0	87.8	0.6						2.0	1.0	3.7
3			100.0								
4			0.1	67.7	32.2						
5				3.2	96.4	0.4	0.0				
6				34.5	48.4	6.3	10.7				
7							94.0	6.0			
8							1.6	98.4			
9				0.6	2.2	1.2	0.0	14.7	81.3		
10		0.0		1.2	5.3	12.9			10.0	54.4	16.1
11	1.0	1.6		0.8	2.9	5.8			7.8	10.4	69.6